**Musculoskeletal Ultrasound**

Author(s) Beggs, Ian

Imprint Lippincott Williams & Wilkins, 2014

ISBN 9781451144987, 1451144989

Permalink https://books-scholarsportal-info.myaccess.library.utoronto.ca/en/xml/chapter?id=/ebooks/ebooks1/lww/2014-07-29/1/01762492&chapterId=B01762492-C5

Chapter 5
Hand and Wrist
Monique Reijnierse
Nicole C. Fernandes

## INTRODUCTION

The complex soft tissue structures of the hand and wrist are ideally suited for ultrasound examination. They are superficial and accessible. Dynamic examination can be performed in real-time and vascularity assessed by color or power Doppler. Standard linear array transducers are adequate for most purposes, but small footprint transducers operating at high frequency (>10MHz) may be valuable.

## ANATOMY OF THE WRIST

### Bones and Ligaments

Two carpal rows with eight carpal bones form the wrist. From radial to ulnar, the proximal carpal row is formed by scaphoid, lunate, triquetrum, and pisiform, and the distal carpal row by trapezium, trapezoid, capitate, and hamate (Fig. 5.1). Stability is maintained by extrinsic (radiocarpal and ulnocarpal) and intrinsic (intercarpal) ligaments. Palmar and dorsal ligaments are differentiated and are named for the bones from which they originate and into which they insert, starting from proximal to distal and from radial to ulnar.[1,2]

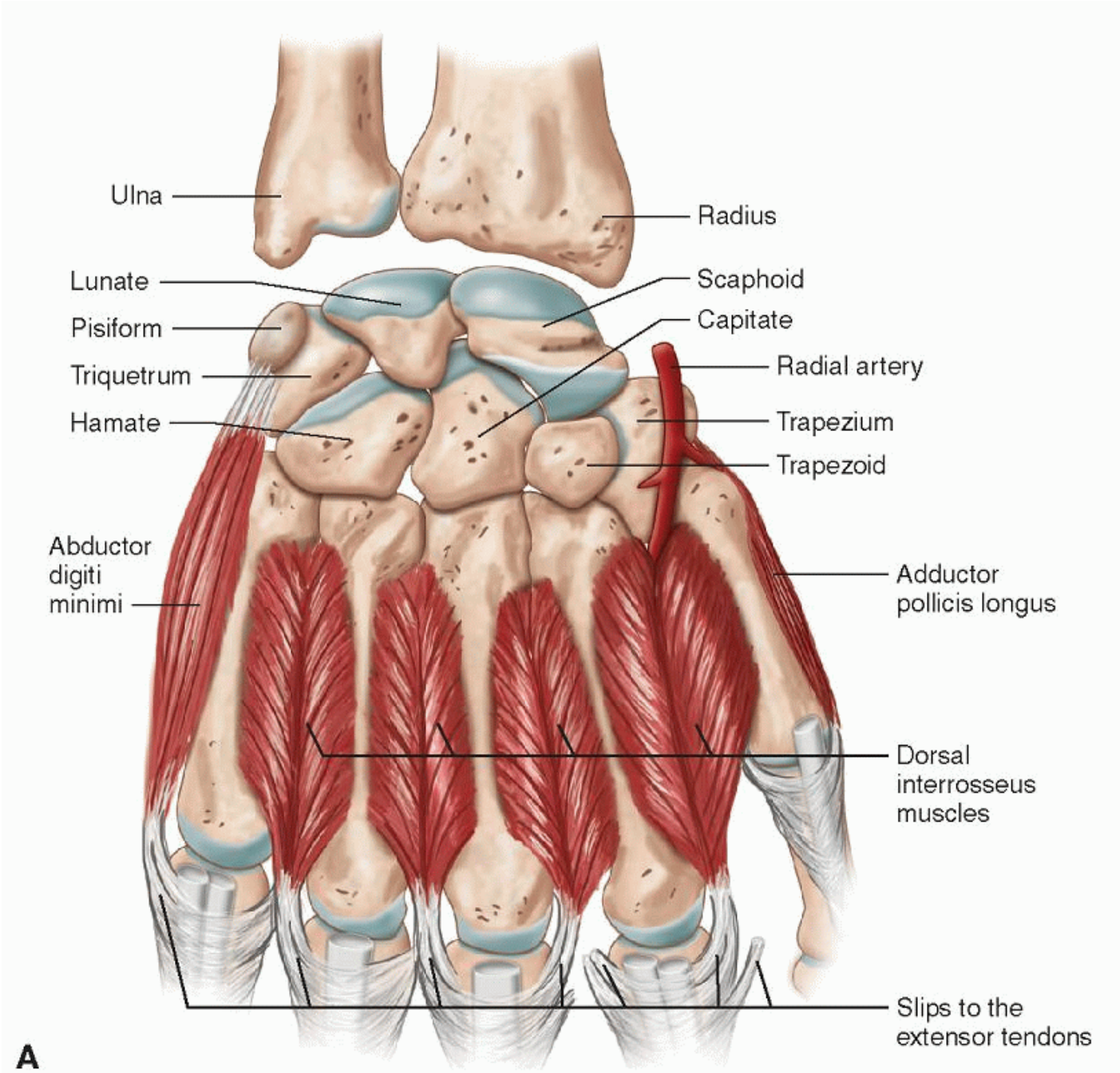


Figure 5.1. Bony anatomy. A, B: The anatomy of the proximal and distal carpal rows, as seen from the dorsal (A) and palmar (B) sides is shown. The landmarks for the carpal tunnel proximally—scaphoid and pisiform—and distally—trapezium and hamate—

are clearly visible in B. The carpal bones are connected by intrinsic ligaments. The interosseous and lumbrical muscles contribute lateral and central slips to stabilize the extensor tendons.
(Adapted from Netter FH, Woodburne RT, Crelin ES, et al. Upper limb, wrist and hand. In: Musculoskeletal System, Part 1: Anatomy, Physiology and Metabolic Disorders. NJ: Ciba-Geigy; 1987:55-73, with permission.)
The scapholunate (SLL) and lunotriquetral ligaments (LTL) are the most important intrinsic ligaments. They have thick palmar and dorsal components and thinner central portions.[3]
The triangular fibrocartilage is a biconcave disk between the ulnar styloid and the radius, with a variable thickness. Together with the meniscus homologue,
P. 74

the ulnar collateral ligament (UCL), the radioulnar ligament, and the sheath of the extensor carpi ulnaris (ECU) tendon, the triangular fibrocartilage forms the triangular fibrocartilage complex (TFCC).[3] It increases stability of the ulnar side of the wrist.

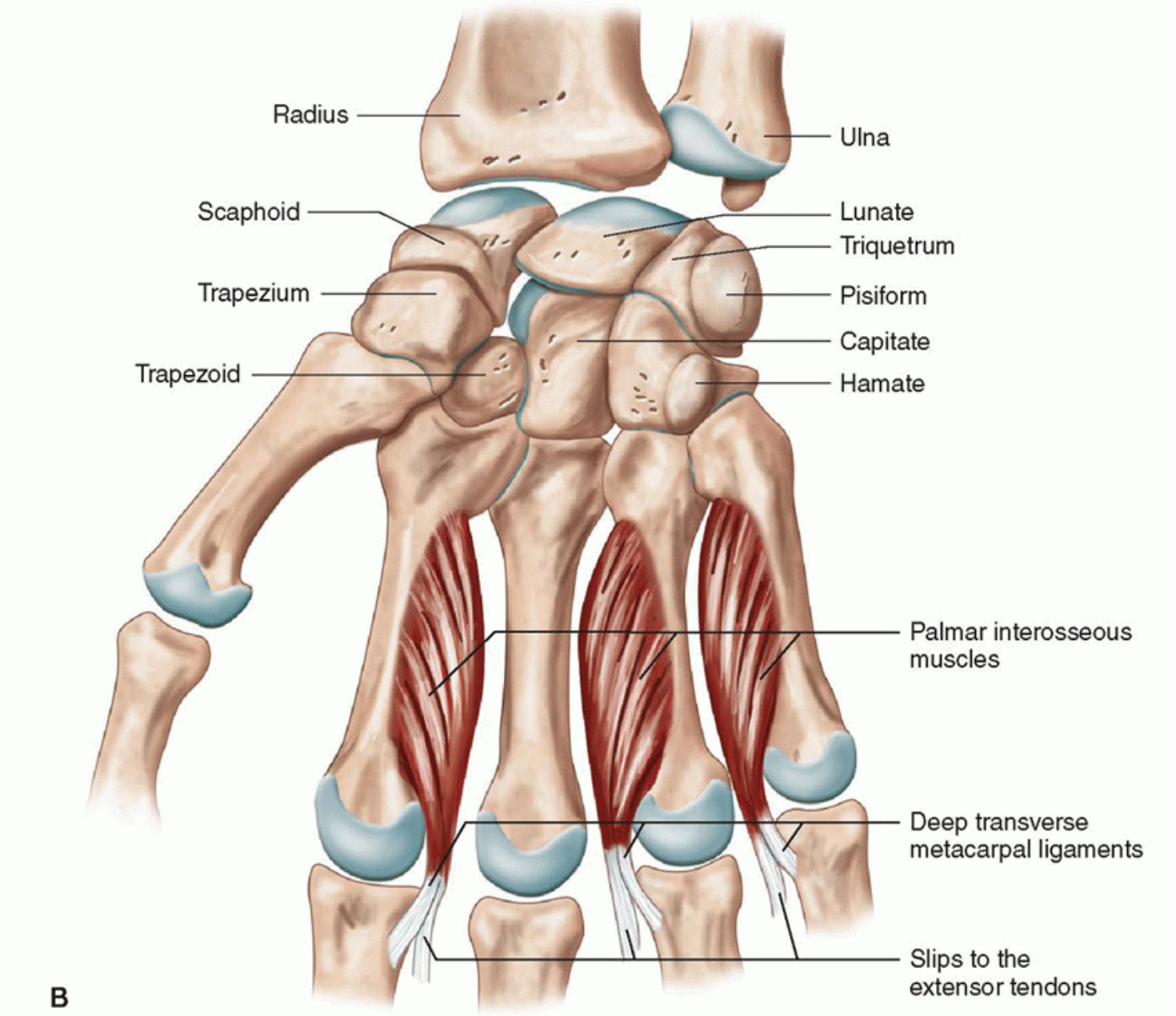


Figure 5.1. (Continued)
Tendons and Synovium
Extensor Tendons at the Wrist
The extensor tendons run across the dorsum of the wrist held in position by the extensor retinaculum, a focal thickening of the deep fascia that is attached to the radius laterally and to the triquetrum and pisiform medially. Fibrous bands extend from the deep surface of the retinaculum and attach to the radius and ulna, resulting in six separate compartments numbered 1 to 6, starting from the radial side.
Compartment one is at the level of the styloid process of the radius and contains the tendons of abductor pollicis longus (APL) and extensor pollicis brevis (EPB).

Compartment two lies on the radial side of Lister's tubercle, a bony prominence on the dorsal aspect of the distal radius, and contains the extensor carpi radialis longus (ECRL) and extensor carpi radialis brevis (ECRB) tendons. Ulnar to Lister's tubercle, compartment three contains the extensor pollicis longus (EPL) tendon. The fourth compartment is the last compartment on the ulnar side of the radius, and contains the four tendons of the extensor digitorum muscle and the tendon of extensor indicis, which is deeper. Compartment five lies over the ulna, at the level of the distal radioulnar joint, and contains the extensor digiti minimi (EDM) tendon. Compartment six contains the tendon of the ECU in the groove of the distal ulna (Fig. 5.2).

The tendons of each compartment are enveloped by double-layered synovial sheaths to prevent friction.[4] These sheaths extend proximally and distally from the extensor retinaculum. The sheaths surrounding the tendons to the fingers are longer than those of ECU, ECRB, and ECRL. The tendons of ECRB and ECRL insert on the bases of the second and third metacarpals, and ECU inserts on the base of the fifth metacarpal. Abductor pollicis longus inserts on the base of the first metacarpal. The extensor tendons are vulnerable at the dorsum of the hand, since they are located superficially. The extensor digitorum tendons show intertendinous connections that limit separate movement. Since the tendon of the extensor indicis is extra, separate extension of the index finger is possible.

P. 75

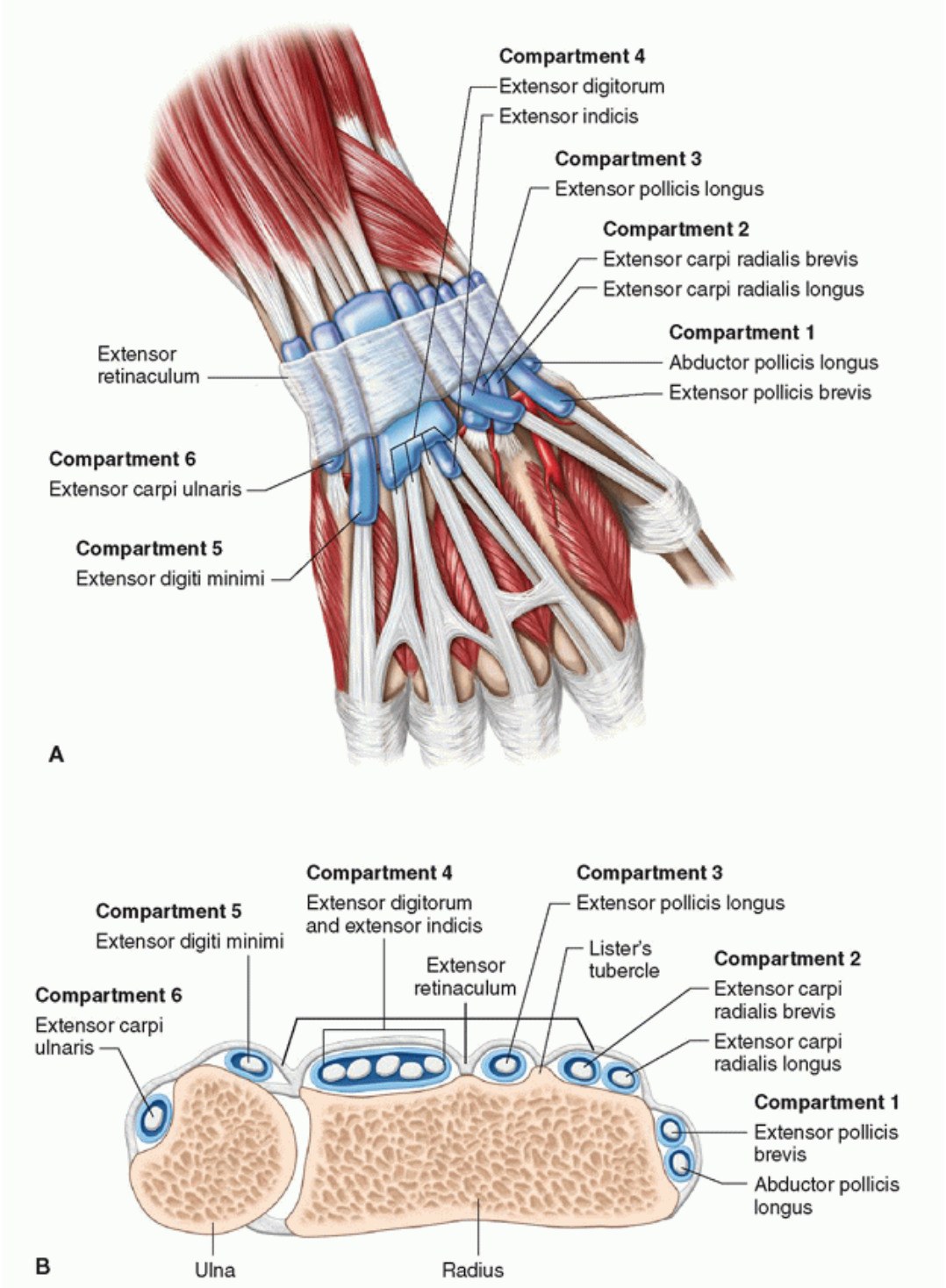

Figure 5.2. Extensor tendon anatomy at the wrist. A: Dorsal view. The extensor tendons lie in six compartments. Each compartment contains a synovial sheath for the tendon(s) it contains. The sheaths extend proximal and distal to the extensor retinaculum. The tendons of compartments two and six insert on the bases of the second/third and fifth metacarpals, respectively. Intertendinous connections are visible on the dorsum of the hand. B: Axial view. The extensor compartments are numbered from the radial to the ulnar side. Lister's tubercle is the bony landmark that separates compartments two and three.
(Adapted from Netter FH, Woodburne RT, Crelin ES, et al. Upper limb, wrist and hand. In: Musculoskeletal System, Part 1: Anatomy, Physiology and Metabolic Disorders. NJ: Ciba-Geigy; 1987:55-73, with permission.)
P. 76

Proximal to the extensor retinaculum the tendons of compartment one cross superficial to the tendons of compartment two. Distal to Lister's tubercle, EPL crosses over extensor compartment two.

Flexor Tendons at the Wrist

There are nine flexor tendons in the carpal tunnel. The flexor tendons of the fingers, the flexor digitorum superficialis (FDS) and flexor digitorum profundus (FDP), are arranged in the carpal tunnel, superficial and deep, respectively, and continue distally in pairs to each finger except the thumb (Fig. 5.3). They are invested by a common tendon sheath that starts proximal to the carpal tunnel and extends to within 5 mm of the insertion of the profundus tendon on the distal phalanx. A separate ulnar bursa envelops the flexor tendons of the little finger. There is a gap between ulnar bursa and the synovial sheaths of the index, long, and ring fingers in the distal palm of the hand. The other tendon in the carpal
P. 77

tunnel is the flexor tendon of the thumb, flexor pollicis longus, which has a separate synovial covering, the radial bursa (Fig. 5.4).

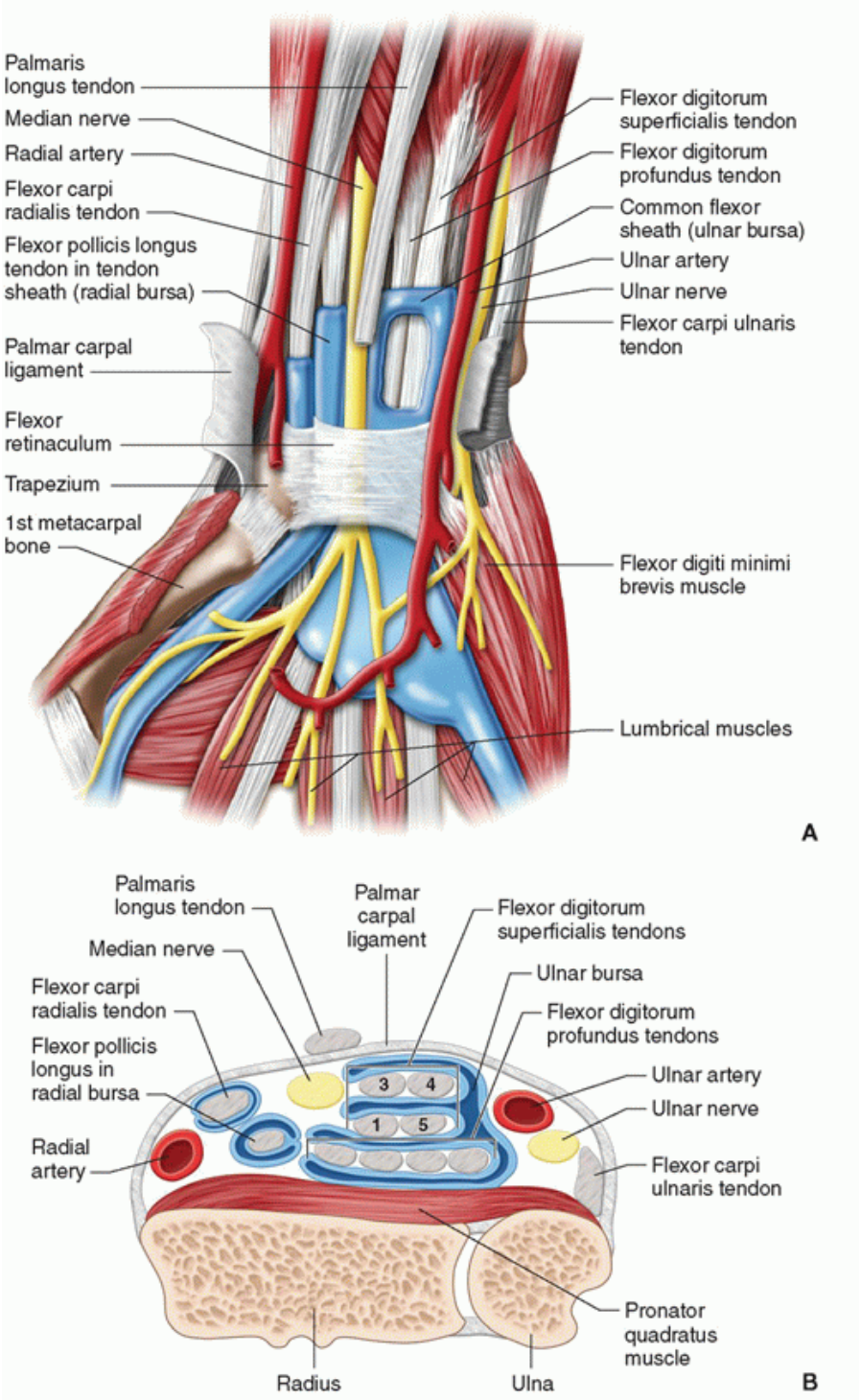


Figure 5.3. Flexor tendon anatomy at the wrist. A: Volar view. The palmar ligament is proximal and superficial to the flexor retinaculum. The tendons of FPL, FDP, and FDS (nine in total) run through the carpal tunnel, accompanied by the median nerve. Flexor carpi radialis runs in a separate compartment and inserts on the bases of the second and third metacarpals and the tuberosity of the trapezium. Flexor carpi ulnaris inserts on the pisiform and has no synovial sheath. The palmaris longus is the only other flexor tendon without a sheath. B: Axial view, proximal to the carpal tunnel. Appreciate the typical position of the tendons surrounded by the ulnar bursa.

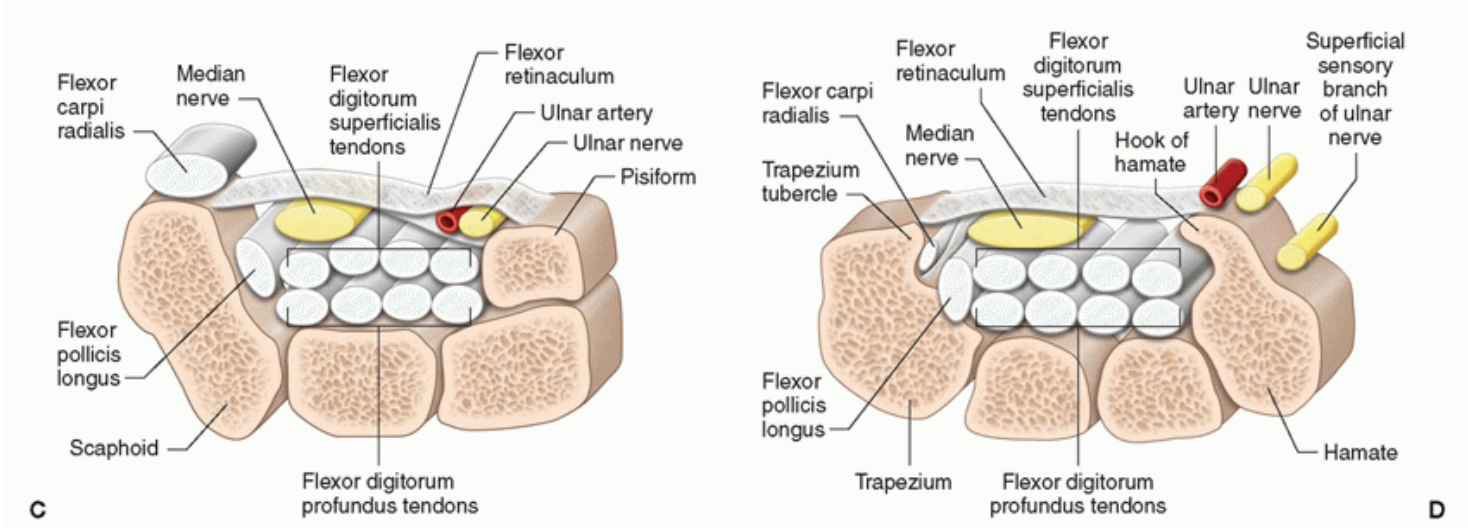


Figure 5.3. (Continued) C: At proximal carpal tunnel. The bony landmarks are the scaphoid tubercle and the pisiform. The flexor retinaculum forms the roof of the carpal tunnel and the floor of Guyon's canal that contains the ulnar artery and nerve. D: Distal carpal tunnel. The bony landmarks are the trapezium tubercle and the hook of the hamate. The FCR tendon sits in a groove in the trapezium separated from the other tendons by a split in the attachment of the retinaculum.
(Adapted from Netter FH, Woodburne RT, Crelin ES, et al. Upper limb, wrist and hand. In: Musculoskeletal System, Part 1: Anatomy, Physiology and Metabolic Disorders. NJ: Ciba-Geigy; 1987:55-73, with permission.)

There are two primary wrist flexors. They are superficial to the carpal tunnel. The flexor carpi radialis (FCR) tendon inserts on the base of the second metacarpal. It has a separate synovial sheath. Flexor carpi ulnaris (FCU) contains the pisiform, a sesamoid bone, and inserts on the hook of the hamate and the base of the fifth metacarpal. The FCU does not have a tendon sheath. The palmaris longus tendon is a thin, variable tendon that inserts on the transverse carpal ligament and the palmar aponeurosis and is absent in 20% of cases.[4]

Nerves at the Wrist

The median nerve (MN) enters the carpal tunnel with the FDP and FDS tendons of the fingers. The MN is located superficial to the flexor pollicis longus tendon and the FDS tendon of the index finger. Distal to the carpal tunnel, it divides into recurrent motor and common palmar digital nerves.[5] It provides the motor supply for the muscles of the thenar eminence and the sensory supply to the palmar aspect of the thumb, index, and middle fingers and the radial half of the ring finger.[3] Anatomic variants include a persistent median artery of the forearm and bifid MN.

The ulnar nerve and artery run through Guyon's canal. The floor of this small tunnel is formed by the transverse carpal ligament, its ulnar wall by the pisiform, and its roof by the palmar carpal ligament, which is an extension of the flexor retinaculum. The tunnel is demarcated by the pisiform proximally and the hook of hamate distally. The ulnar nerve divides in the distal canal into a superficial sensory branch and a deep motor branch, located on either side of the flexor digiti minimi brevis muscle.[5,6] The sensory branch supplies the palmar aspect of the ulnar portion of the ring finger and the little finger, and the motor branch supplies the muscles of the hypothenar eminence, ulnar lumbrical, and interosseous muscles and the adductor pollicis.[4]

The radial nerve at the wrist is a small superficial branch in the subcutis and pierces the deep fascia proximal to the extensor retinaculum. It crosses the first extensor compartment, subdivides into two branches, which usually split into four or five dorsal digital nerves, and provides sensation to the dorsum of the wrist, hand, thumb, and proximal fingers.[6,4]

ANATOMY OF THE FINGERS

The five metacarpal bones and their phalanges form the metacarpophalangeal (MCP) and proximal (PIP) and distal interphalangeal (DIP) joints, except for the thumb, which has a metacarpal joint and a single interphalangeal joint. In each joint, the bones are united by a loose articular capsule, radial and ulnar collateral ligaments, and a palmar ligament. Dorsally the joints are reinforced by the expansion of the digital extensor tendon.[4]

The collateral ligaments are strong, fan-shaped, cordlike bands that stabilize the joint.

P. 78

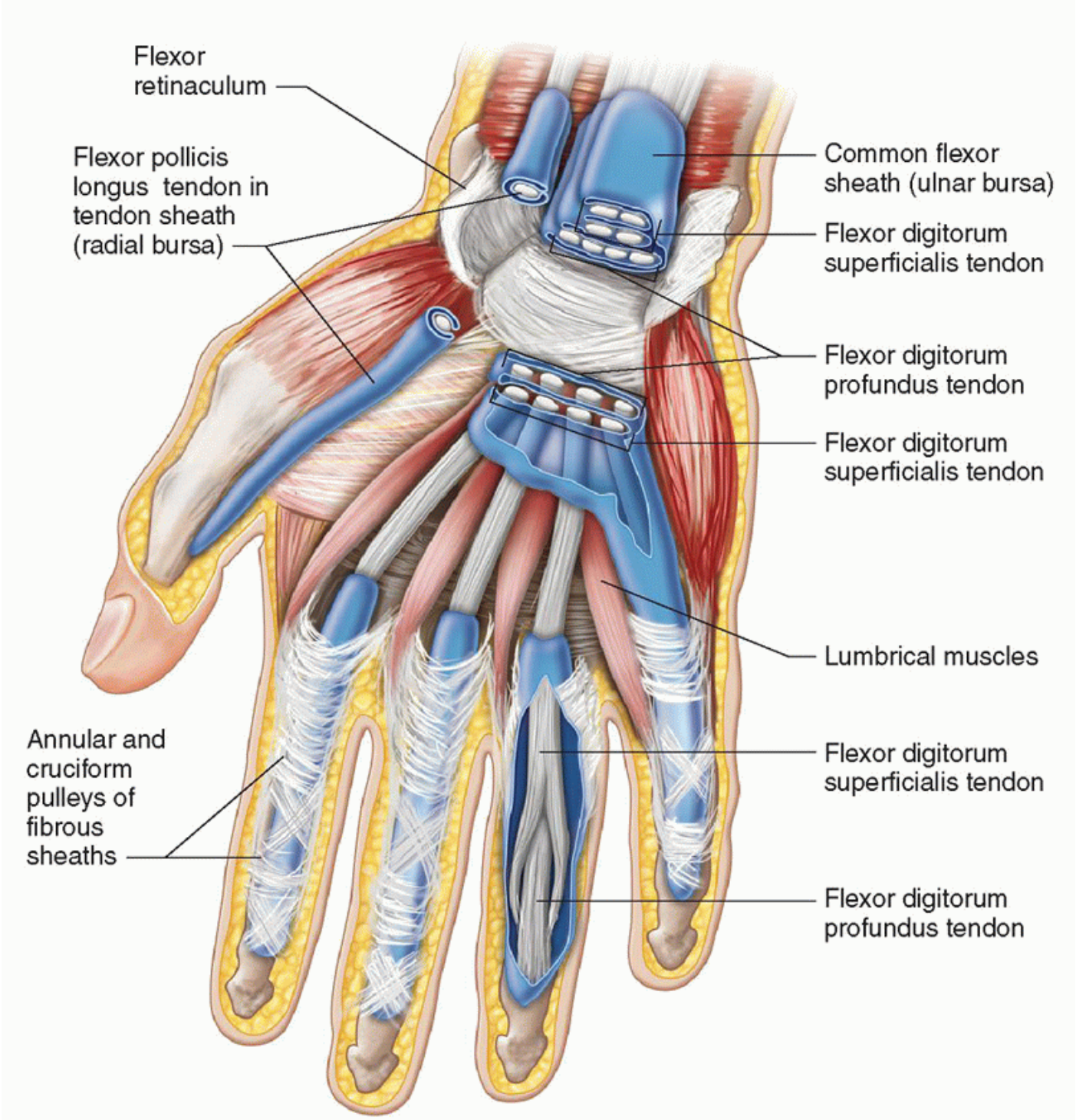


Figure 5.4. Volar wrist and hand synovial anatomy. The flexor pollicis longus tendon is surrounded by the radial bursa, which extends distally. The other flexor tendons are surrounded by the ulnar bursa, which extends to the little finger. Note the gap between this bursa and the synovial sheaths of the second, third, and fourth digits.
(Adapted from Netter FH, Woodburne RT, Crelin ES, et al. Upper limb, wrist and hand. In: Musculoskeletal System, Part 1: Anatomy, Physiology and Metabolic Disorders. NJ: Ciba-Geigy; 1987:55-73, with permission.)

The palmar ligament, also called the palmar or volar plate, consists of thick fibrocartilage, extending from the neck of the proximal bone to the base of the distal bone. Proximally it is loosely attached, distally firmly. At the sides, it is continuous with the collateral ligaments, and at the level of the MCP joints it is also continuous with the deep transverse metacarpal ligament. On the volar side of the palmar plate, a groove holds the flexor digitorum tendons. Fibrous sheaths cover the synovial sheaths and extend from the head of the metacarpals distally. The fibrous sheaths have thick, transversely running fibers, pulleys, which insert on the palmar plate (Fig. 5.5). The pulley system refers to a number of ligaments, including annular pulleys (A1-A5) and cruciform pulleys (C1-3).

Their task is to keep the tendons close to the bone in flexion and to prevent “bowstringing.” The A2 and A4 pulleys are broader than the others and are functionally more important. (Fig. 5.5)

The tendon of FDP inserts on the base of the distal phalanx. The tendon of FDS splits at the level of the proximal phalanx and inserts on the shaft of the middle phalanx (Fig. 5.5B).
The four tendons of extensor digitorum longus flatten distally from the MCP joints and divide into three slips: the central slip inserts on the base of the middle phalanx, and the two lateral slips insert on the base of the distal phalanx (Fig. 5.5C). The extensor tendons are closely related to the joint capsule, and an extensor expansion for the MCP, PIP, and DIP joints is formed by the tendons of the lumbrical and interosseous muscles of the hand.[4] At the level of the MCP joint this dorsal expansion is called a hood. A triangular aponeurosis is formed over the distal end of the middle phalanx, with the apex inserting on the distal phalanx. The thumb has two separate extensor tendons: the EPL inserting on the base of the distal phalanx and the EPB inserting on the base of the proximal phalanx. Thus the extensor tendons are attached to the bone by a complex ligamentous structure and do not have a synovial sheath.

ULTRASOUND TECHNIQUE

The patient is seated opposite the examiner, with the hand placed on the examination couch. The height of the couch is adjusted such that it is comfortable for both the patient and the examiner. Abundant ultrasound gel is required to ensure that the ultrasound probe is in good contact with the underlying skin, without the need to exert excessive pressure. The hand is placed on an absorbent pad.

P. 79

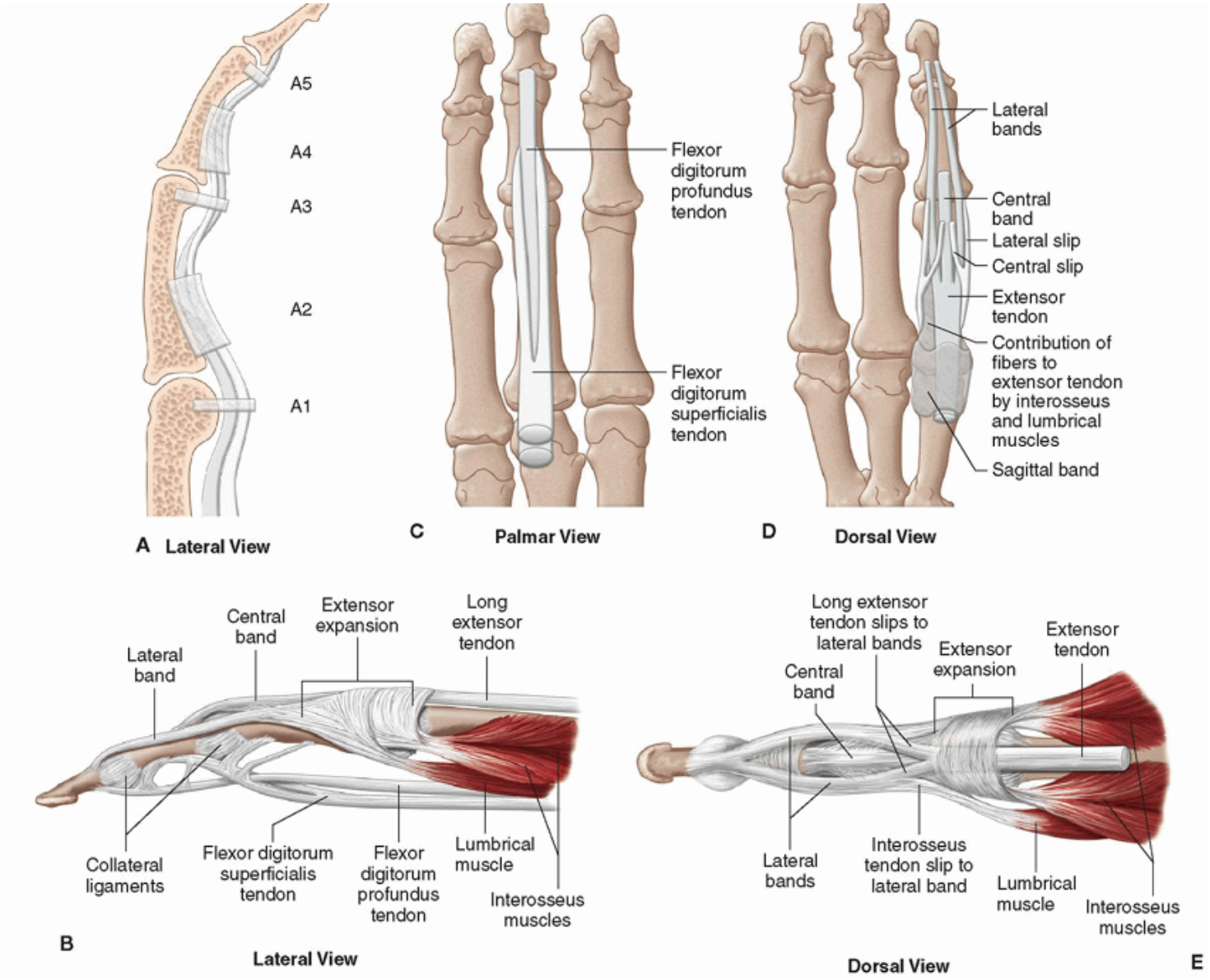


Figure 5.5. Tendon anatomy of the fingers. A: Lateral view of annular pulley system that stops the flexor tendons from bowstringing. B: Lateral view: insertion of the extensor and flexor tendons. The extensor tendon has three slips and flattens distally. Flexor tendons are thicker than extensor tendons and have superficial and deep components. The stabilizers of the extensor tendon include the interosseous and lumbrical insertions and a dorsal expansion at the level of the MCP joints. C: Palmar view: flexor tendon insertion. The FDP tendon inserts on the base of the distal phalanx, the FDS tendon divides into two at the level of the proximal phalanx and inserts on the shaft of the middle phalanx. D,E: Dorsal views: extensor tendon insertion. The extensor tendon

with three slips, the lateral ones inserting distally and the central one inserting on the middle phalanx, is stabilized by slips of the interosseous and lumbrical muscles and a dorsal expansion at the level of the MCP joints.
(Adapted from Netter FH, Woodburne RT, Crelin ES, et al. Upper limb, wrist and hand. In: Musculoskeletal System, Part 1: Anatomy, Physiology and Metabolic Disorders. NJ: Ciba-Geigy; 1987:55-73, with permission.)

In general, anatomy is identified using a standardized protocol[3,5,7] and important landmarks. Be aware of normal variations.

Dorsal Wrist

Start the examination of the wrist in a transverse plane. Identification of the different tendons is achieved by using the important landmark of Lister's tubercle, a bony prominence on the distal radius that separates the second and third compartments. The six extensor compartments are identified. Compartment one contains the tendons of the APL (palmar) and the EPB (dorsal), which are best shown with the hand placed on its ulnar side, thumb upward (Fig. 5.6). A septum may divide this compartment into two. This is important in the case of therapeutic injections as the two sub-compartments may have to be injected separately.
P. 80

The APL may have multiple tendinous slips, a normal finding. The radial artery and the sensory branch of the radial nerve lie palmar to the APL. The artery crosses deep to the tendons, and the nerve crosses superficial. To exclude accessory tendons at the first compartment, the APL should be followed distally over the scaphoid.

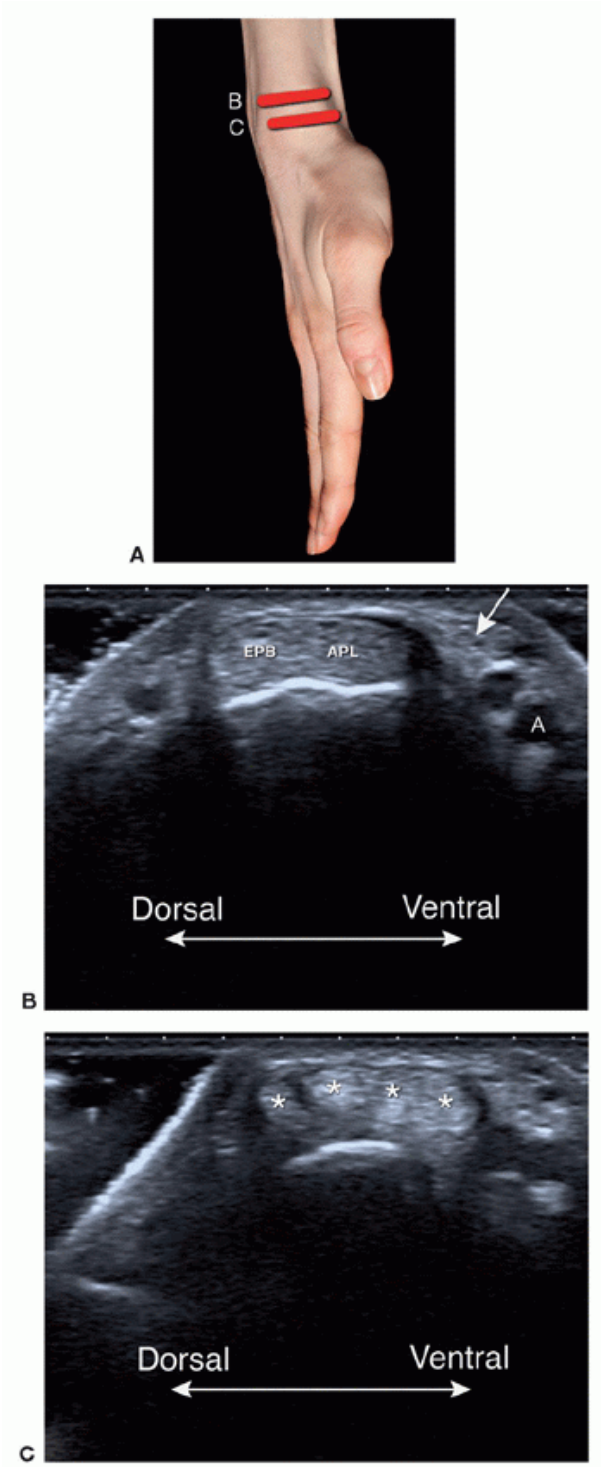


Figure 5.6. Compartment one. A: The right hand is examined on its side, thumb upward. B: Extensor pollicis brevis (EPB) is dorsal, and abductor pollicis longus (APL) lies ventral. The radial artery (A) crosses deep to the tendons more distally, and the superficial branch of the radial nerve (arrow) crosses superficially. C: Distal image demonstrates the multiple tendon slips (asterisks) of APL.

The wrist is then turned prone. The second compartment (Fig. 5.7) contains ECRL and ECRB. Moving the transducer proximally from Lister's tubercle, the point where the first compartment crosses superficial to the second compartment is identified, the site of intersection syndrome.

Extensor compartment three lies immediately medial or ulnar to Lister's tubercle and contains the tendon of EPL. Distally, the tendon of EPL (Fig. 5.8) crosses superficial to the tendons of compartment two.

The fourth compartment contains the extensor digitorum communis (EDC) tendon and the tendon of the extensor indicis proprius (EIP), which is located deeper. The compartment has a thick, hypoechoic retinaculum that should not be mistaken for fluid. The fifth compartment is small and contains the tendon of EDM (Fig. 5.9).

The sixth compartment (Fig. 5.10) contains the tendon of ECU, and is best examined with the hand in extreme pronation, that is, with the thumb on the examination couch and the ulnar surface of the wrist upward.

Tip:

To remember the names of the tendons in the extensor compartments one to three, start from the radial side with longus (L) and alternate with Brevis (B): APL, EPB (1), ECRL, ECRB (2), and EPL (3).
The TFCC is located in the space between the distal ulna and the proximal carpal row, but is not well demonstrated by ultrasound. Suspected TFCC tears should be investigated by magnetic resonance imaging (MRI) or MR arthrography.
To identify the SLL (Fig. 5.11), the transducer is moved distally from Lister's tubercle. Only the dorsal part of the SLL can be seen as a thin band running between the scaphoid and the lunate, but this is a useful screening tool in suspected SLL tears. The LTL may be seen ulnar to the SLL.
Tip:
Use Lister's tubercle as a landmark to identify the second and third compartments. By moving distally from Lister's tubercle, you will find the scapholunate ligament.
Longitudinal imaging is used to image the radiocarpal joint and screen for synovial hypertrophy or joint
P. 81

P. 82

effusion. The distal radio ulnar (DRU) joint is imaged transversely and lies just proximal to the radiocarpal joint.

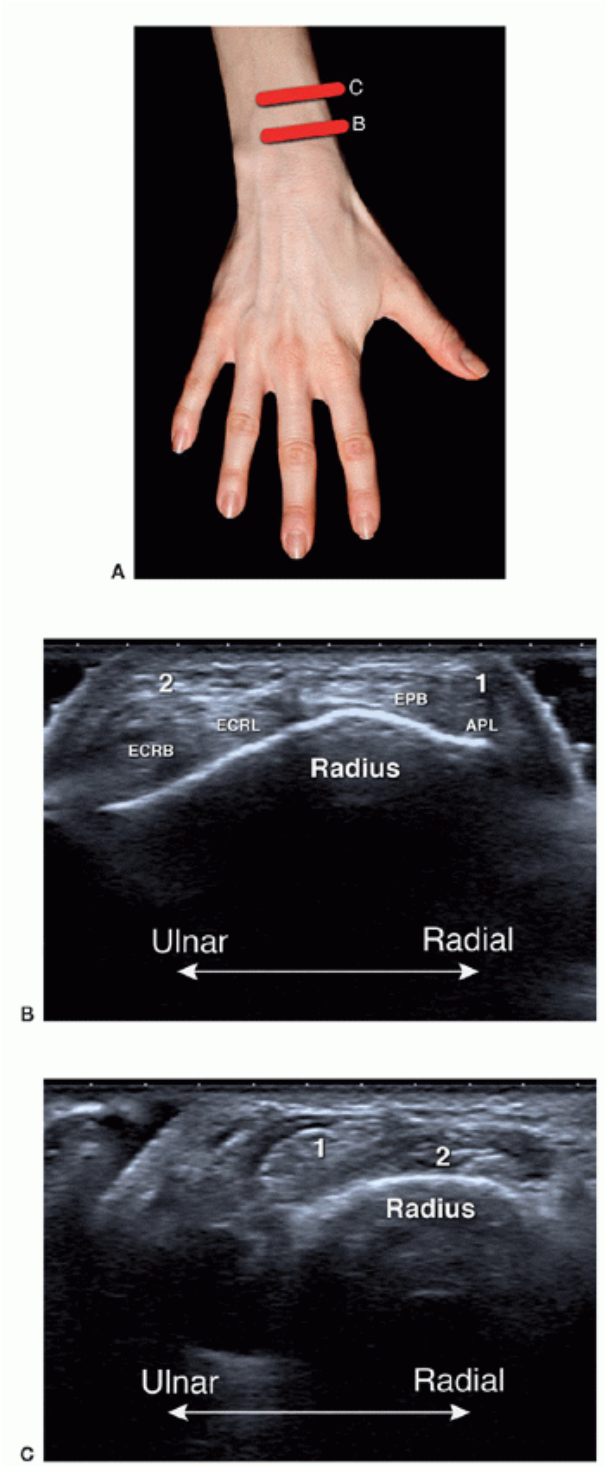


Figure 5.7. Compartment two. A: Hand pronated. B: Axial image of the second extensor compartment illustrating the extensor carpi radialis longus (ECRL) and extensor carpi radialis brevis (ECRB). EPB, extensor pollicis brevis; APL, abductor pollicis longus. C: Moving the transducer proximally shows the first compartment crossing superficial to the second compartment.

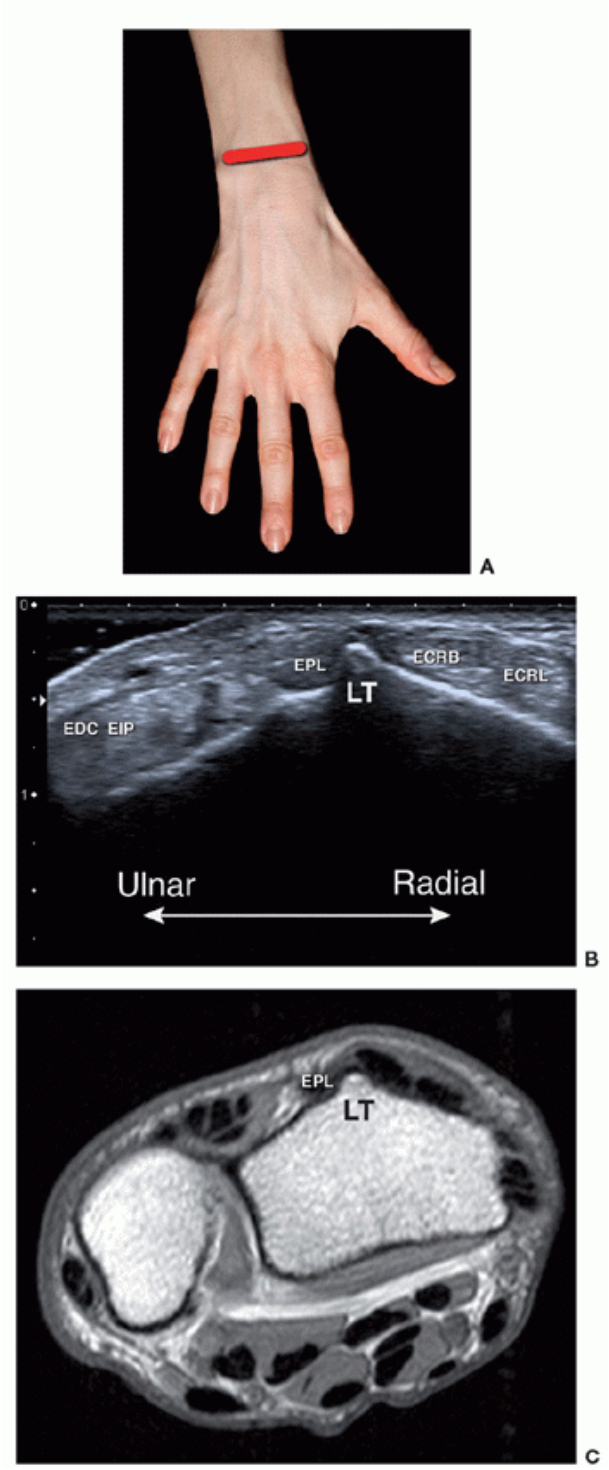


Figure 5.8. Compartments two, three, and four. A: Hand pronated. B: Axial ultrasound: Lister's tubercle (LT) is the bony landmark that separates compartments two (ECRB, ECRL) and three (EPL). ECRL, extensor carpi radialis longus; ECRB, extensor carpi radialis brevis; EPL, extensor pollicis longus; EDC, extensor digitorum communis; EIP, extensor indicis proprius. C: Axial T1 weighted image. EPL lies immediately medial to Lister's tubercle. EPL, extensor pollicis longus.

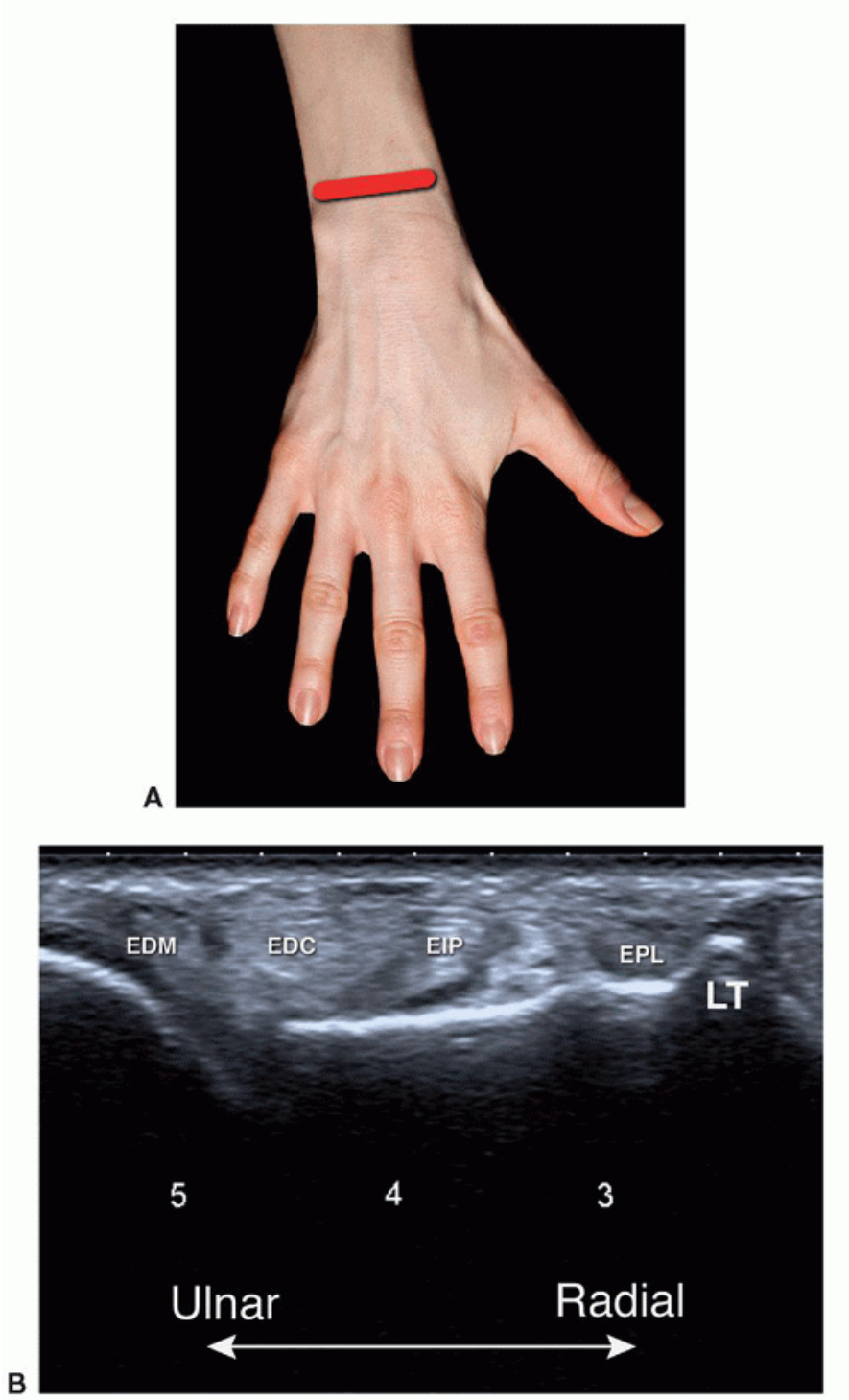


Figure 5.9. Compartment three, four, and five. A: Hand pronated. B: Axial ultrasound image. Moving the transducer ulnar from Lister's tubercle and EPL demonstrates the fourth compartment with the extensor indicis proprius (EIP) and extensor digitorum communis (EDC), and the fifth compartment with extensor digiti minimi (EDM). Moving the fingers can be used to identify individual tendons. EPL, extensor pollicis longus; LT, Lister's tubercle.

Volar Wrist

Carpal Tunnel

The volar wrist is examined with the wrist supinated and slightly extended. The transverse plane is most valuable in identifying the anatomic landmarks. The bony landmarks for the proximal carpal tunnel are the scaphoid tubercle (radial) and pisiform (ulnar). By placing the transducer on these marks, the flexor retinaculum, nine flexor tendons, and MN are demonstrated. (Fig. 5.12) Attention should be paid to possible anomalous muscles in the carpal tunnel. The landmarks for the distal carpal tunnel are the trapezium tubercle (radial) and hamate hook (ulnar) (Fig. 5.13). Adjustment of the orientation of the probe or slight flexion of the wrist can help to optimize imaging.

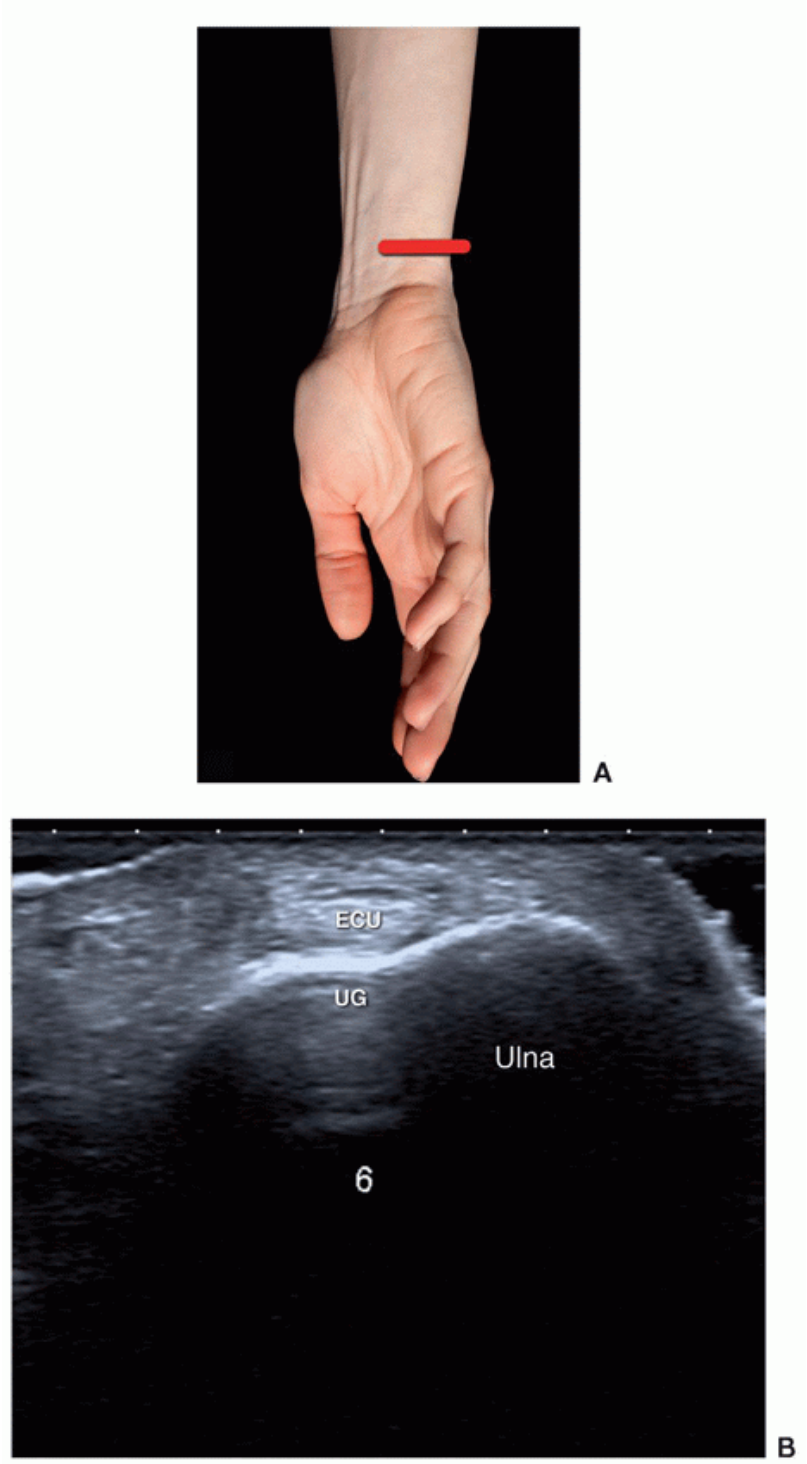


Figure 5.10. Compartment six. A: Extreme pronation of the hand is the ideal position for examining the sixth compartment. B: Extensor carpi ulnaris (ECU) is situated in the ulnar groove (UG).
P. 83

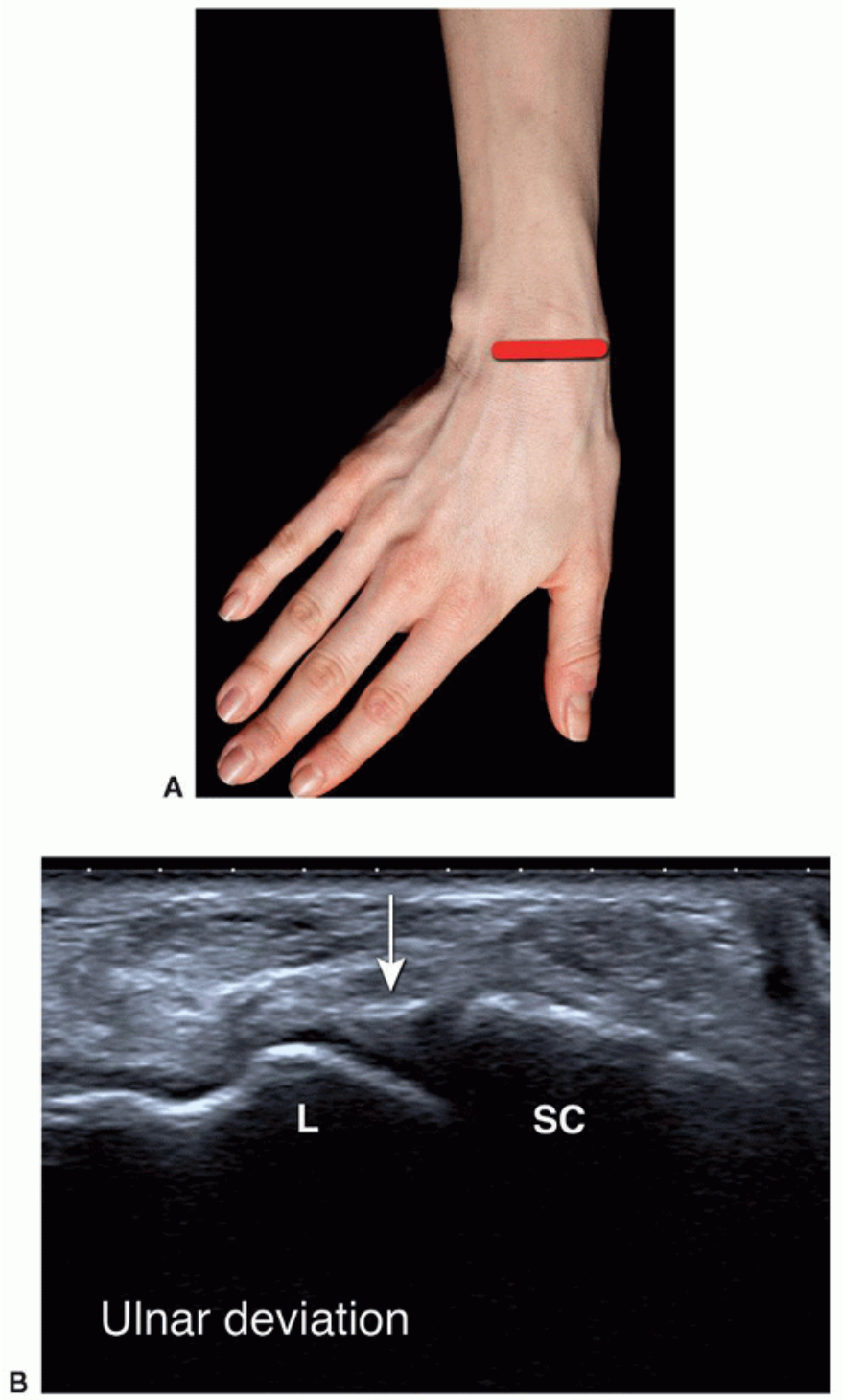


Figure 5.11. Scapholunate Ligament. A: Hand pronated and in ulnar deviation. B: Moving the transducer distally from Lister's tubercle shows the scapholunate ligament as a thin hyperechoic structure (arrow) running between the scaphoid (SC) and the lunate (L).

The MN is identified in the carpal tunnel in the transverse plane by rocking the transducer back and forward. As transducer angulation alters, the tendons change between hypoechoic and hyperechoic due to anisotropy, whereas the MN does not, or at least not to the same degree. On longitudinal scans, the flexor tendons show quite long excursions on finger flexion/extension, whereas the MN has a shorter excursion. Another way to identify the MN is to scan transversely in the mid-forearm and demonstrate the nerve between the muscle bellies of FDS and FDP, then trace the nerve distally to the carpal tunnel. The cross-sectional area (CSA) of the MN can be calculated proximal to and in the carpal tunnel (see section on carpal tunnel syndrome).[5] As it runs distally through

P. 84

the carpal tunnel, the nerve changes shape from oval to more flattened.[3]

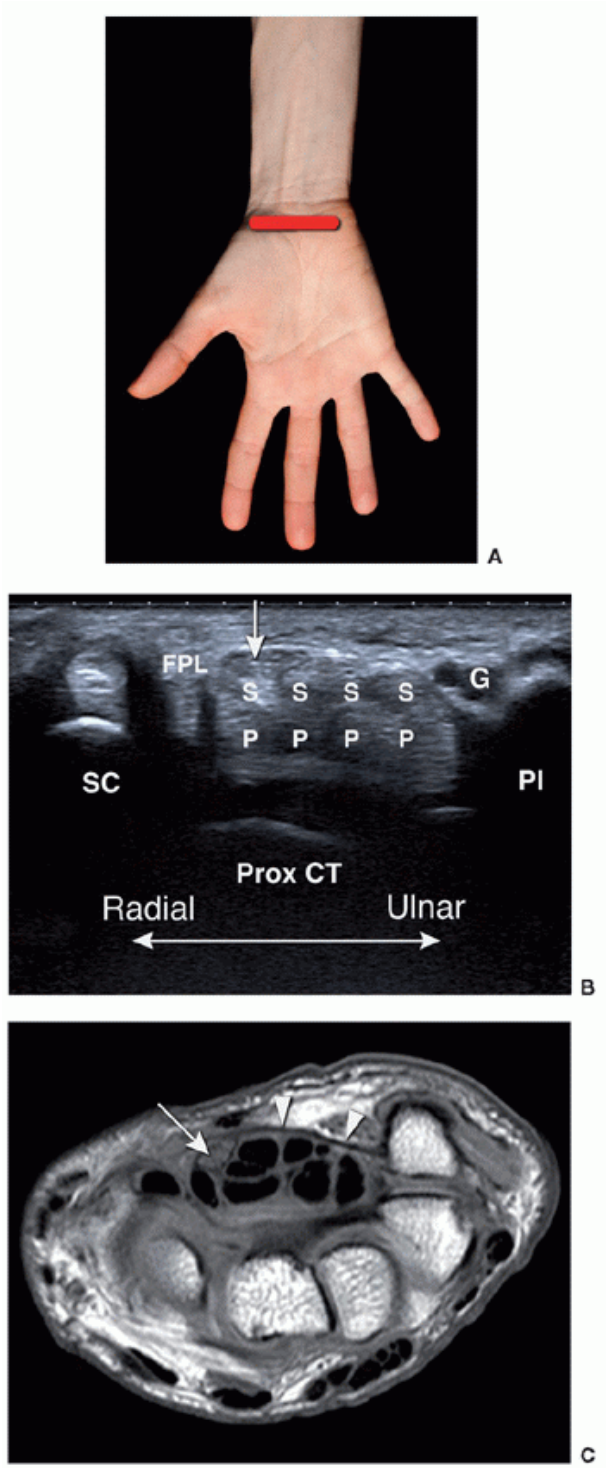


Figure 5.12. Proximal carpal tunnel. A: Hand supinated. B: Axial ultrasound of the proximal carpal tunnel (CT): the bony landmarks are the scaphoid (SC) and pisiform (PI). Arrow, median nerve and nine tendons run in the carpal tunnel: four tendons of flexor digitorum superficialis (S), four tendons of flexor digitorum profundus (P), and the flexor pollicis longus (FPL) radially. Note Guyon's canal (G). C: Axial T1-weighted image of the proximal carpal tunnel. The retinaculum (arrowheads) is the roof of the carpal tunnel. The median nerve (arrow) lies immediately deep to the flexor retinaculum.

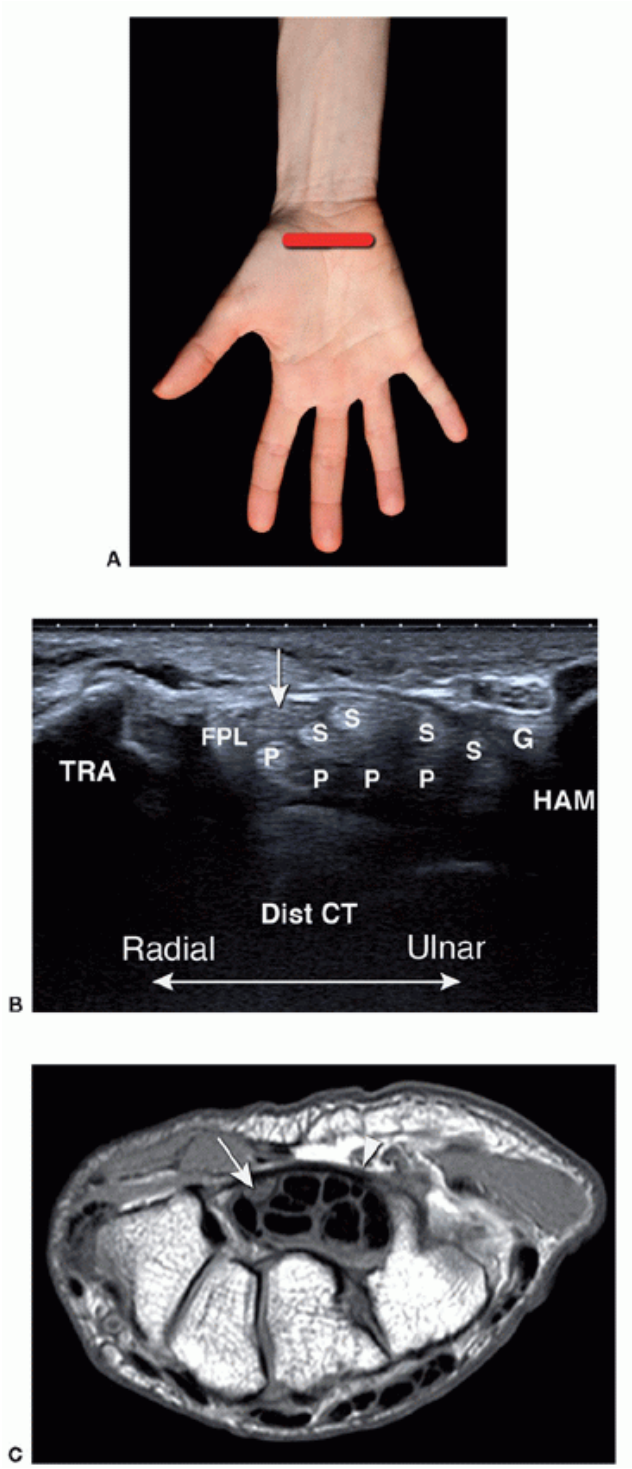


Figure 5.13. Distal carpal tunnel. A: Hand supinated. Axial ultrasound (B) and T1-weighted MR images (C) of the distal carpal tunnel. The bony landmarks are the trapezium (TRA) and the hook of hamate (HAM). The median nerve (arrow) is superficial. G, Guyon's canal; arrowhead, flexor retinaculum.

Potentially important normal variants may occur here such as a persistent median artery and a bifid MN, which may coexist.

Tip:

Use anisotropy to distinguish tendons from the MN by rocking the transducer: tendons change between bright and dark; MN echogenicity does not change as much.

Guyon's Canal

On the volar ulnar side of the wrist, the pisiform is the landmark for Guyon's canal (Fig. 5.14). The ulnar nerve lies between the pisiform and the ulnar artery. Color Doppler demonstrates the ulnar artery and its companion paired veins, which are effaced by pressure and refill when pressure is removed. Moving the transducer distally identifies the division of the ulnar nerve into a superficial sensory branch and a deep motor branch. The hook of hamate is a landmark for the deep motor branch.

Fingers

Abundant gel is essential and allows good contact and visualization. Start the examination in a sagittal plane to get a first impression of the anatomy. Joint fluid is more easily detected dorsally, as the thick volar plate and capsule form a tighter structure,

than the dorsal capsule. The synovial pouch, which extends distally and proximally from the joint, can be filled with fluid. Synovial thickening is less hypoechoic than fluid. Color/power Doppler differentiates between active and chronic synovitis. Appreciate the lateral pouches and collateral ligaments in the axial and coronal planes.

Examination of the flexor tendons starts axially in the palm of the hand, where the superficial and deep tendons are separately identified. Differentiation may be more difficult distally, but tilting the transducer back and forward at the level of the proximal phalanx and PIP joint shows anisotropy affecting the tendons inversely, that is, when FDP is hypoechoic, FDS is echogenic, and vice versa. The two slips of the superficialis tendon insert on the volar aspect and sides of the base of the middle phalanx, separated by the profundus tendon, which inserts distally on the base of the distal phalanx (Fig. 5.15). The distal FDP tendon and its insertion are best examined on longitudinal scans.

Dynamic imaging helps distinguish between superficialis and profundus tears. The transducer is placed sagittally at the level of the metacarpal joint, and passive movement of the PIP or DIP joints shows the tendons moving in the sheath.

The extensor tendons are smaller and more band-like than the flexor tendons and more difficult to examine.

P. 85

P. 86

A small cushion underneath the carpus allows movement and facilitates discrimination between a proximal or distal tendon tear (Fig. 5.16).

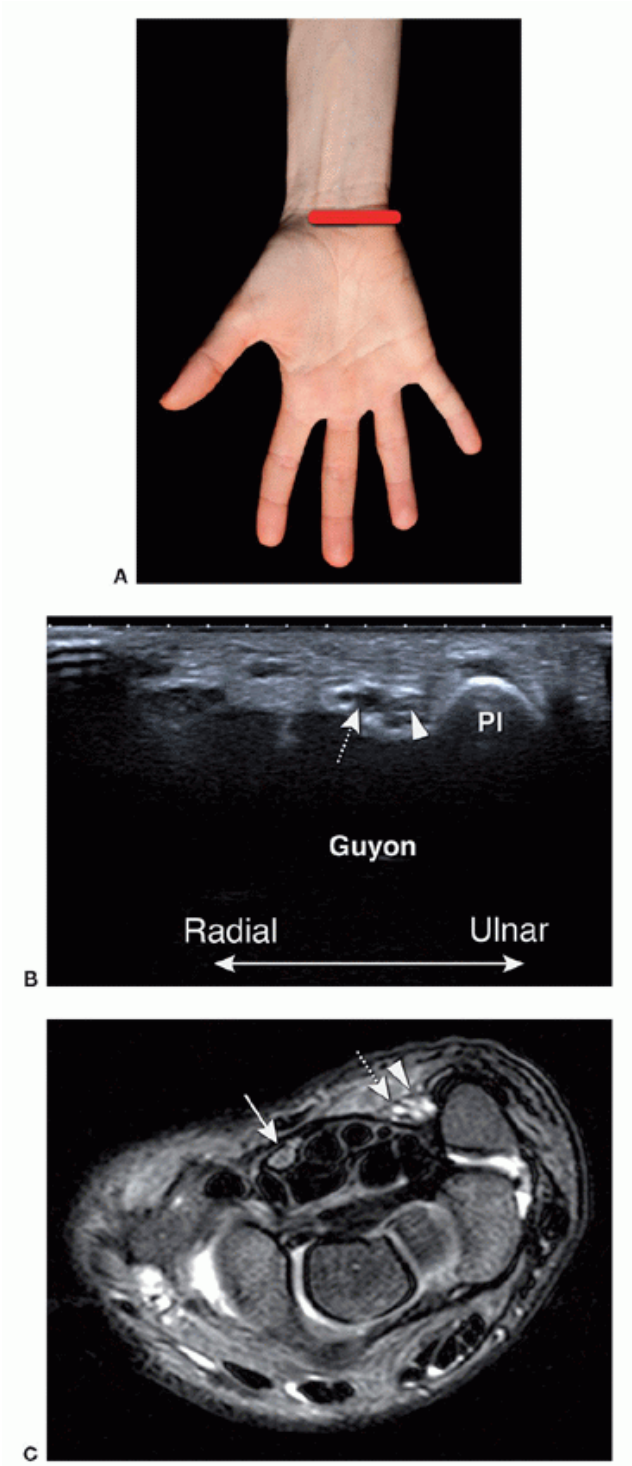


Figure 5.14. Guyon's canal. A: Hand supinated. Axial ultrasound (B) and T2-weighted MR image with fat suppression (C). The pisiform (PI) is the bony landmark. The ulnar nerve (arrowhead) lies radial to the pisiform, the ulnar artery (stippled arrow) more laterally. On MR the flexor retinaculum roofs the carpal tunnel, and the ulnar nerve and artery show high signal intensity; the median nerve (arrow) is superficial to the flexor tendons.

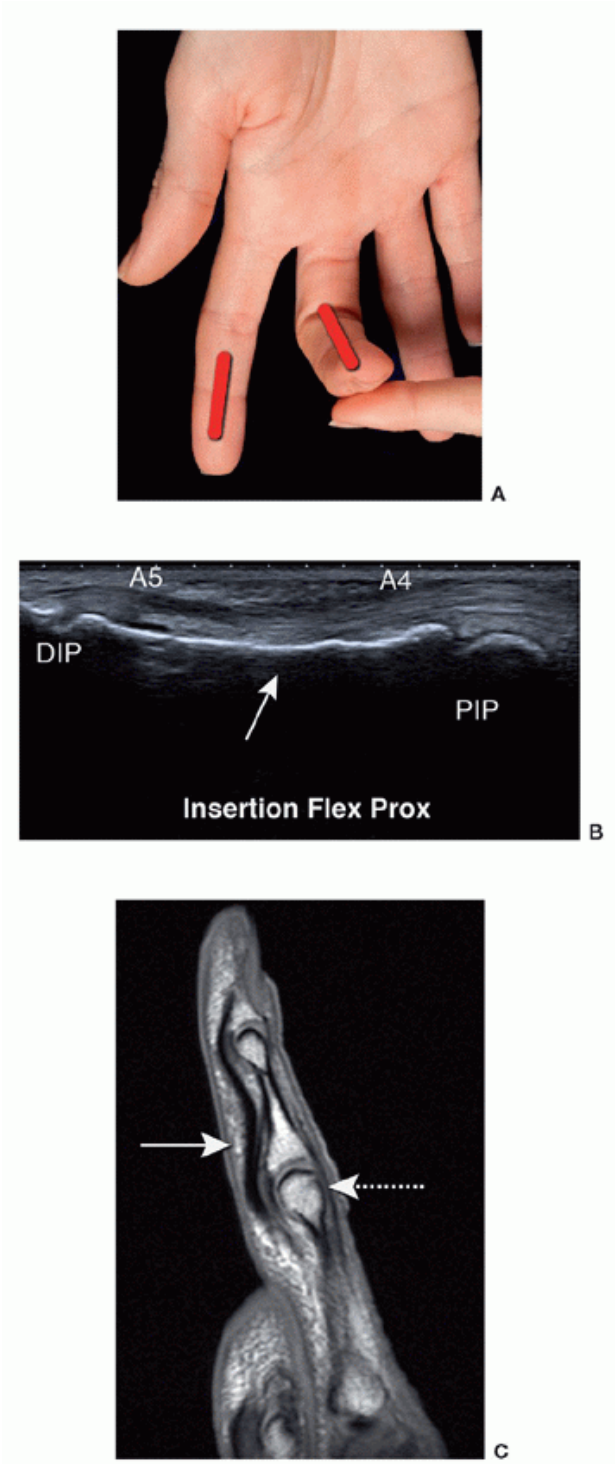


Figure 5.15. Flexor tendons of the finger. A: Flexor tendons are examined with the hand supine and the finger initially extended. B: Longitudinal ultrasound shows the distal insertion of the profundus tendon on the base of the distal phalanx just distal to the distal interphalangeal joint (DIP). The proximal insertion of one of the slips of the flexor superficialis tendon on the base of the middle phalanx is appreciated (long arrow). A5 and A4 are flexor pulleys. C: Corresponding sagittal T1-weighted MR. Note the difference in thickness of the flexor (arrow) and extensor (stippled arrow) tendons.

The synovial sheath of a flexor tendon is normally not visible, although a thin hypoechoic rim <0.1 mm may surround the flexor digitorum tendons just proximal to the A1 and A2 pulleys[3] and has to be differentiated from tenosynovitis.

The five annular pulleys are small hypoechoic linear structures at the level of the MCP (A1), PIP (A3), and DIP (A5) joints and the proximal shaft of the proximal (A2) and mid-shaft of the middle (A4) phalanges (Fig. 5.17). Dynamic imaging shows a pulley tear as an increased distance between the tendon and the bone (bowstringing). The C-pulleys are more difficult to visualize with ultrasound.

The palmar digital nerve branches of the median and ulnar nerves are detected by locating the palmar digital arteries with Doppler. The nerves run alongside the arteries.

Ultrasound of the UCL of the thumb is performed with the hand prone. The transducer is placed lengthwise on the ulnar side of the MCP joint for long-axis scans, and rotated 90 degrees for short-axis images. Imaging is performed at rest. Additional imaging

during flexion and cautious valgus stress can be performed. However, varus and valgus stressing should be employed with caution for fear of aggravating an injury. The normal UCL is hyperechoic and lamellar and extends from the metacarpal head to the base of the proximal phalanx. The deep fibers demonstrate anisotropy and may be hypoechoic. The adductor aponeurosis, a thin hyperechoic band superficial to the UCL, is demonstrated by flexing the interphalangeal joint while scanning in the long axis (Fig. 5.18).

Tips:

Use abundant gel, an "ice cream cone," to maintain contact and avoid excessive pressure. Hypervascularity can be missed using too much pressure.

Use dynamic imaging by flexing and extending the finger to identify a tendon.

If there is fluid in a joint or around a tendon, always use color or power Doppler to identify hypervascularization.

Accessory Muscles

Accessory muscles are frequent incidental findings at the wrist. They have typical locations and are frequently bilateral. Most are asymptomatic, but they may present as soft tissue masses or cause nerve compression in the carpal tunnel or Guyon's canal. Ultrasound shows a mass with similar morphology and echogenicity to other muscles, and dynamic imaging shows muscle contraction, confirming the diagnosis (Fig. 5.19). The most common

P. 87

anomalous muscles include the accessory abductor digiti minimi (AADM), extensor digitorum brevis manus (EDBM), the digastric FDS of the index finger, a proximal origin of the lumbrical muscles and variants of palmaris longus.[8]

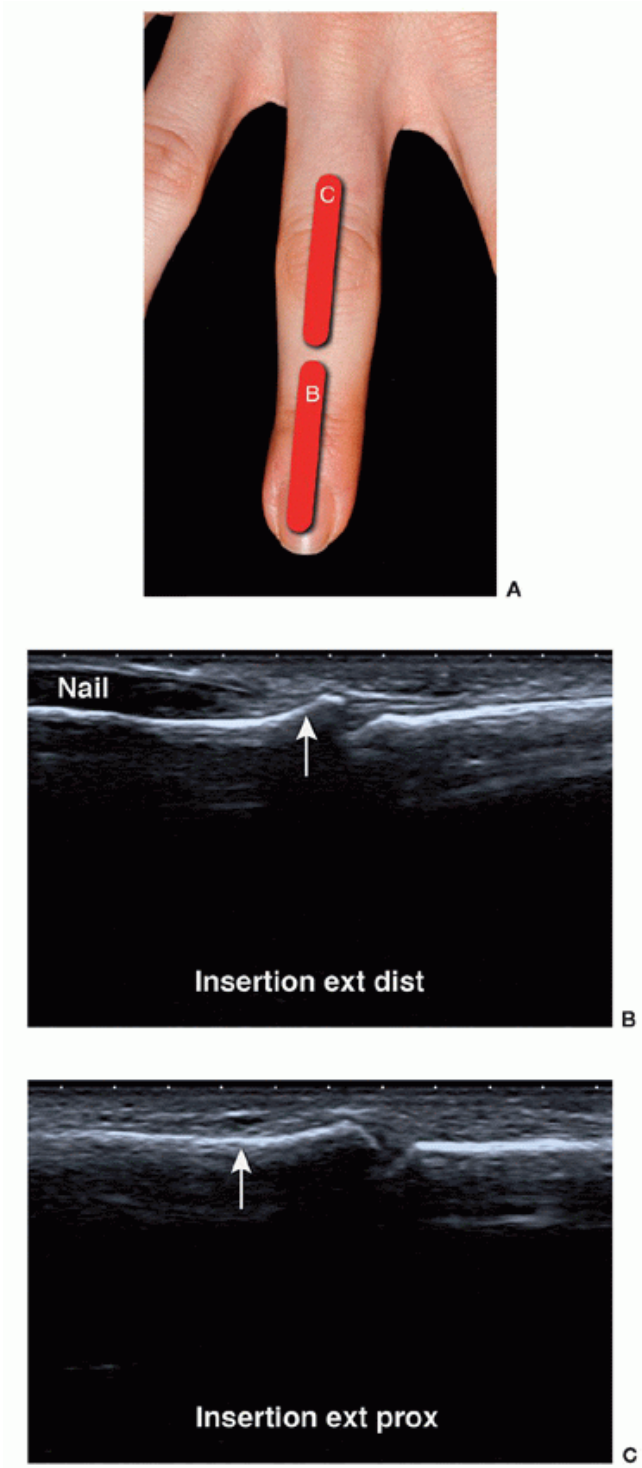


Figure 5.16. Extensor tendons of the fingers. A: Extensor tendons are examined on the dorsum of the finger. B: The lateral slips of the extensor tendon insert on the dorsal aspect of the base of the distal phalanx (arrow). C: The central slip inserts on the base of the middle phalanx (arrow).

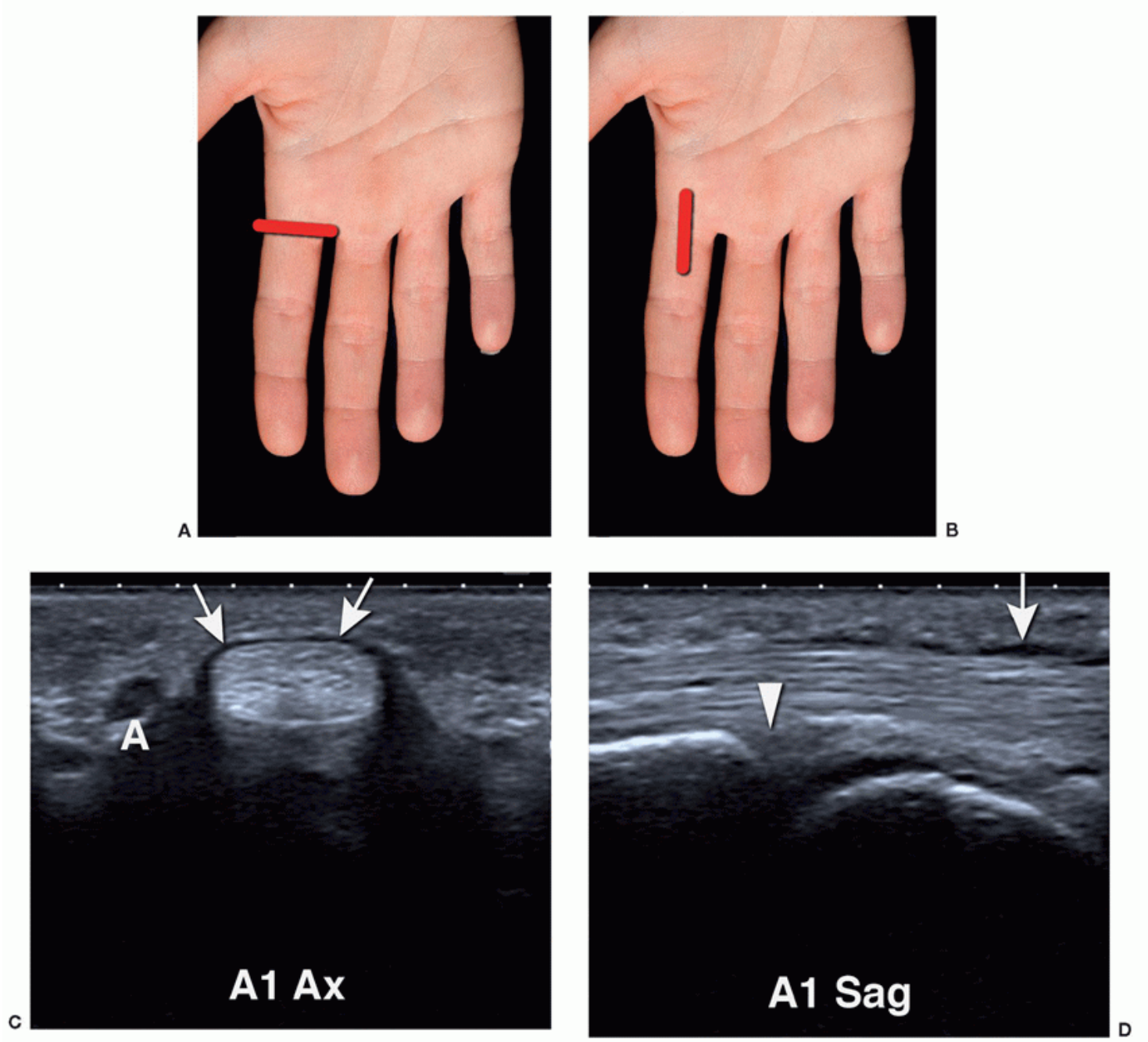


Figure 5.17. A1 Pulley. Transducer position to examine A1 pulley in short (A) and long (B) axis. C, D: The A1 pulley is a thin hypoechoic band (arrows) superficial to the tendon. The volar plate is deep to the flexor tendon (arrowhead). Notice the digital artery (A).

The AADM occurs in 24% to 47% of the normal population and is bilateral in 50% of cases.[9,10] Sites of origin include the palmar carpal ligament, the palmaris longus tendon, and the antebrachial fascia of the forearm. The tendon of AADM inserts with the abductor digiti minimi on the ulnar aspect of the proximal phalanx of the little finger. The pisiform can be used as a landmark in identifying this accessory muscle.[8] Most AADMs are small and asymptomatic, with a mean muscle thickness of 1.7 mm. The size of the accessory muscle (mean thickness 4 mm in symptomatic cases) is an important factor in determining if nerve compression at Guyon's canal is significant.[9]

The EDBM muscle occurs in 3% of individuals and is bilateral in 54% of cases. It lies on the dorsum of



the wrist on the ulnar side of the extensor tendon of the index finger. It originates from the distal radius and posterior radiocarpal ligament and inserts on the index finger, at the level of the metacarpal head, less frequently the long finger.[11,12] It is considered to be a variant of the EIP muscle, and the two are often joined and have the same nerve and arterial supplies and insertion. However, in 40% of individuals with an EDBM muscle, the EIP is absent or hypoplastic.[13,8]

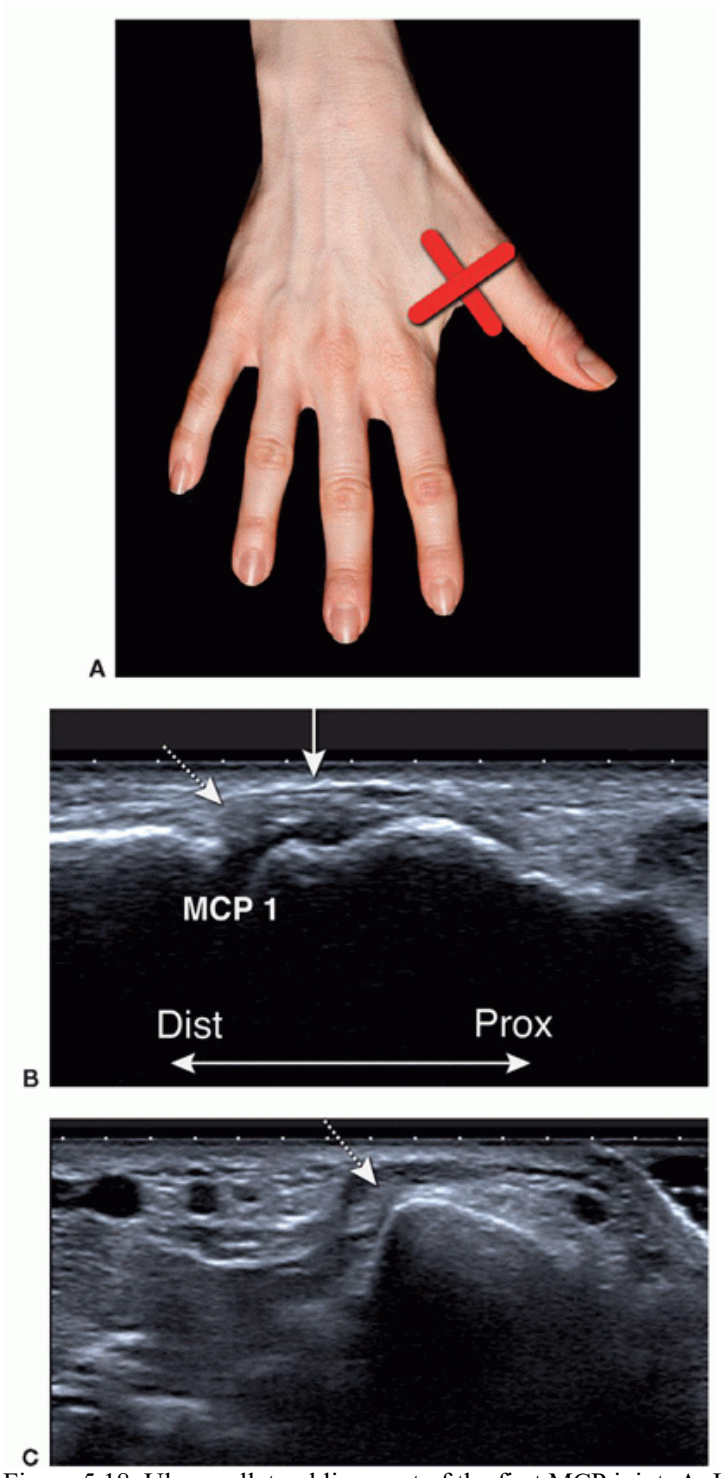


Figure 5.18. Ulnar collateral ligament of the first MCP joint. A: Hand prone. The transducer is placed on the ulnar side of the thumb for long- and short-axis scans. B, C: Long and short-axis scans. The UCL is a hyperechoic band (stippled arrow) spanning the joint. The thin hyperechoic band superficially is the adductor aponeurosis (solid arrow), which can be demonstrated by flexing the interphalangeal joint of the thumb.

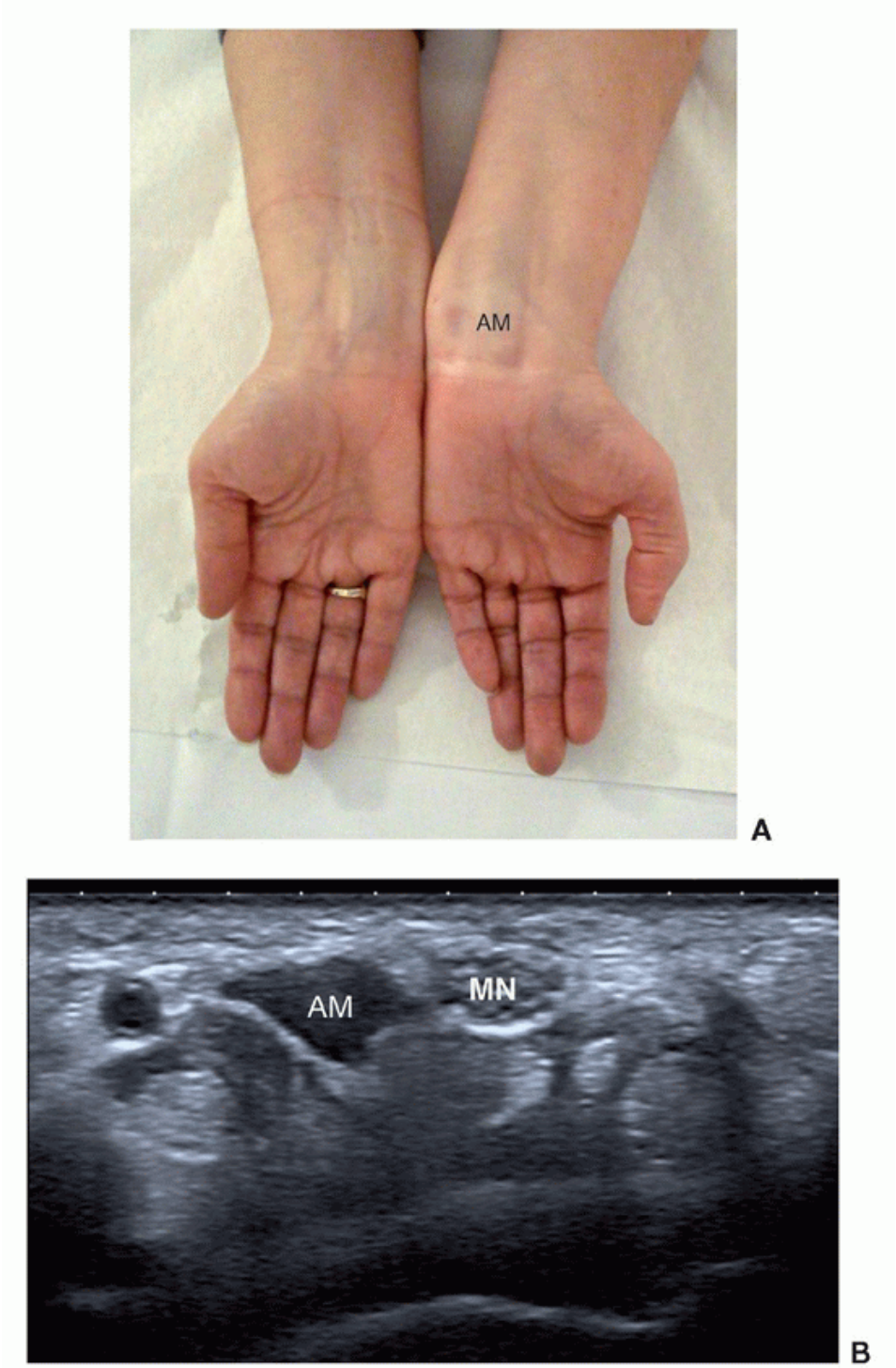


Figure 5.19. Accessory muscle. A: Asymptomatic mass at the left wrist. B: Axial ultrasound shows a hypoechoic mass consistent with an aberrant muscle proximal to the carpal tunnel. On dynamic imaging, the muscle moves with the index finger. AM, aberrant muscle; MN, median nerve.

The anomalous belly of the FDS muscle in the palm of the hand is usually related to the index finger. The anomalous muscle can be seen in the carpal tunnel and can cause carpal tunnel syndrome (CTS) or it can be appreciated as a mass at the base of the index finger.[14],[15] The muscle can be seen moving distally in or into the carpal tunnel on finger extension and proximally when the fingers are flexed. Comparison with the opposite side may be helpful.

P. 89

A proximal origin of the lumbrical muscles inside the carpal tunnel is seen in 22% of individuals and may cause CTS. Normally, the lumbricals arise from the FDP muscle and insert on the radial aspect of the extensor expansion at the level of the proximal phalanx.[8],[16] As with the anomalous FDS, dynamic imaging may be helpful.

Palmaris longus tendon anomalies include variants of its insertion deep to the retinaculum and a distal belly. Both can cause compression of the MN in the carpal tunnel. An accessory palmaris longus can compress the ulnar nerve during repeated contractions.[17] A hypertrophied palmaris longus muscle has also been reported.[18]

## TENDONS

### Tenosynovitis

Inflammation of the synovial lining of tendon sheaths can be caused by mechanical overload due to sporting or occupational activities, mechanical irritation due to bony spurs or orthopedic material, infection, or rheumatologic diseases. Tenosynovitis is common in rheumatoid arthritis (RA),[19] and typically involves flexor digitorum, extensor digitorum, and extensor carpi ulnaris. Tenosynovitis of ECU may be an early manifestation of RA.[20],[21],[22] Ultrasound shows the tendon surrounded by hypoechoic fluid in the tendon sheath. Hyperemia on color or power Doppler indicates active inflammation (Figs. 5.20 and 5.21). Chronic disease shows synovial hypertrophy with (Fig. 5.20) or without (Fig. 5.21) hypervascularization (Fig. 5.22).

Increased flow indicates disease exacerbation.[23] Retinacula may be thickened.[24]Tendons may appear normal in tenosynovitis, but may become swollen and hypoechoic in chronic disease.[25] Intra- and peritendinous vascularity may be detected. Rheumatoid nodules may be located centrally in the tendon or superficially attached to the tendon and particularly involve flexor tendons.[26] Scanning while moving the finger shows if the mass is in or attached to the tendon. Rocking the transducer on axial ultrasound also helps. Normal tendons show anisotropy. Pannus does not. Chronic RA may result in a partial or complete tendon tear, most often involving the extensor tendons of the ring and little fingers at the level of the wrist. Peritendinous effusion, hyperemia, soft tissue thickening, and cortical erosions may be seen.[27]

Tips:

In the presence of synovial hypertrophy, always use color Doppler to appreciate the presence or absence of hypervascularization, indicating active or chronic synovitis.

Rocking the transducer while scanning in the axial plane will show anisotropy of normal tendons. It can help in differentiating from pathology.

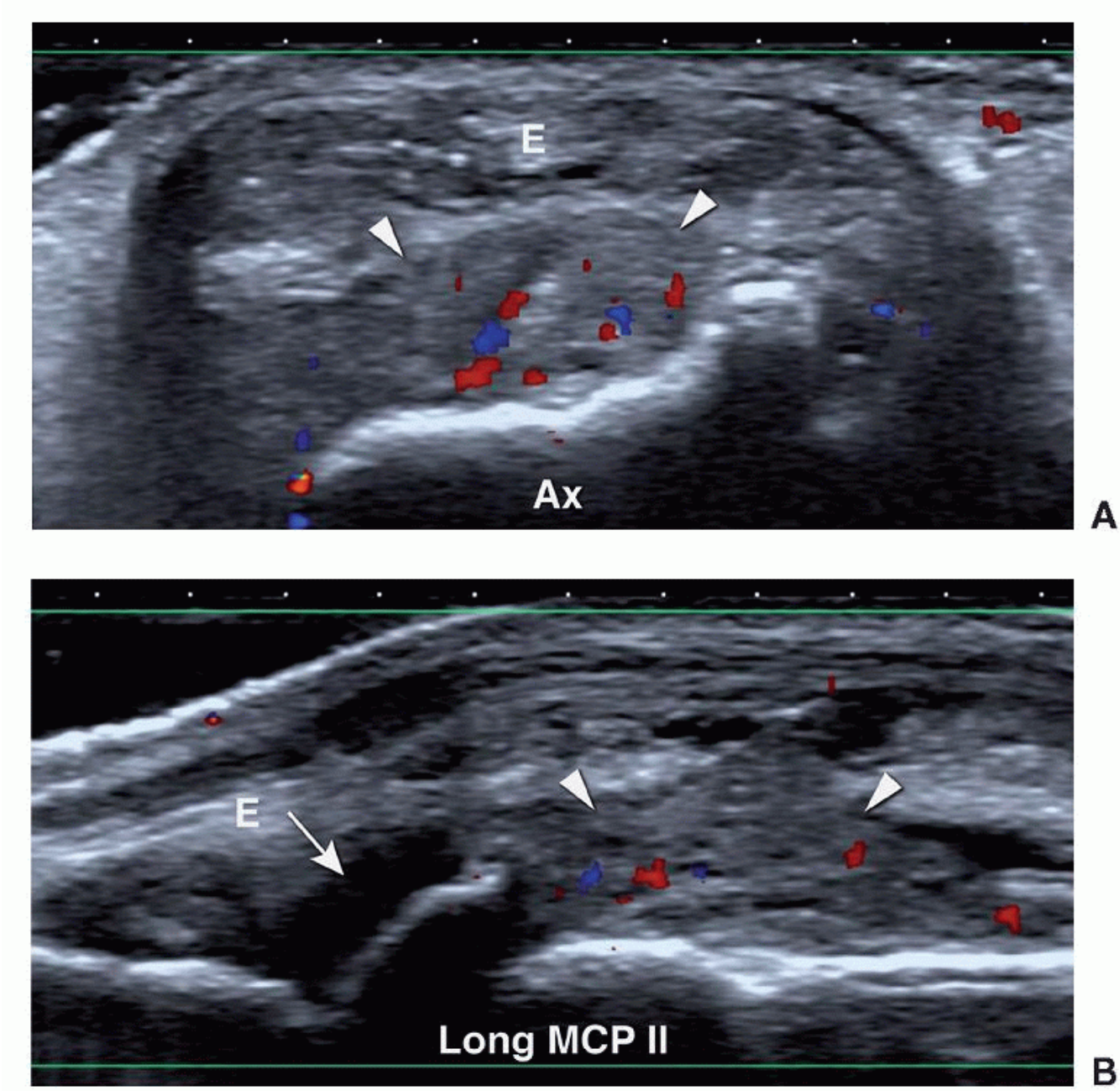


Figure 5.20. Rheumatoid arthritis. Axial (A) and longitudinal (B) images of the dorsal aspect of the MCP joint of the long finger. Synovial hypertrophy and hypervascularization (arrowheads) indicate active synovitis. There is a small amount of fluid (arrow). The tendons (E) are elevated by the synovium and are thickened and surrounded by fluid in keeping with tenosynovitis.

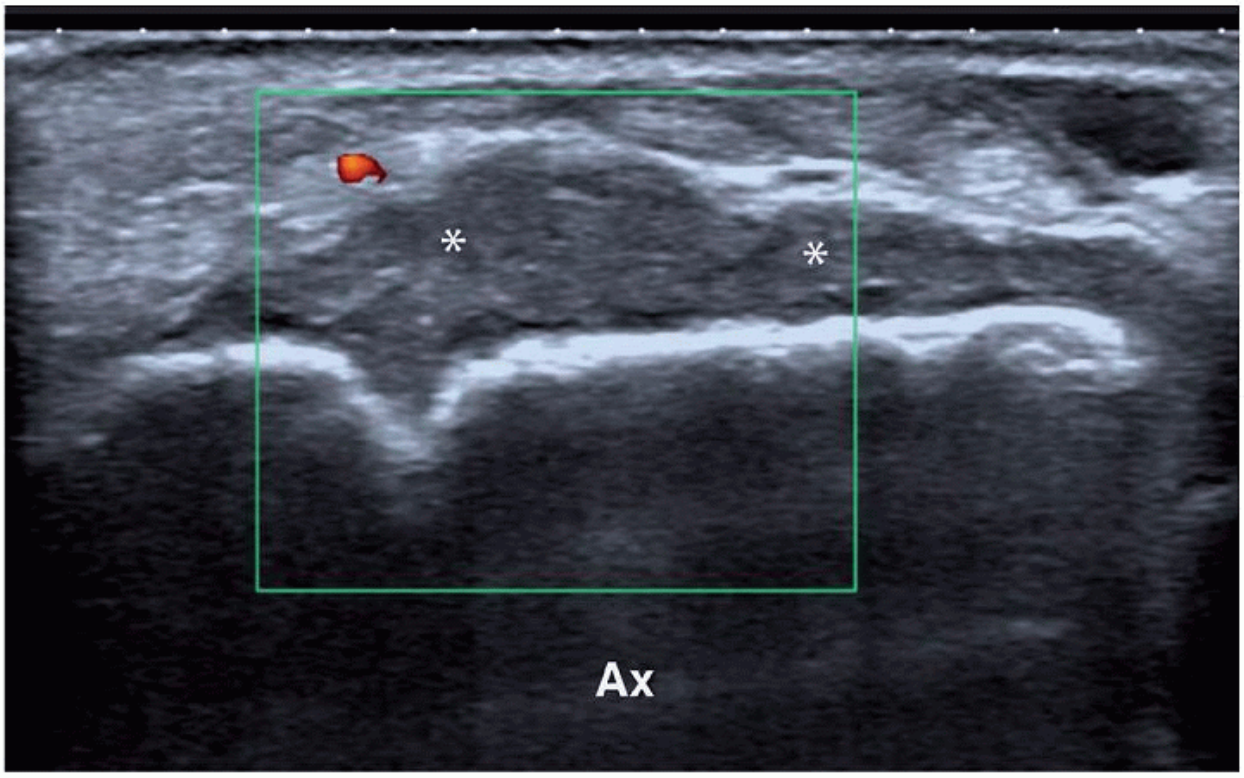


Figure 5.21. Chronic RA. Axial image of the dorsum of the wrist showing thickened synovium (asterisks) without hypervascularization in chronic RA.

The distribution of tenosynovitis depends on anatomy. For instance, at the dorsal wrist the tendons run in six separate compartments, which may be individually affected (Fig. 5.23), and fluid does not extend distally to the fingers. The flexor tendons in the carpal tunnel communicate with the palm of the hand and the little finger only, whereas the radial bursa surrounds the flexor pollicis longus, and tenosynovitis can be seen extending distally in the thumb. Fluid may accumulate proximal and

P. 90

distal to retinacula and pulleys producing a lobulated appearance (Figs. 5.24 and 5.25).

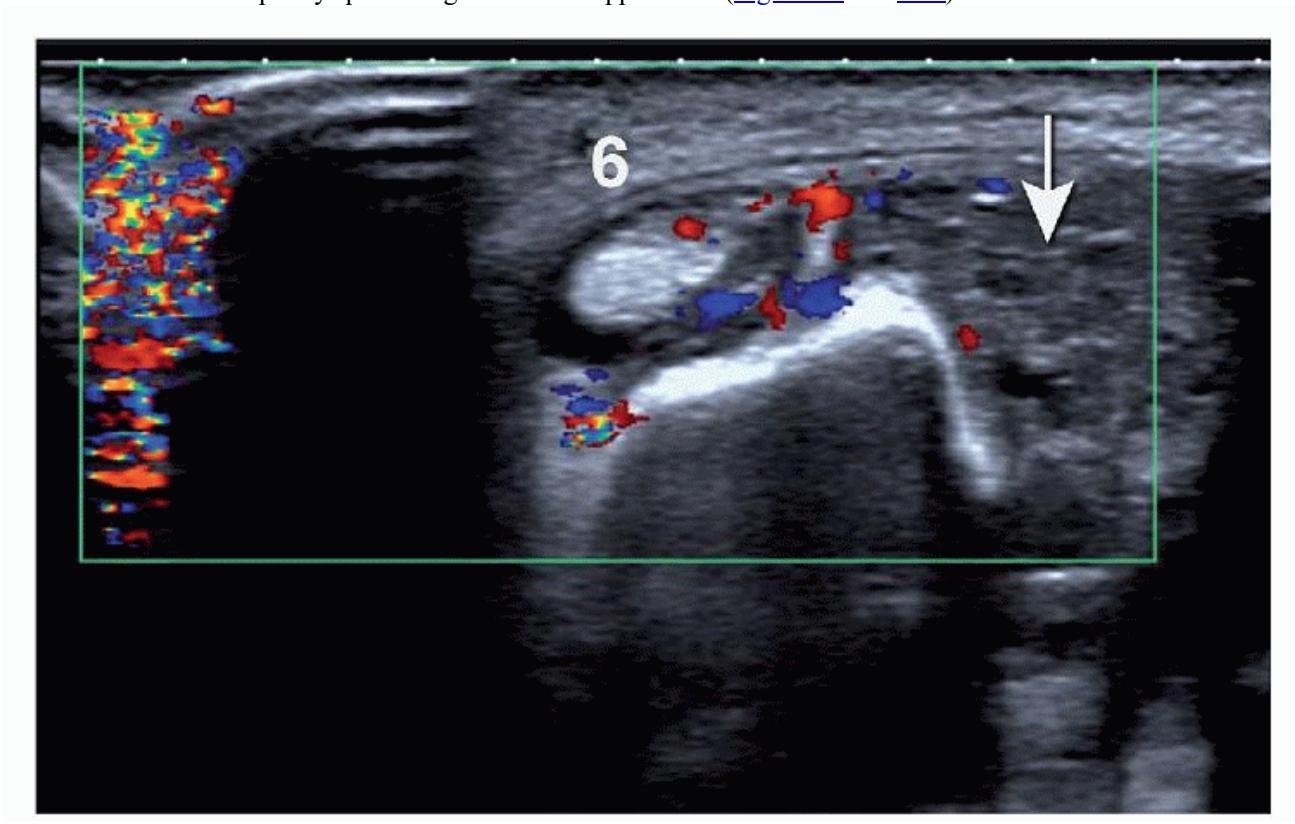

Figure 5.22. Axial image of ECU demonstrating active synovitis of the ulnocarpal joint (arrow) extending into the ECU tendon sheath.

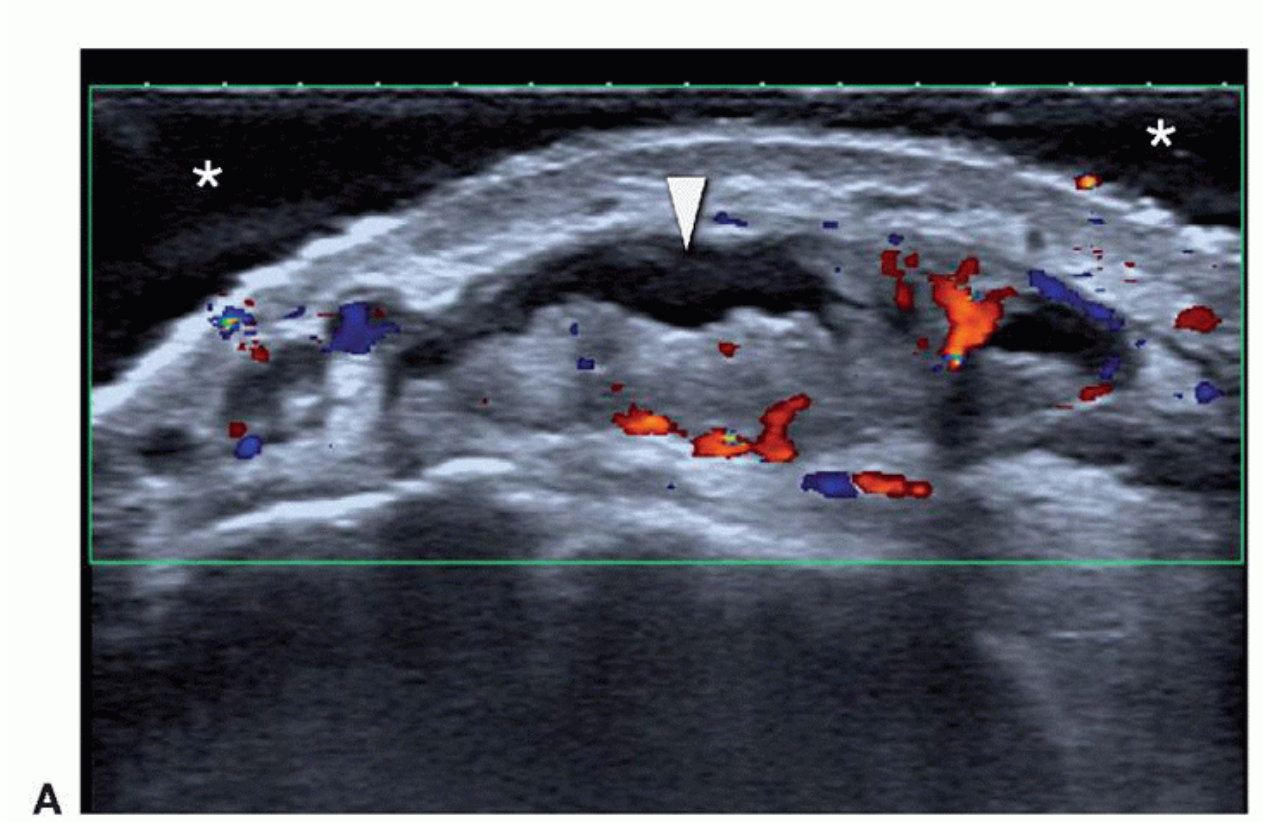


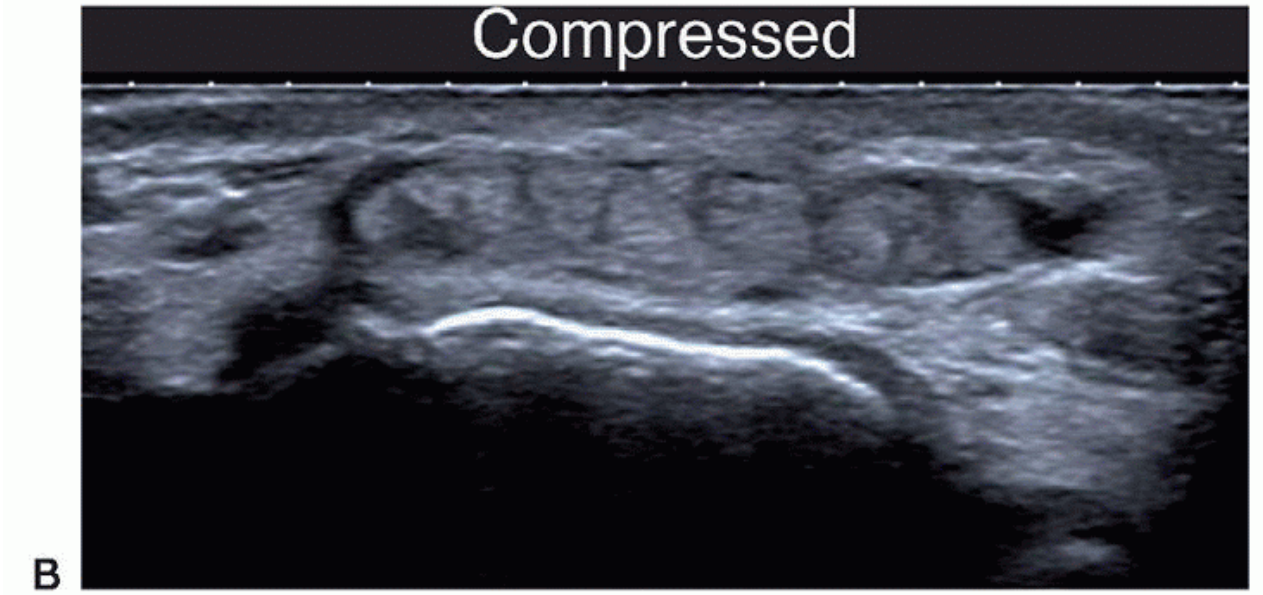


Figure 5.23. A, B: Axial ultrasound images of the dorsal wrist showing fluid (arrowhead) and hypervascularization around the tendons of compartment four, consistent with tenosynovitis. Compression (B) displaces the fluid, confirming that it is not pannus. The Doppler signal is effaced; therefore, abundant gel and light pressure should be used to avoid missing hypervascularity.
Flexor carpi ulnaris and palmaris longus are the only tendons at the wrist without synovial sheaths, and therefore they cannot be affected by tenosynovitis. Flexor carpi ulnaris may be affected by calcific tendinitis. Rupture of the calcium into adjacent soft tissues results in acute, severe pain and erythema in the region of the pisiform. Standard radiographs are often normal, but an oblique radiograph shows soft tissue calcification. Ultrasound shows echogenic foci of calcification and may also show hyperemia in the soft tissues adjacent to the tendon.

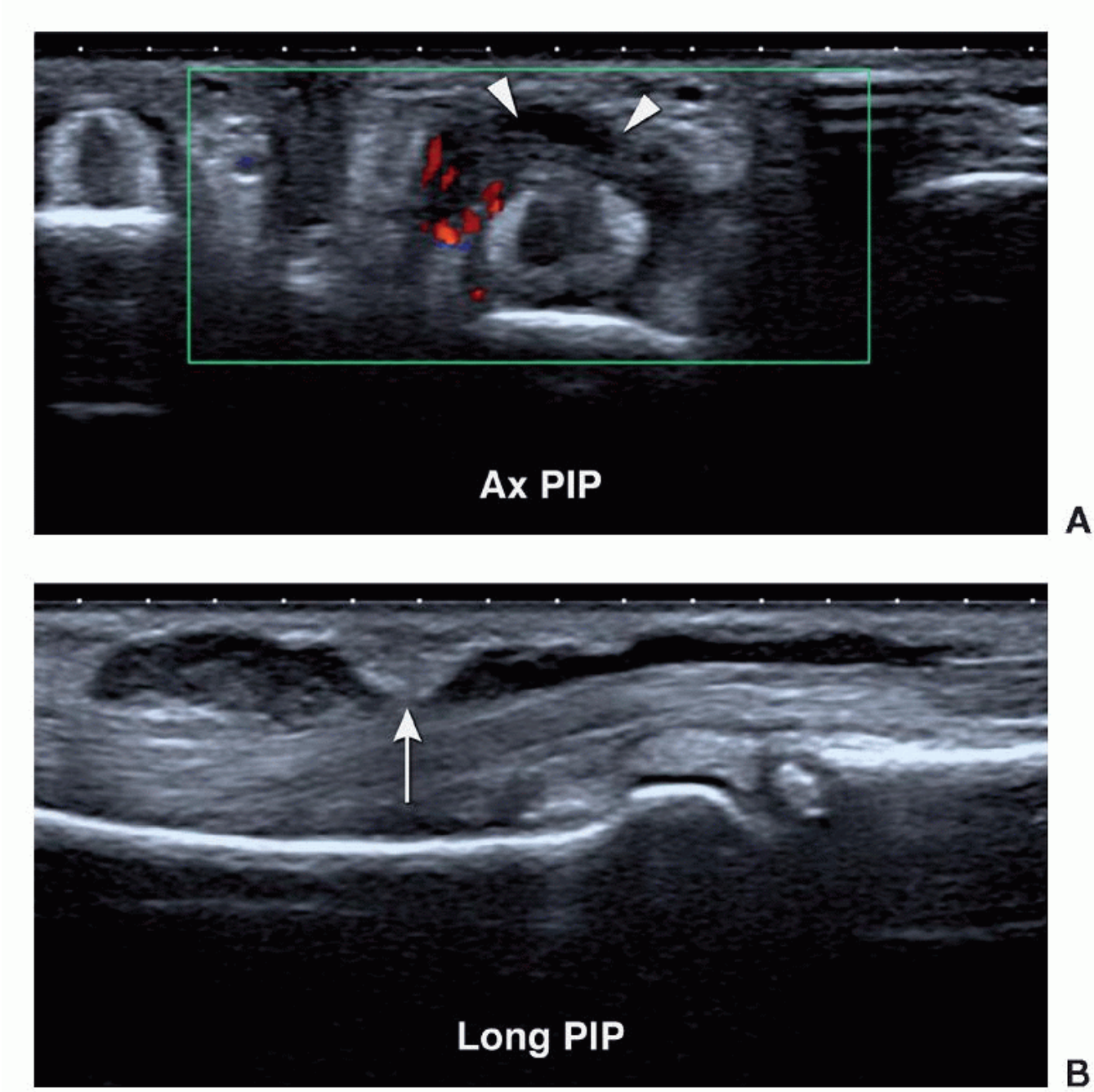


Figure 5.24. Flexor tenosynovitis. Axial (A) and longitudinal (B) ultrasound images demonstrate synovial thickening (arrowheads) of the tendon sheath and vascularization due to tenosynovitis. The FDP tendon is hypoechoic in A due to anisotropy and is surrounded by the echogenic FDS slips. The A2 pulley indents the tendon sheath (arrow). PIP, proximal interphalangeal.

DeQuervain Disease

DeQuervain tenosynovitis involves the first extensor compartment and presents with pain and swelling on the lateral aspect of the wrist. It is usually a clinical diagnosis. The tendons are thickened and surrounded by a hypoechoic mass of synovium (Fig. 5.26) with increased vascularity on Doppler ultrasound. The retinaculum may also be thickened. A vertical septum dividing the compartment into two tunnels[28] may be seen and may cause failure of steroid injections performed without image guidance. Ultrasound confirms the diagnosis and can ensure correct needle placement, avoiding intratendinous injection.[29]

Intersection Syndrome

Intersection syndrome occurs where the first extensor compartment crosses superficial to the second extensor compartment. Overuse due to repetitive flexion and extension of the wrist is seen in sports such as rowing ("oarsman's forearm") and weight lifting. Clinically,

P. 91

intersection syndrome mimics de Quervain disease, which is more distal (Fig. 5.26).

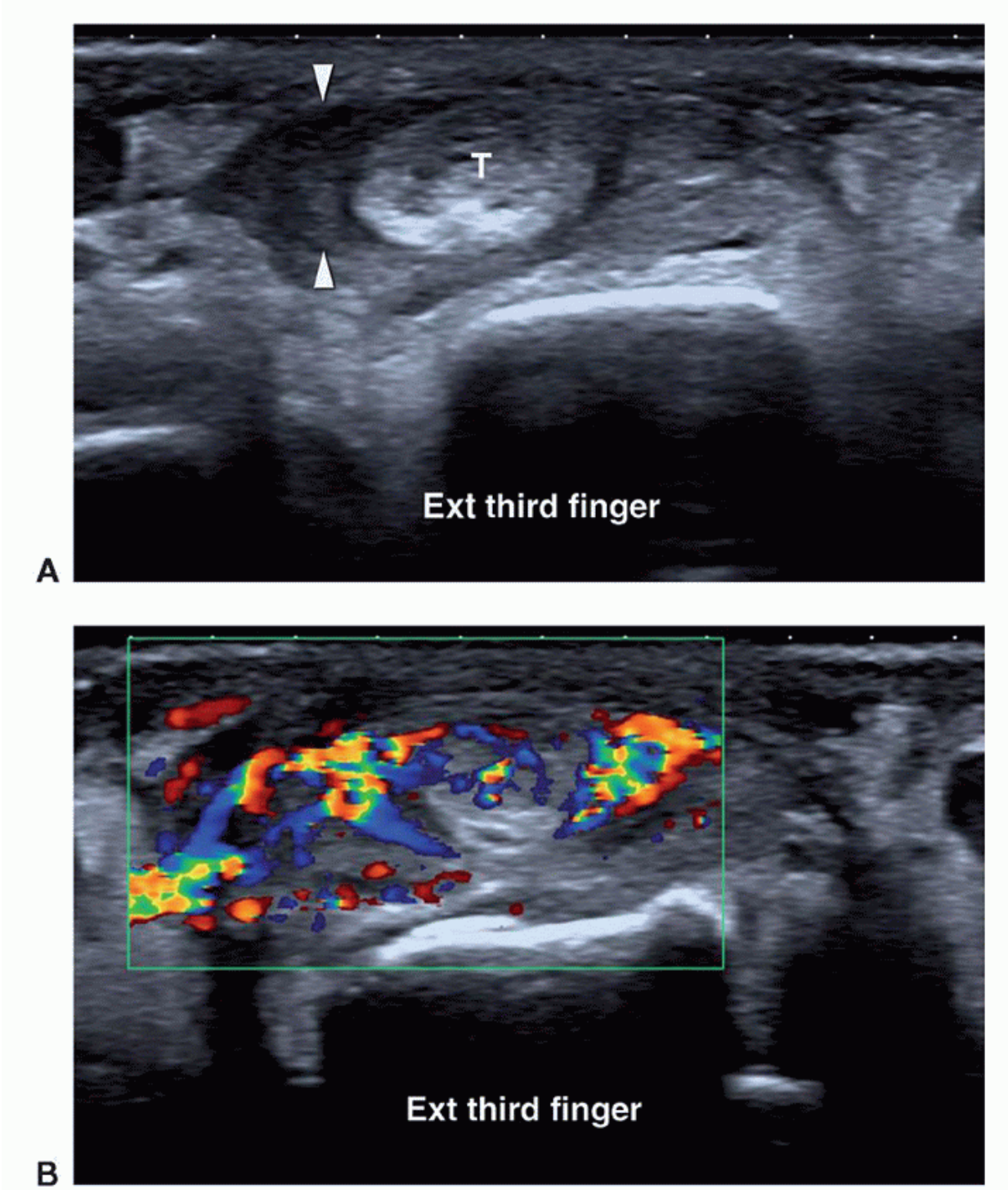


Figure 5.25. Extensor tendinitis. A: Axial image of extensor tendon (T) at the level of the proximal phalanx. The tendon is thickened and surrounded by hyper and hypoechoic tissue (arrowheads). B: Color Doppler shows hypervascularization in the tendon and surrounding soft tissues. The extensor tendons do not have a tendon sheath at the level of the fingers.

Ultrasound shows fluid in the tendon sheaths at the crossing point several centimeters proximal to Lister's tubercle. The two compartments are less well defined than usual, and there is an intervening hypoechoic area due to local soft tissue edema.[3] More distally, where the third extensor compartment crosses over the second compartment, a distal intersection syndrome or decussation syndrome can be caused by bony spurs secondary to degeneration or fracture. Minimal amounts of loculated fluid, fascial or soft tissue edema, and tendon abnormalities, including tenosynovitis and tendon tears, may be found.[30]

Tendon Tears

Ultrasound can confirm if a tendon is torn and define the exact location of the tendon stumps, providing essential preoperative information for the surgeon (Fig. 5.27).

Tendon tears result from chronic tendinosis, acute or repetitive trauma, inflammatory arthropathy, steroid injections, and as side effects of drugs such as chloroquinolones.[31] Repetitive trauma may be occupational, sporting, or the result of mechanical irritation from a fracture fragment, callus, or orthopedic hardware (Fig. 5.28). Tendon rupture is a recognized complication of distal radius fracture and has an incidence of 0.2% to 3%.[31]

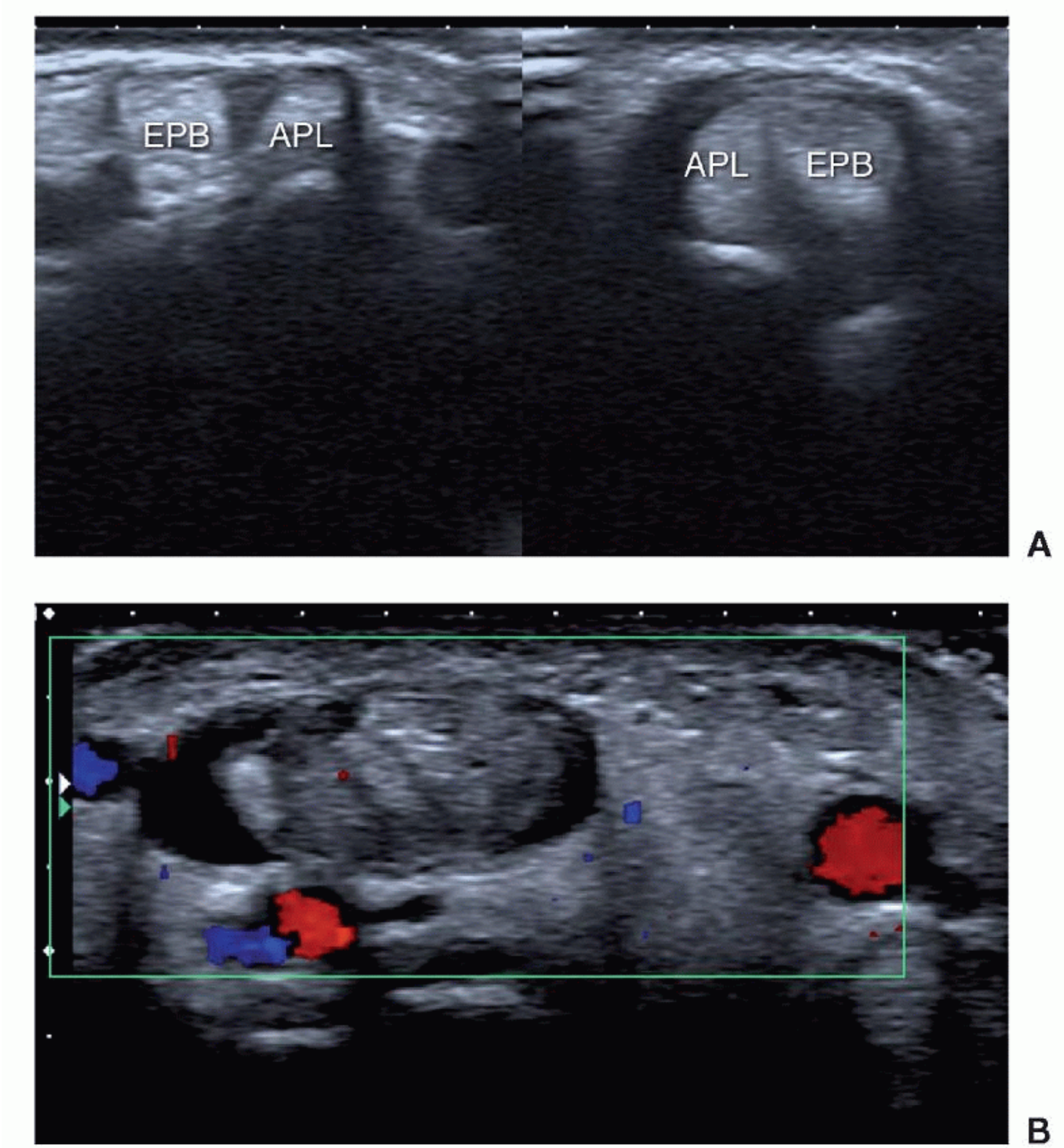


Figure 5.26. Two examples of de Quervain tenosynovitis: one with predominant synovial thickening (A) and the other with fluid (B). A: Axial images of the wrists demonstrate thickening of the right extensor pollicis brevis (EPB) and abductor pollicis longus (APL) tendons (on the right of the image) that are surrounded by hypoechoic synovium. The left side is normal. B: Axial image of the left wrist shows thickened EPB and APL tendons surrounded by fluid.

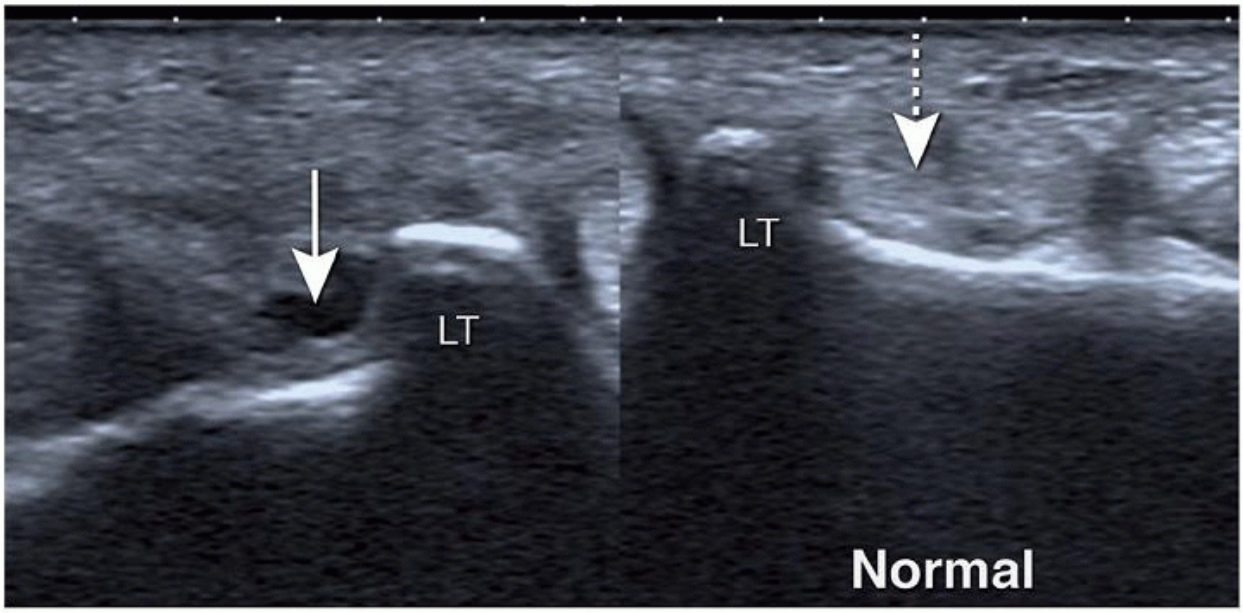


Figure 5.27. Extensor pollicis longus tendon tear. Axial ultrasound image of the right wrist at Lister's tubercle (LT) shows fluid (arrow), but no tendon in extensor compartment three. Echogenic EPL tendon is present on the other side (stippled arrow). Loss of normal tendon structure can be identified with ultrasound. Chronic tendinosis causes focal tendon
P. 92

thickening and reduced echogenicity and may be complicated by a partial or complete tear.

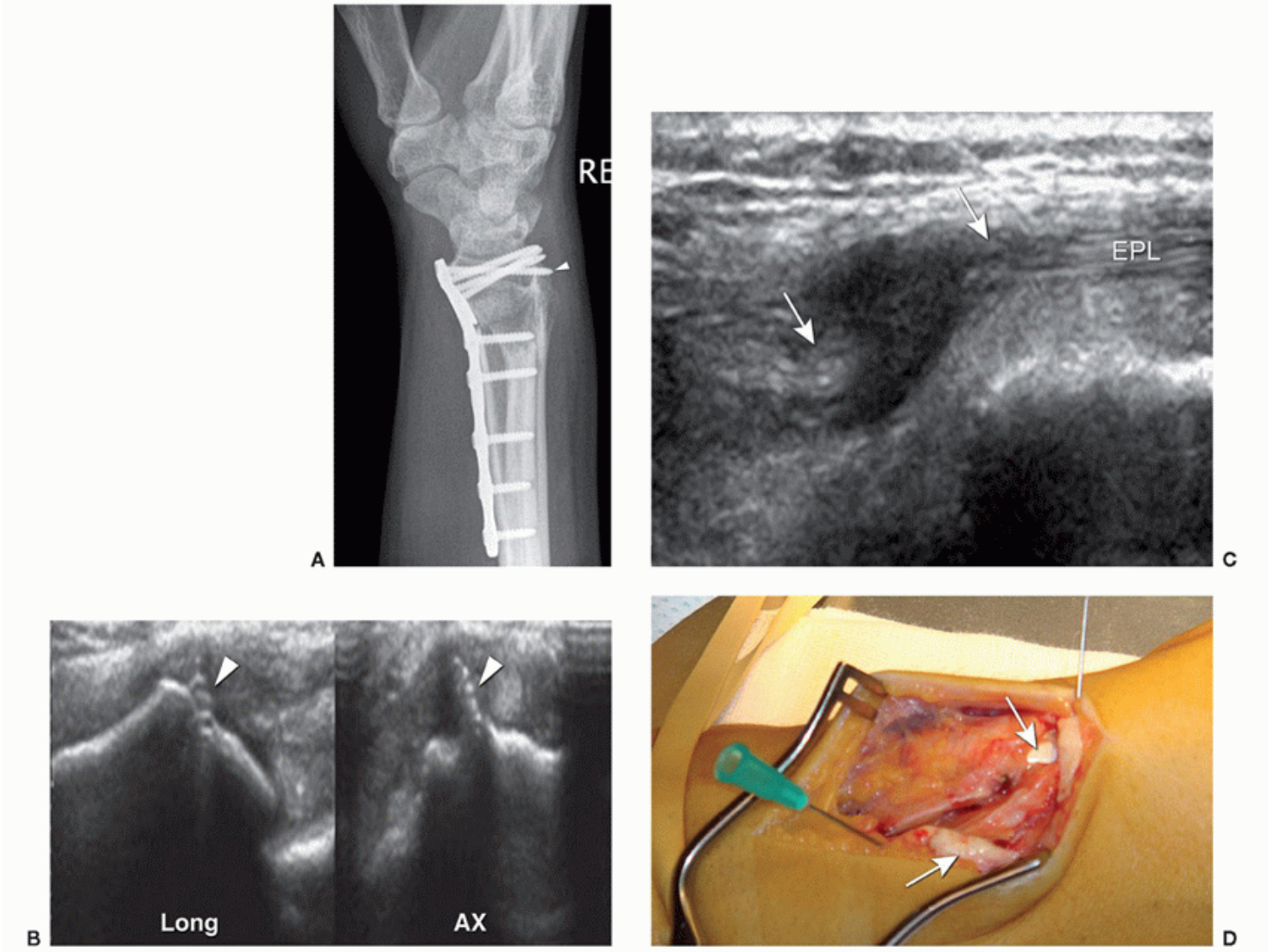

Figure 5.28. Extensor pollicis tendon tear due to screw. A: Lateral radiograph of the wrist shows volar plate fixation of a distal radial fracture. One of the screws protrudes through the dorsal cortex (arrowhead). The patient presented with sudden loss of extension of the thumb. B: Ultrasound shows the protruding screw (arrowheads). C: Longitudinal ultrasound shows a complete tear of EPL. A fluid-filled defect lies between the torn ends (arrows) of the tendon. D: Operative photograph showing the edges of the tear (arrows).

The tendons on the dorsum of the wrist are vulnerable to injury due to their superficial location. The EPL tendon is the most frequently ruptured tendon. The clinical diagnosis is usually clear as the patient is unable to extend the distal phalanx of the thumb. However, ultrasound can identify the position of the two tendon ends and help plan surgery. Typically, at the level of Lister's tubercle, a fluid collection is identified in the tendon sheath instead of the tendon (Fig. 5.27), but the gap may be filled with fluid, debris, or residual fibers. The tendon ends may be thickened, stump-like, and displaced from the site of the tear. Histological examination shows that the tendon is degenerate and that inflammatory changes are present.[32] Ultrasound, computed tomography (CT), or MRI can be used to identify tendon tears. Ultrasound has a distinct advantage in the presence of orthopedic hardware (Fig. 5.28). The torn tendon is often reconstructed using the EIP.

Distal extensor tendon tears cause typical deformities. Mallet finger is a flexion deformity of the DIP joint caused by rupture at the tendon insertion. Ultrasound shows discontinuity of the extensor tendon, fluid in the tendon sheath at the insertion site, and tendon retraction. Mallet finger due to avulsion of the bony insertion of the extensor tendon is diagnosed on radiographs. Rheumatoid arthritis and osteoarthritis may cause similar joint deformities due to extensive inflammation of the synovium in the DIP joint or osteophytes.[33] Ultrasound easily demonstrates hypervascular synovial hypertrophy.

P. 93

A boutonniere deformity is typical of rupture of the extensor tendon at its proximal insertion site on the base of the middle phalanx. On longitudinal scanning the central slip is ruptured, and fluid is seen in its place. The lateral slips continue distally and are probably better demonstrated by transverse scans. Dynamic scanning with the finger passively flexed and extended is necessary to appreciate the presence of a rupture or differentiate a partial from complete tear.[3] Extensor tendon tears are treated by splinting or by surgery if there is a large bony fragment.

Subluxation of the extensor tendon should be considered if the tendon is not found in its expected position on longitudinal scanning. This results from injury to the sagittal bands (boxer's knuckle) located at the MCP joint.[34] Transverse scanning, particularly during flexion and extension, shows tendon instability. The tendon itself appears normal or slightly swollen and hypoechoic. The sagittal band is hypoechoic and thickened, and minor hyperemia may be present. Complete rupture of the sagittal band results in frank tendon dislocation. The index and little fingers have two extensor tendons that may dislocate in opposite directions.

Tip:

Dynamic scanning of the finger with passive and active movements helps to diagnose a tendon tear and differentiate a partial tendon tear from a complete tear.

Flexor tendon tears are less common than extensor tears. Clinical examination shows loss of function, although pain and swelling from other causes may present with impaired or absent function. This is not unusual after tendon repair. Ultrasound shows loss of fibrillar pattern and a gap at the rupture site. In the acute phase, fluid fills the tendon sheath. In a chronic tear, hyperechoic fibrinous material can be appreciated in the sheath.[35] The tear ends may retract, often over quite long distances, and ultrasound is especially helpful in locating the two stumps preoperatively. Partial tears may be difficult to diagnose and appear as focal hypoechoic areas.

Distinguishing superficial from deep flexor tendon tears requires appreciation of the normal anatomy (Fig. 5.3). Dynamic imaging, transverse scanning, and comparison with another finger may help. The commonest site of a flexor tendon tear is distally, due to traumatic avulsion of the FDP tendon (jersey finger), when an actively flexed DIP joint is forced into extension.[36] Radiographs may show avulsion of the volar lip of the distal phalanx, and this is diagnostic. Retraction of the bone fragment is usually limited by the A5 or A4 pulley.[37] Ultrasound is indicated if there is no bone fragment. The sheath of the torn tendon may fill with blood and debris, mimicking the tendon; therefore dynamic imaging is essential. Moving the distal phalanx will not show movement in the tendon sheath.[36] The proximal stump of the torn tendon, sometimes retracted to the mid-palm, has to be located.

Pulley Lesions

Rock Climber's Finger

Pulley lesions occur in climbers, classically in mountain climbers, but are increasingly seen following the introduction of artificial rock-climbing walls. They are encountered in the young and the old. The typical favorite climber's grip is the crimp grip or pocket grip when the climber's weight is taken on flexed fingers, resulting in maximum force on the PIP joint and the pulley system. Lifting a heavy object with the finger tips or trauma, for example, in sports, may have the same result. Pulley tears can also be secondary to chronic tenosynovitis in RA.

Acute tears occur in maximal resisted flexion of the fingers and present with a sudden sharp pain on the volar side of the finger, typically the ring or middle finger. The A2 (proximal phalanx) and A4 (middle phalanx) annular pulleys are broader and more important than the other pulleys. Tears occur more frequently at the A2 than A4 level and are usually solitary, although A2 and A3 tears can be seen in combination.[38,39] Diagnosis and treatment of pulley tears can prevent restricted range of motion, flexion contractures, and the development of osteoarthritis.

A pulley tear results in volar bowstringing. As a result of the tear, the pulley is no longer able to keep the tendon apposed to the bone on finger flexion, and the distance between the tendon and bone increases. This is evaluated on dynamic ultrasound[38] with the finger in extension and forced flexion (Fig. 5.29A, B). The patient is asked to keep the fingertip in flexion against the pressure of the examiner: about 10 degrees at the DIP joint, 40 degrees at the PIP joint with the MCPJ extended,[38] and longitudinal scanning is performed. Bowstringing is defined as a tendon-bone distance greater than 1.0 mm.[40] For the A2 pulley, the transducer is positioned at the base of the proximal phalanx, and for the A4 pulley at the middle phalanx. An increased distance up to 2.5 mm (A4) or 3 mm (A2) indicates an incomplete tear. Greater measurements indicate complete tears. A combined tear of the A2 and A3 pulleys is diagnosed with a distance of >5 mm at both levels. High sensitivity (98%) and specificity (100%) are reported using these parameters.[38] Hypoechoic fluid is seen in the tendon sheath in the acute setting, but may be absent in older injuries. Scar tissue can form between the phalanx and the tendon[41] (Fig. 5.29C, D) and lead to flexion deformity. MR and CT imaging can be used in evaluating pulley injuries,[40],[38],[41],[42] but are more time consuming and expensive. Since pulley lesions are usually not associated with other traumatic lesions, ultrasound is the preferred imaging technique. In elite rock climbers, complete combined A2 and A3 pulley lesions are repaired surgically. Isolated A2 pulley lesions are primarily treated
P. 94

without surgery,[43] although reconstruction of isolated A2 or A4 pulley tears is performed in selected cases.[3],[44] Other patients are treated conservatively.

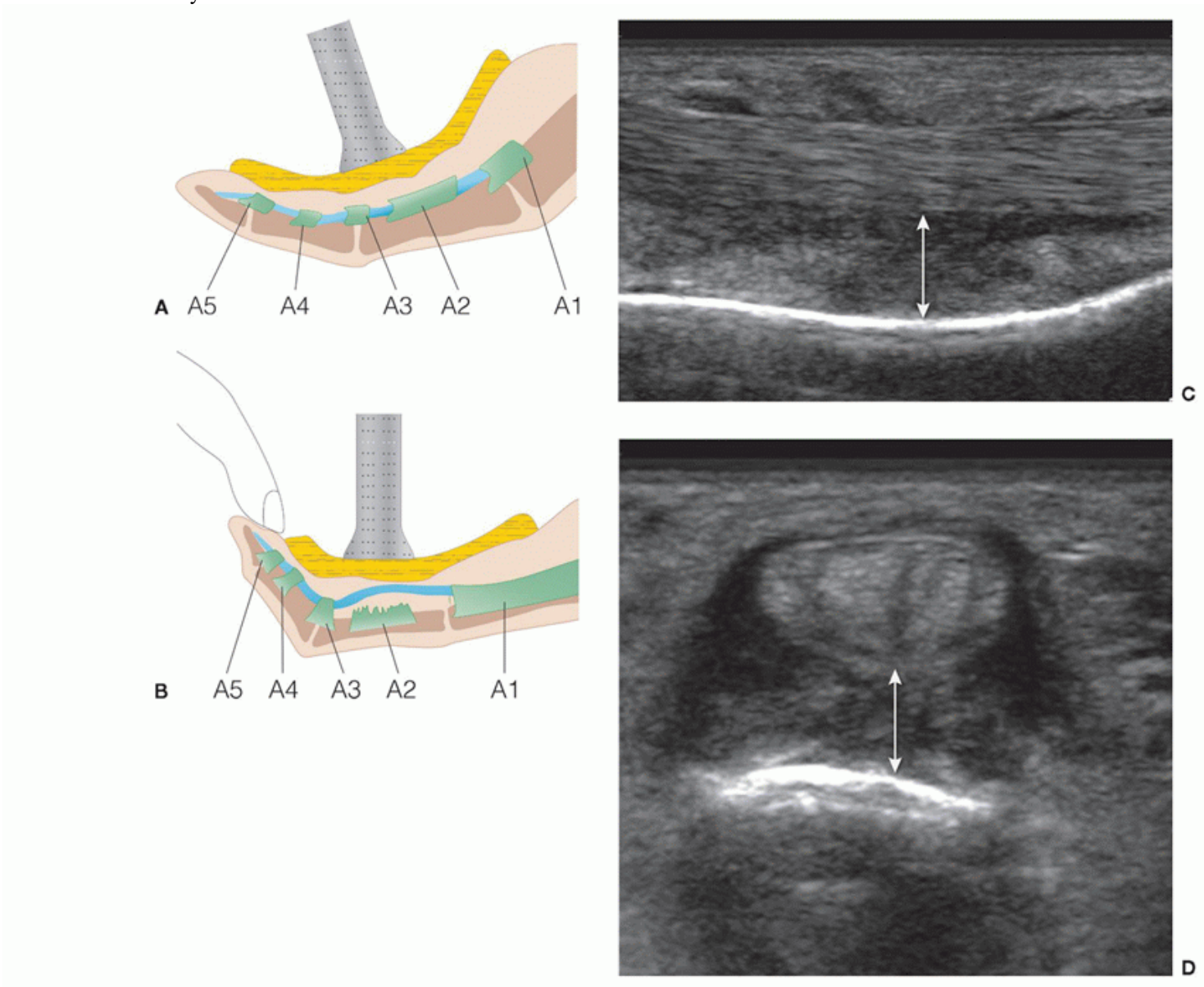


Figure 5.29. A2 pulley tear. A, B: Drawing of dynamic imaging of the annular pulleys. The transducer is placed longitudinally on the finger at rest (A) and with forced flexion against the tip of the examiner's finger (B). The A2 pulley demonstrates bowstringing, consistent with a complete tear. (A, B: Adapted with permission from Klauser A, Frauscher F, Bodner G, et al. Finger pulley injuries in extreme rock climbers: depiction with dynamic US. Radiology. 2002;222(3): 755-761.) Acute A2 pulley tear longitudinal (C) and

axial (D) images show the increased distance between the flexor tendon and the proximal phalanx. (C, D: Courtesy: Dr Carlo Martinoli. Associate Professor of Radiology. University of Genoa, Italy.)

Trigger Finger

Trigger finger is transient locking of the finger in flexion, followed by a painful snapping sensation during extension. It is a clinical diagnosis. Most cases are idiopathic, but activities requiring repetitive flexion and extension may lead to chronic, stenosing tenosynovitis with secondary thickening of the A1 pulley. The incidence of triggering is increased in patients with diabetes mellitus, RA, gout, amyloid, and acromegaly.[45] Ultrasound shows a thick, hypoechoic A1 pulley constricting the tendon sheath and may show hypervascularization. Tendinosis and tenosynovitis may be observed.[46] Dynamic ultrasound performed in the long axis at the level of the metacarpal joint during flexion and extension of the finger may show the tendon "blocking" at the A1 pulley, followed by sudden release. Comparison with adjacent fingers can help. Treatment is often corticosteroid injection near the level of the A1 pulley or in the tendon sheath[46,47] (Fig. 5.30) and can be performed under ultrasound guidance. Failed conservative management may require surgical release.[48] Ultrasound-guided release using a bent 19 or 25 G hypodermic needle has been described.[49]

LIGAMENTS

Ligaments of the wrist can be divided into extrinsic, that is, radiocarpal and ulnocarpal, and intrinsic, that is, intercarpal and involved in carpal stability.

The SLL and LTL are important stabilizers of the wrist. They have volar and dorsal segments and a central segment, which is also known as the proximal or

P. 95

membranous component. The site and extent of a tear may be used to differentiate between traumatic (peripheral) and degenerate (central) tears.[50] Tears of the dorsal segment of the SLL alter the normal relationship between the scaphoid and the lunate and may result in dynamic scapholunate instability, causing wrist pain and instability with a normal radiograph.[1]

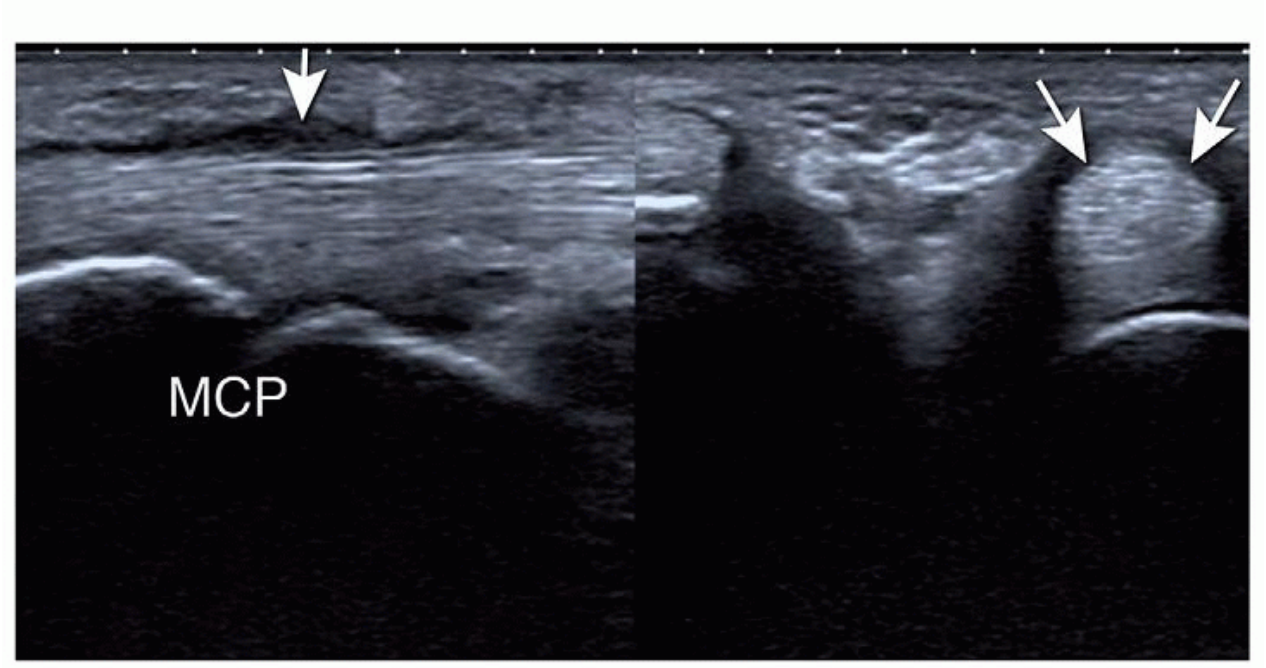


Figure 5.30. Trigger finger. Longitudinal and axial scans showing thickening (arrows) of the A1 pulley, resulting in triggering.

Diagnostic modalities advocated in the diagnosis of ligament tears include radiography in ulnar and radial deviation, arthrography, scintigraphy, and CT and MRI with and without arthrography.[51,52] In cadaver wrists, CT arthrography and MR imaging are almost equally accurate in depicting palmar and central segment tears, whereas CT arthrography is superior to MR imaging in detecting dorsal segment tears.[53] The diagnostic performance of MR varies considerably, and the sensitivity for SLL tears is consistently better than that for LTL tears.[54]

Ultrasound studies focus on the SLL. The dorsal aspect of the SLL can be depicted as a thin hyperechoic structure (Fig. 5.11),[55,56] completely or partially visible in 78% of normal wrists. Its detection following injury excludes scapholunate dissociation (Fig. 5.31), but the absence of a visible SLL does not necessarily indicate injury.[55] There is considerable variation in scapholunate interval widths on sonography and an unpredictable response with stress testing.

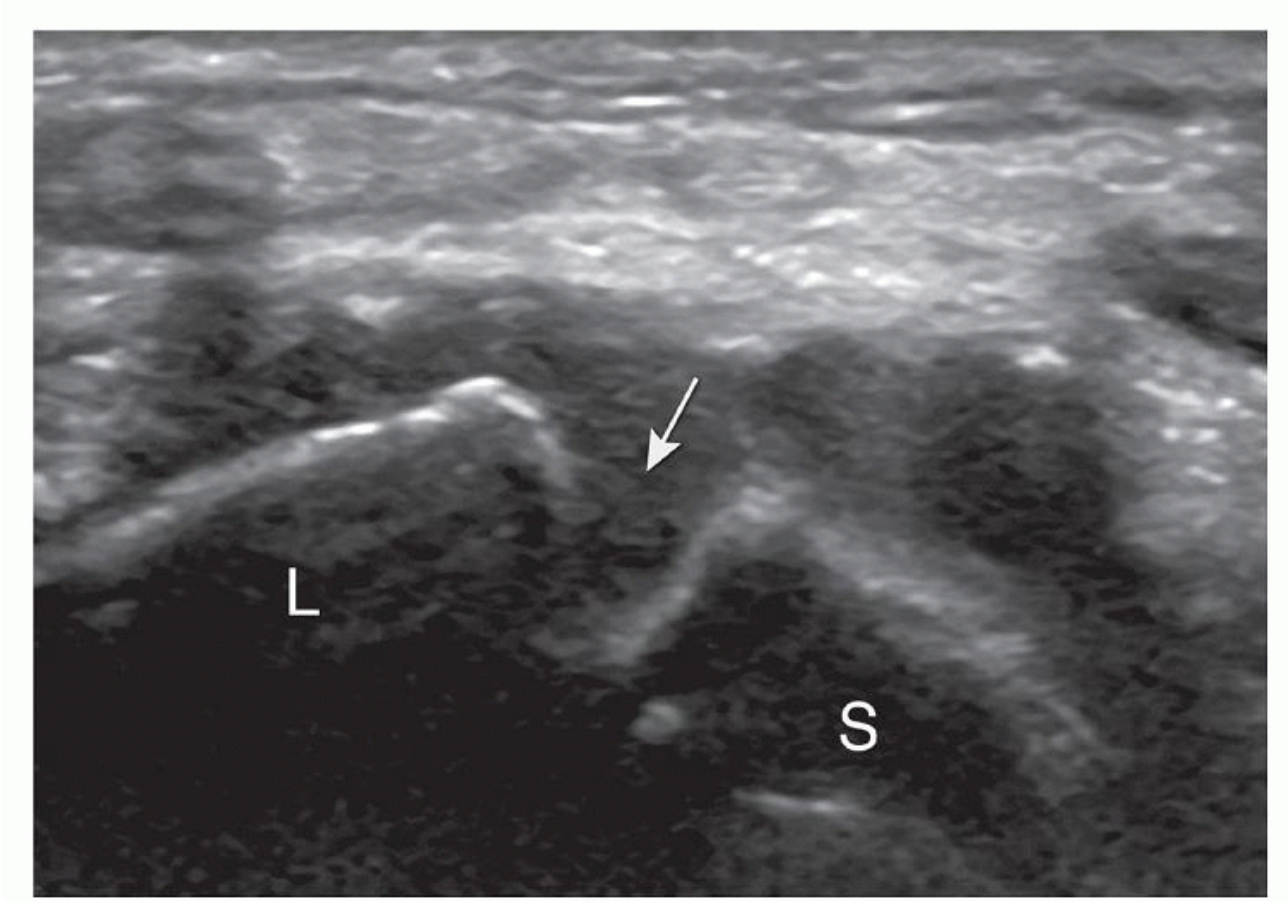


Figure 5.31. Scapholunate ligament tear. Axial ultrasound image shows an SL ligament tear with hematoma. (Courtesy: Dr. Eugene McNally, Consultant Musculoskeletal Radiologist at the Nuffield Orthopaedic Centre & University of Oxford.)

In spite of this, ultrasound distinguishes between normal and abnormal or possibly abnormal wrists.[57] Comparison with tricompartmental arthrography shows that ultrasound accurately detects SLL tears, but misses many LTL and TFCC tears.[58]

The introduction of a new generation of ultrasound machines with advanced probes and software and increased spatial resolution has improved visualization of the extrinsic and intrinsic carpal ligaments[59],[60] as thin fibrillar hyperechoic structures. Dynamic examination in flexion and extension may be useful,[60] but the radioscapholunate and UCL of the wrist are not usually seen. A standardized protocol has been proposed for evaluating the intrinsic and extrinsic wrist ligament and the TFC as a screening tool,[2] but as the imaging of chronic wrist pain wrist includes assessment of the TFCC, hyaline cartilage, ligaments, tendons, and bones, ultrasound can only be used as part of the diagnostic work-up and the role of ultrasound remains to be determined.

Triangular Fibrocartilage Complex

The TFC is a triangular structure of homogeneous hyperechogenicity on transverse and oblique sagittal scans at the level of the distal radioulnar joint, and is normally thicker than 2.5 mm on both transverse and oblique sagittal sections. A tear appears as a hypoechoic region or as thinning of the TFC (<2.5 mm) on either transverse or oblique sagittal sections.[61]

Ultrasound[62] shows a degree of correlation with MRI and arthroscopy for TFCC tears, but is not sufficiently accurate for clinical practice.[63],[64]

MR arthrography with injection of contrast into the distal radioulnar joint is recommended for evaluation of the TFCC. Clinically meaningful ulnar-sided peripheral tears are otherwise hard to diagnose.[54] Multi Detector Computed Tomography (MDCT) arthrography may also be used.[65]

Ulnar wrist pain has a large differential diagnosis including ECU tendinitis (Fig. 5.32), FCU tendinitis, pisotriquetral arthritis, TFCC lesions, ulnar impaction, LT instability, and distal radioulnar joint instability.[66]

Ulnar Collateral Ligament Tears of the Thumb and Stener Lesion

Acute injury of the UCL of the MCP joint of the thumb, “gamekeeper’s thumb,” or “skier’s thumb” is due to valgus stress (hyperabduction) and hyperextension. Acute thumb pain after trauma requires prompt evaluation of structural integrity to avoid long-term morbidity from instability, chronic pain, and osteoarthritis.[67]Clinical examination is limited by pain and swelling. Imaging of the



thumb is indicated to identify injuries that require surgery, that is, a displaced bone fragment or a Stener lesion.[67],[68]

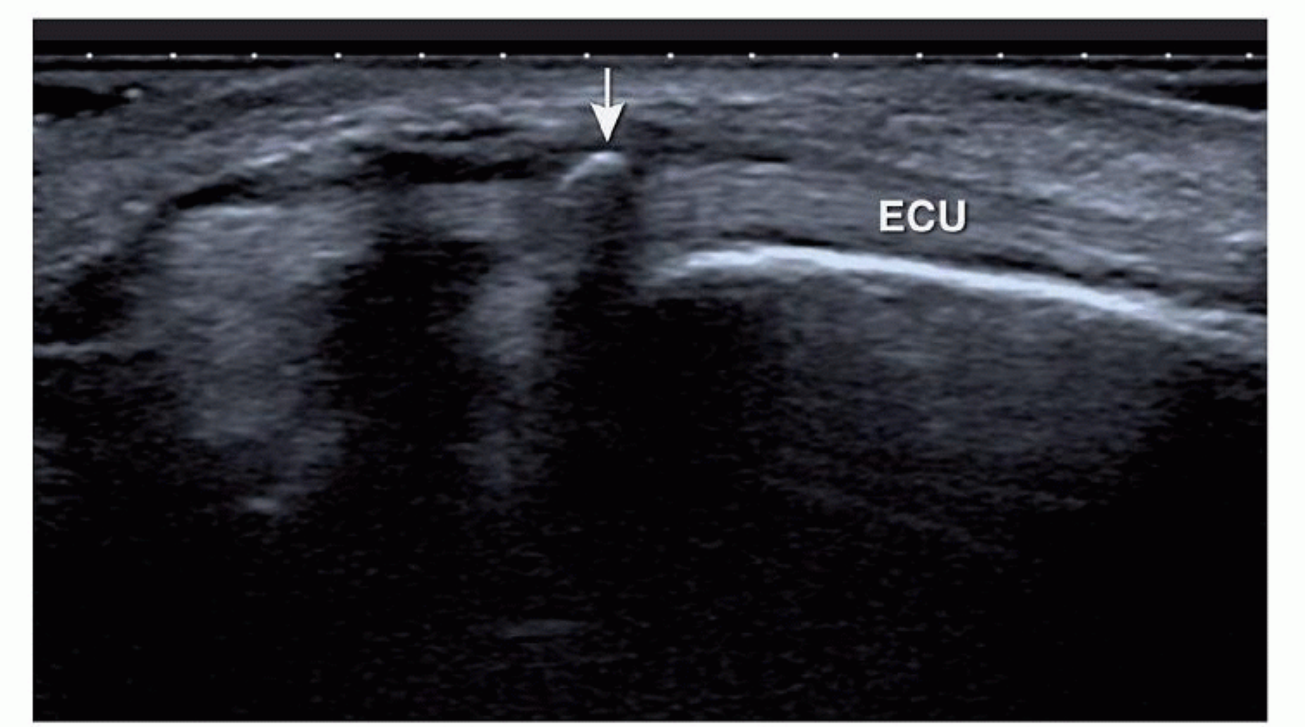


Figure 5.32. Extensor carpi ulnaris calcific tendinitis. Longitudinal image of the ECU tendon at the level of the distal ulna. The patient presented with acute wrist pain. A small calcific deposit (arrow) is present.

A tear of the UCL usually occurs at its distal insertion at the base of the proximal phalanx. An avulsed bone fragment may be identified on radiographs. “Stress radiographs” are sometimes requested, but are often difficult to interpret and may increase damage. Both ultrasound and MRI offer detailed anatomic information. Ultrasound is easy to perform and is quick (Fig. 5.18).[67] Ulnar collateral ligament injury is graded into sprain, partial tear, and full thickness tear (Fig. 5.33A). Sprained ligaments appear thickened and hypoechoic owing to edema and hemorrhage. Tears usually occur at the distal insertion and remain deep to the adductor aponeurosis. Ultrasound shows obvious discontinuity in the ligament. Additional findings may include bone avulsion, joint effusion, and volar plate injury.[67] Full-thickness UCL tears are divided[68] into intra-aponeurosis tears, when the ligament remains deep to the adductor aponeurosis, and extra-aponeurosis tears, when the displaced proximal fragment of the torn ligament is retracted and trapped superficial to the aponeurosis, the so-called Stener lesion (Figs. 5.33B, and 5.34). Ultrasound of a Stener lesion shows the hypoechoic mass of torn and retracted proximal ligament superficial to the adductor aponeurosis at the level of the metacarpal head. The torn ligament cannot return to its normal position and the two torn ends of the ligament are not in contact; therefore, healing is impossible. Surgery is indicated to prevent chronic instability of the joint.[67],[69] The diagnosis is more difficult if the injury is more than 1 week old because of reactive changes.

NERVES

Carpal Tunnel Syndrome

Compression of the MN in the carpal tunnel is a clinical diagnosis and confirmed by electrodiagnostic testing (EDX). Ultrasound is not routinely performed in CTS. A recent meta-analysis confirms that ultrasound-derived CSA measurement of the MN is not an alternative to EDX, but gives complementary results (Fig. 5.35).[70] The diagnostic accuracy of ultrasound is increased by comparing CSA measurements of the MN at the levels of the carpal tunnel and the pronator quadratus muscle.[71]

Color Doppler ultrasound may confirm the severity of CTS by showing intraneural hypervascularity.[72],[73]

Ultrasound can identify normal variants such as a persistent median artery (incidence 2% to 4%) and a bifid MN (incidence 3%)[74] and mass lesions including anomalous muscles (Fig. 5.19), ganglion cysts, and tenosynovitis.[75]

Steroid injections into the carpal tunnel can be performed under ultrasound guidance and produce short-term benefits compared with placebo, oral steroids, anti-inflammatories, and splinting.[76]

Surgical decompression results in decreased MN caliber within 2 weeks of surgery,[77] although EDX studies take much longer to normalize. Surgery is associated with a greater decrease in MN CSA than nonsurgical treatment. Smaller postoperative CSAs may be associated with better clinical outcomes.[78]

Guyon’s Canal

There is a high prevalence of anomalous muscles in Guyon’s canal (see Normal anatomy: anomalous muscles), and if the AADM muscle is not significantly thicker than 1.7 mm,[6] alternative causes of ulnar nerve compression should be sought. A ganglion cyst is the most frequent cause. Ultrasound shows a well-defined anechoic/hypoechoic mass.[79] The pedicle, which is often difficult to identify, originates from the joints between the hamate and triquetrum or between the pisiform and triquetrum. Other causes of compression are neuritis, ulnar artery disease (pseudoaneurysm or thrombosis), fracture (hook of hamate), or nerve sheath tumor. At the level of the hook of the hamate, the deep branch of the ulnar nerve and the ulnar artery may be injured by compression

against the hook owing to single or repeated episodes of trauma, often occupational, causing hypothenar hammer syndrome. Intimal damage causes ulnar artery thrombosis or pseudoaneurysm. In thrombosis, the artery is increased in size, filled with echogenic thrombus, and shows no flow on Doppler. With pseudoaneurysm, the artery is dilated and shows swirling, abnormal flow on Doppler.[80]

Radial Nerve

The radial nerve at the wrist can become inflamed, for example, by a tight watch strap or wrist band, as it crosses the first extensor compartment to reach the dorsal aspect of the wrist. This Wartenberg syndrome has to be differentiated from de Quervain tenosynovitis and

P. 97

P. 98

intersection syndrome. The radial nerve can also be injured by intravenous cannulation.

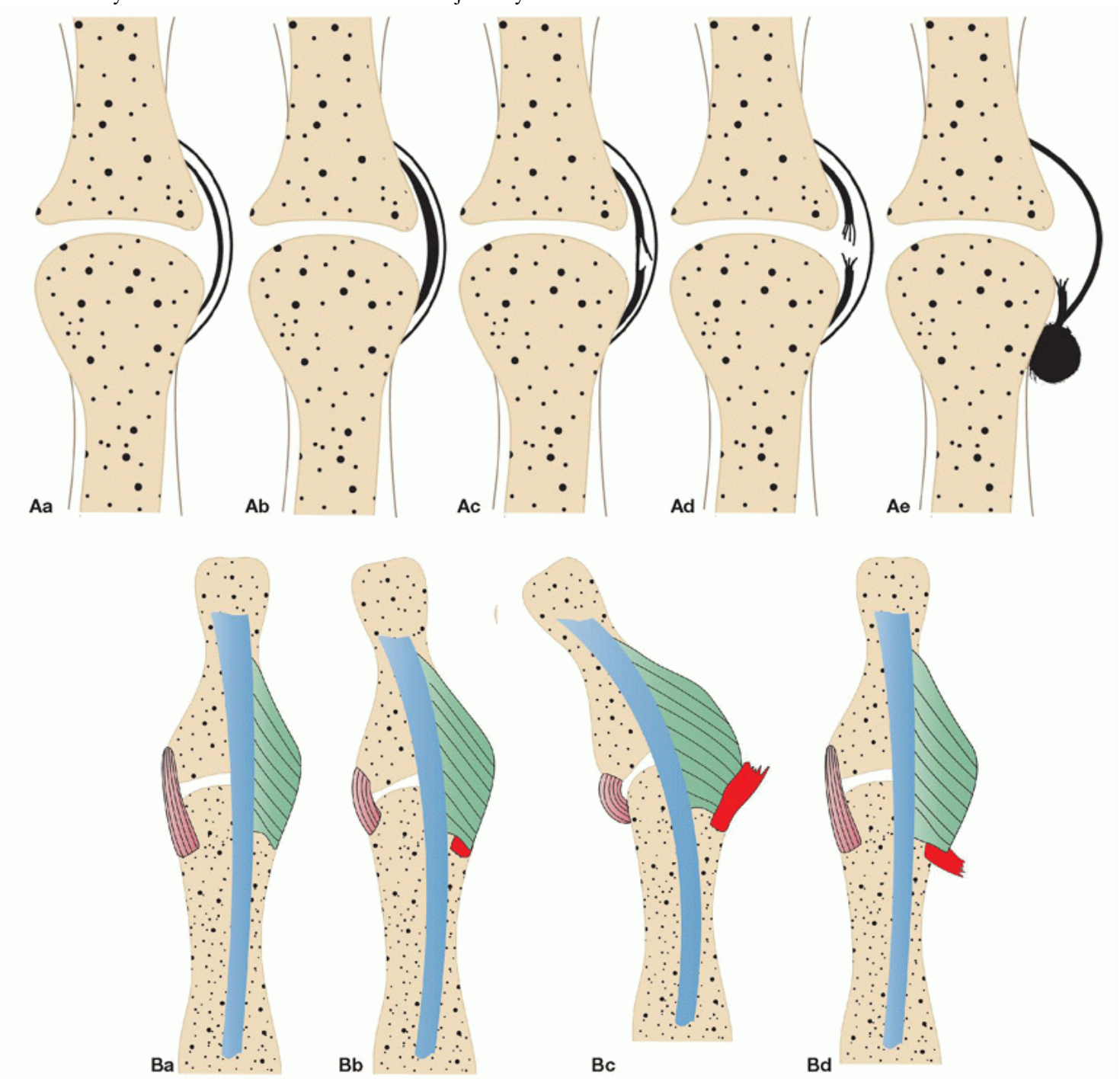


Figure 5.33. Tears of the UCL of the thumb. A: Drawing showing UCL pathology of the thumb. a. normal appearance, b. sprain, c. partial-thickness tear, d. full-thickness tear, and e. Stener lesion. The adductor aponeurosis remains intact in all grades of UCL injury. In a Stener lesion, the aponeurosis becomes interposed between the proximally retracted UCL and its distal insertion. (Drawings adapted with permission from Ebrahim FS, De Maeseneer M, Jager T, et al. ultrasound diagnosis of UCL tears of the

thumb and Stener lesions: technique, pattern-based approach, and differential diagnosis. Radiographics. 2006;26(4):1007-1020.). B: Mechanism of a Stener lesion. a. The normal UCL is covered by the adductor aponeurosis (green). b. In abduction, the ligament (red) is torn distally, deep to the aponeurosis. c. In extreme abduction, the torn ligament slips superficial to the aponeurosis. d. With the joint back in the neutral position, the torn ligament remains trapped superficial to the adductor aponeurosis. (Adapted with permission from Shinohara T, Horii E, Majima M, et al. Sonographic diagnosis of acute injuries of the ulnar collateral ligament of the metacarpophalangeal joint of the thumb. J Clin Ultrasound. 2007;35(2):73-77.)

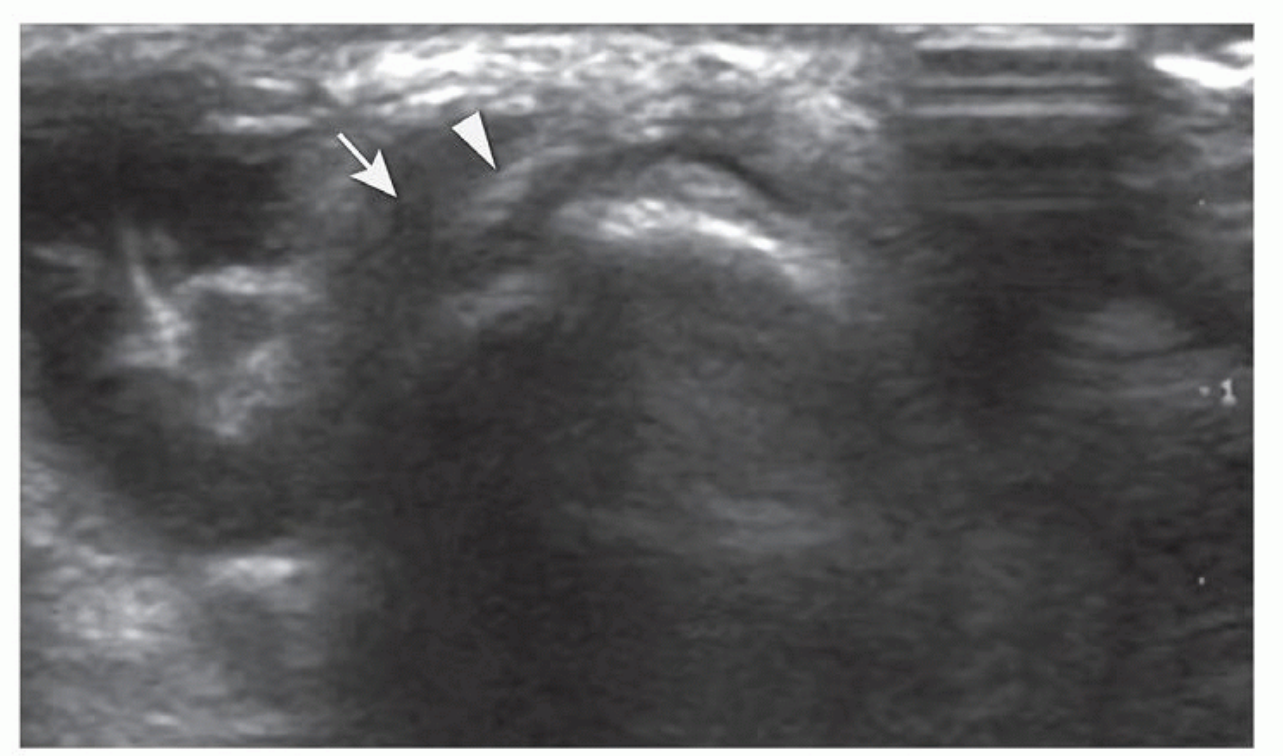

Figure 5.34. Stener lesion. A hypoechoic soft tissue mass (arrow) of retracted UCL lies superficial to the thin hyperechoic band of the adductor aponeurosis (arrowhead).

FOREIGN BODIES

Foreign bodies are frequently encountered in the hand and wrist. Initial radiographs should always be performed. Metal and glass, even lead-free glass, are radiopaque.[81] Non-radiopaque bodies such as wood or plastic can be missed on radiographs, but detected by ultrasound, which also provides exact preoperative localization. Ultrasound-guided removal can be performed,[82] and high success rates have been reported.[83]

All foreign bodies are initially hyperechoic, although wood may become less echogenic over time.[84] Posterior artifacts aid identification, especially of small fragments. Small or irregularly marginated bodies produce “clean” or well-defined acoustic shadows, whereas large or smooth bodies produce “dirty” or poorly defined acoustic shadows.[85] In the acute setting, the initial appearance may be a localized mass secondary to infection or abscess, and the foreign body is surrounded by an irregular, heterogenous, hypoechoic fluid collection with increased vascularity at the periphery. In chronic cases, a soft tissue mass may be caused by a sterile granuloma, and ultrasound shows a hypoechoic halo around the foreign body without hypervascularity.[24],[86]

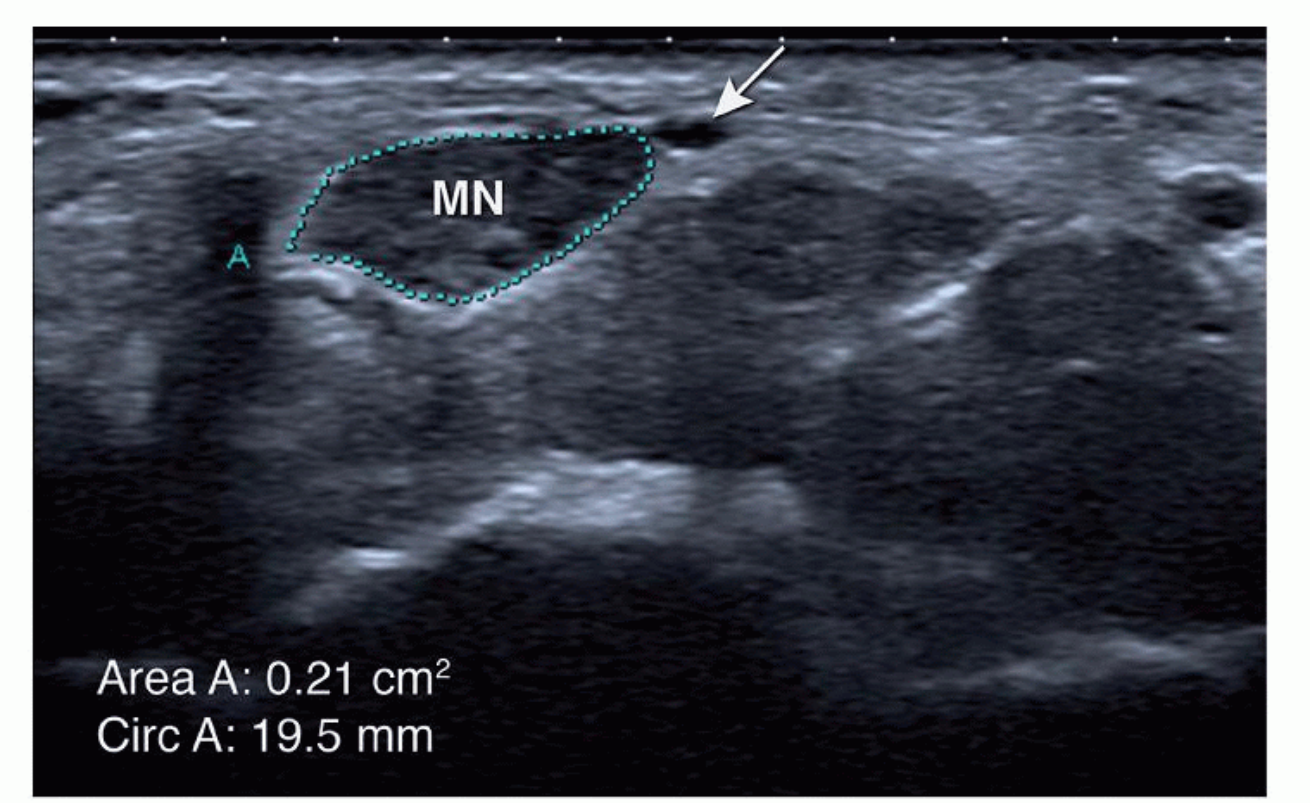


Figure 5.35. Swollen median nerve (MN). Swollen MN in a patient with CTS. The cross-sectional area of the MN is 21 $mm^2$, which is greater than the upper limit of the normal (10 $mm^2$). There is a persistent median artery (arrow).

COMMON HAND TUMORS

Ultrasound is the initial imaging method of choice to evaluate a soft tissue swelling of the hand or wrist. The distinction between a solid or cystic mass is usually easily made. Color Doppler will show if hypervascularity is present, and dynamic imaging with flexion and extension of the fingers shows the relationship of the lesion to the tendon.

Ganglia

The most common masses of the wrist and hand are ganglia. The cyst is filled with thick viscous fluid and surrounded by a fibrous capsule. There is no synovial lining. Ganglia are usually attached to a joint capsule or tendon sheath.[24,87] Most (70%) occur in the dorsal wrist[87] and are attached by a pedicle of variable length to a damaged SLL. Volar wrist ganglia are less common and located radially, originating from the scaphoradial or scaphotrapezial joints, close to the radial artery.

Cysts at flexor tendons, usually near the A1 pulley, are more common than at extensor tendons.[24,86] Ultrasound often shows well-demarcated hypoechoic masses, with posterior acoustic enhancement, but appearances vary depending on size and chronicity. Larger cysts tend to be anechoic/hypoechoic. Septa and hyperechoic contents are seen in older ganglia, which may not appear obviously cystic. Hypervascularity of a thickened wall may be appreciated.[87,88] Identification of the neck of the cyst is not always possible. Flexion of the wrist may help to find small, clinically occult ganglia (Fig. 5.36). Ultrasound can be used to guide aspiration or steroid injection. A mixture of 1:1 corticosteroid and local anesthetic is used. The volume administered depends on the size of the ganglion. The long-term results of aspiration/injection are identical to those of nonintervention.[89]

Tip:

In assessing the vascularity of a soft tissue mass, do not push too hard or the vessels may be effaced. A large amount of gel is helpful.

Giant Cell Tumor of Tendon Sheath

Also called nodular tenosynovitis, it is histologically identical to pigmented villonodular synovitis (PVNS). Giant cell tumor of tendon sheath (GCTTS) is the most



common soft tissue tumor of the hand and wrist, and is usually seen on the volar aspect of the distal fingers.[90] Synovial proliferation with dense collagen and hemosiderin deposition is characteristic. Giant cell tumor of tendon sheath arises from the tendon sheath in close contact with the tendon and may even encase the tendon. Uncommonly, satellite lesions are seen adjacent to the primary lesion, and there may be diffuse involvement of the tendon sheath. The origin of the mass on the tendon sheath can be confirmed by flexing and extending the finger, showing that the tumor is not moving with the tendon.

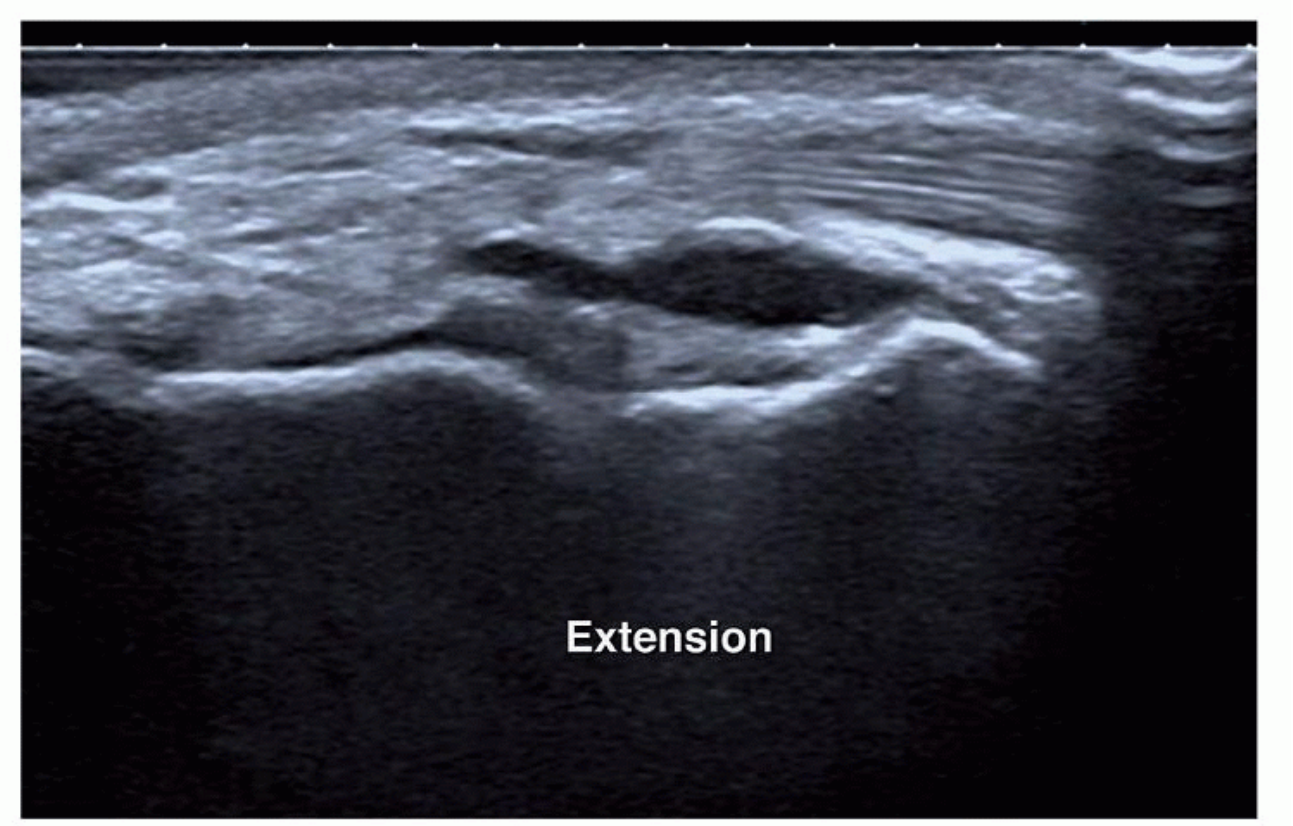


Figure 5.36. Ganglion cyst. Longitudinal image of the dorsal wrist in extension shows a ganglion deep to the extensor tendon. Dynamic imaging can help to identify a clinically occult ganglion cyst.

Ultrasound shows a well-defined, hypoechoic mass, predominantly homogeneous, although heterogeneous lesions are described.[91] Color or power Doppler imaging shows internal vascularity, peripheral or central, or a combination of the two. The ultrasound appearance is not diagnostic, but the proximity to the tendon sheath is highly suggestive of GCTTS.[24] Progressive enlargement can cause bone erosions, predominantly at or distal to the MCP joints, or even present as an intrinsic osseous lesion.[92] MRI[92,93] shows low to intermediate signal intensity on both T1- and T2-weighted images, with a variable degree of heterogeneity, an unusual appearance in other extra-articular soft tissue masses and suggestive of the diagnosis, especially in the hand or foot. Enhancement is seen after intravenous gadolinium. Gradient echo images characteristically show variable “blooming” or susceptibility artifact due to hemosiderin GCTTS.[93]

Nerve and Nerve Sheath Tumors

Tumors of peripheral nerves are rare in the hand and are usually benign and subcutaneous. Benign lesions include schwannoma and neurofibromas, which can originate from any nerve. Most peripheral nerve sheath tumors are homogeneous, hypoechoic, and show posterior acoustic enhancement. Continuity of a mass with a peripheral nerve suggests the diagnosis (Fig. 5.37).

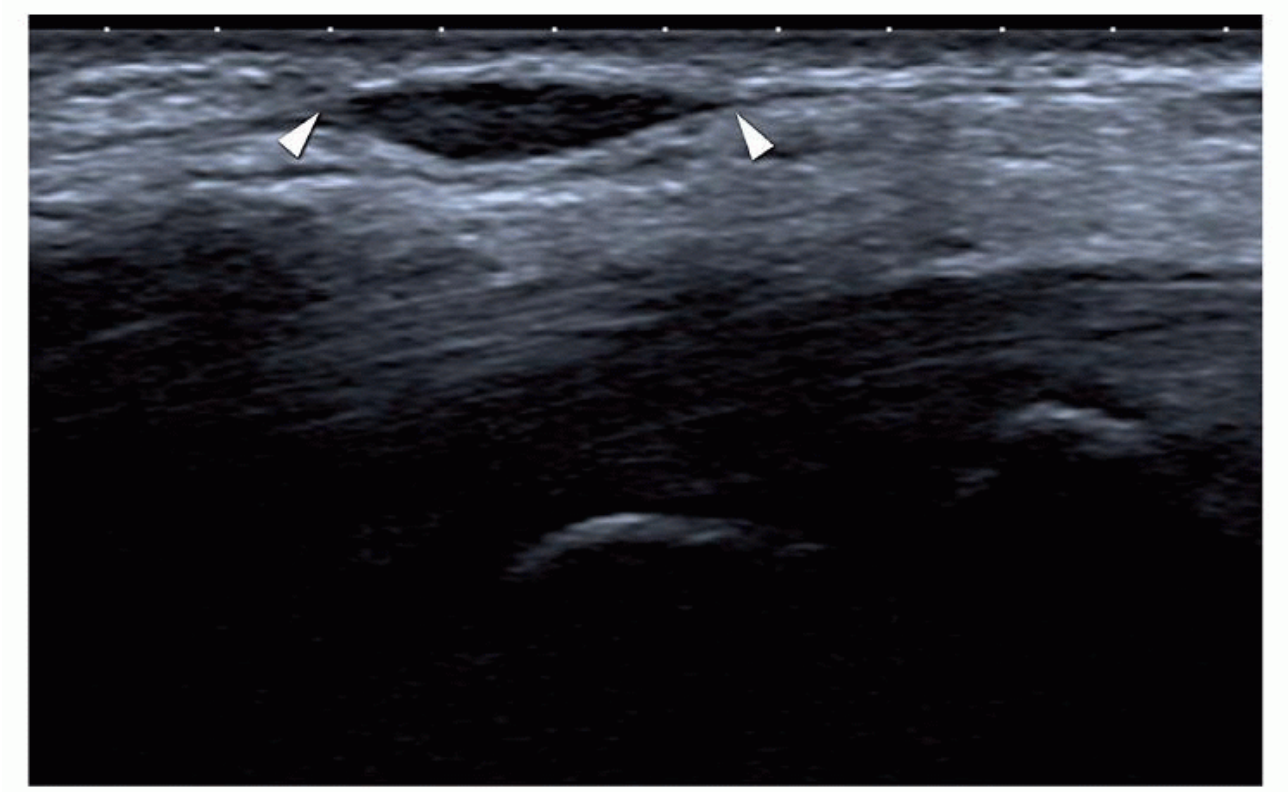

Figure 5.37. Peripheral nerve sheath tumor. Longitudinal image of the volar wrist shows an oval hypoechoic mass in direct continuity with the cutaneous branch (arrowheads) of the MN.

Careful scanning may be needed to identify the nerve proximally and/or distally as it may be displaced.[17] Internal blood flow on Doppler ultrasound helps to differentiate nerve sheath tumors from avascular ganglion cysts. Ultrasound cannot reliably distinguish neurofibromas from schwannomas.[94,95] A rare neurogenic mass with a predilection for the MN is fibrolipohamartoma, also known as neural fibrolipoma or intraneural lipoma. Its presentation is a sausage-like, fusiform mass at the volar wrist usually before 20 years of age. Histology shows fatty and fibrous components surrounding the nerve fascicles.[96] Ultrasound shows fusiform enlargement of the nerve at the level of the distal radius and carpal tunnel. The hypoechoic, enlarged nerve fascicles are separated by echogenic fat.

Vascular Tumors

Glomus tumors are rare, benign hamartomas that develop from the neuromyoarterial glomus bodies that regulate blood flow in the skin. Up to 75% of all glomus tumors occur in the hand, and approximately 65% of these are in the fingertips, particularly the subungual space. They account for 1% to 4.5% of all hand tumors.[97] Patients present with pain, evoked by pressure or cold exposure. Ultrasound shows a hypoechoic mass, which is highly vascularized, with arteriovenous shunting. Comparison with another finger may be valuable as the subungual area is normally highly vascularized. Erosion of the underlying bone may be present (Fig. 5.38). On MR, most glomus tumors are of intermediate signal intensity on T1-weighted images, hyperintense on T2-weighted images, and show inhomogeneous contrast enhancement. The differential diagnosis includes mucoid cyst and angioma.[98] Hemangioma can involve any soft tissue, and may be intramuscular, but in the finger is usually located

P. 100

in the superficial dermis.[97] Ultrasound usually shows a hypoechoic mass that is inhomogeneous due to hypoechoic vascular channels and hyperechoic fat. Slow flow is typical.[99]

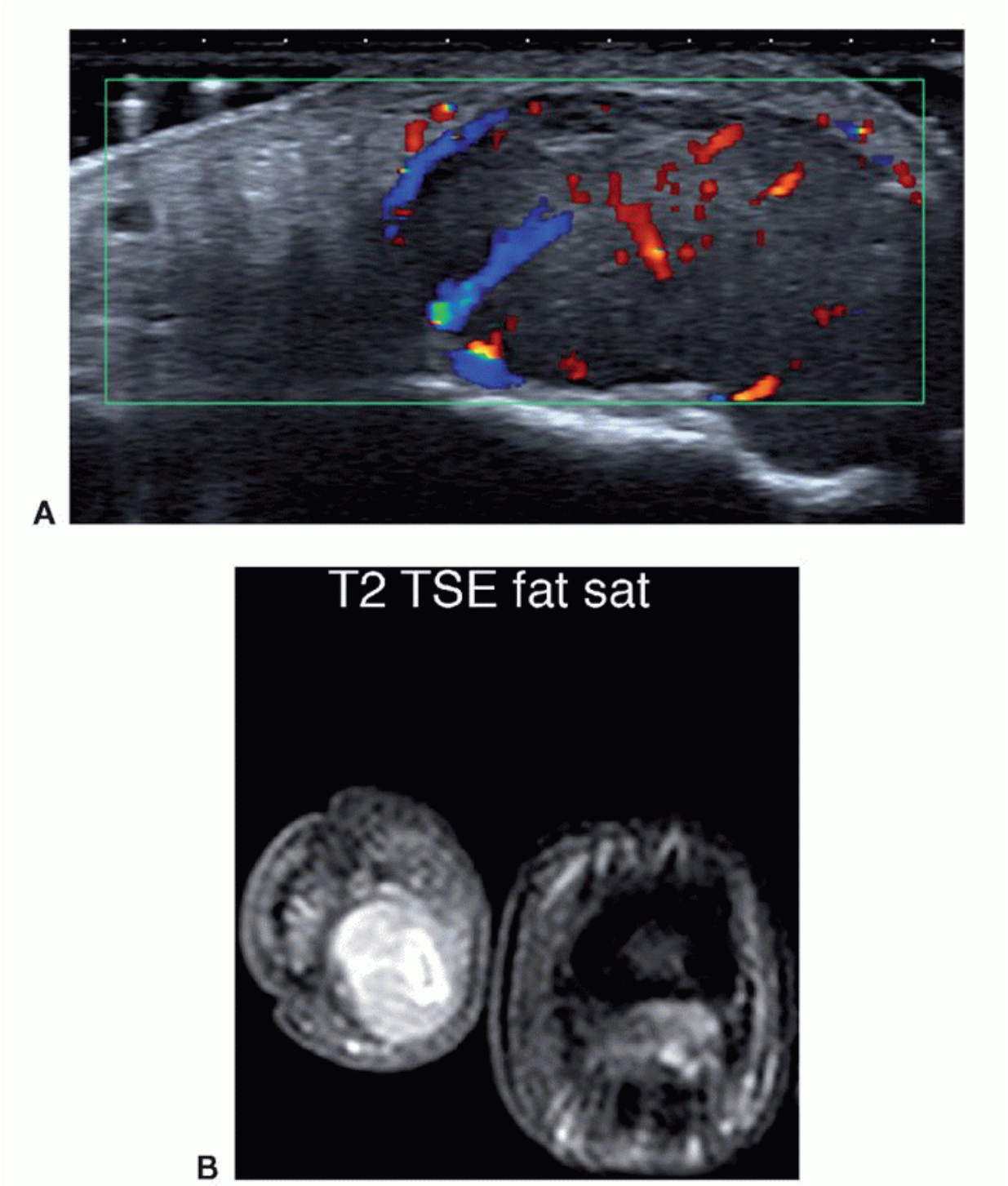


Figure 5.38. Glomus tumor. A: Longitudinal color Doppler image showing a hypervascular hypoechoic well-defined soft tissue mass volar to the distal phalanx of the thumb. B: Axial fat-suppressed T2-weighted TSE image showing a hyperintense mass. Post-contrast images showed enhancement. The location and appearances are consistent with a glomus tumor, although a subungual position is more common.

Lipoma

A superficial lipoma presents as a soft, painless, welldelineated, and mobile mass. Its echogenicity is variable and ranges from hypoechoic to anechoic, related to cellular variability.[100,101] Lipomas have an elongated shape, and most are oriented parallel to the skin. In 66% of cases,[100] superficial lipomas are well marginated, and occasionally a distinct echogenic capsule can be defined. The absence of internal vascularization helps to exclude malignancy. Larger and deeper masses are better evaluated with MRI.[24]

Miscellaneous

Accessory muscles (Fig. 5.19) and tenosynovitis can present as masses and mimic tumors or compress nerves.

If ultrasound fails to provide an answer, MRI is an accurate problem solver for evaluating mass lesions, but is relatively infrequently needed.[96]

ACKNOWLEDGMENT

The authors acknowledge the help of Maria Kelemouridou, MD, Radiology Department, A.H.E.P.A. University Hospital, Thessaloniki, Greece and Gerrit Kracht, Radiology Department, Leiden University Medical Center, The Netherlands.

REFERENCES

1. Taleisnik J. Post-traumatic carpal instability. Clin Orthop Relat Res. 1980;(149):73-82.
2. Taljanovic MS, Goldberg MR, Sheppard JE, et al. US of the intrinsic and extrinsic wrist ligaments and triangular fibrocartilage complex—normal anatomy and imaging technique. Radiographics. 2011;31(1):E44.
3. Bianchi S, Martolini C. Wrist and hand. In: Ultrasound of the Musculoskeletal System. Berlin Heidelberg, NY: Springer; 2007:425-548.
4. Netter FH, Woodburne RT, Crelin ES, et al. Upper limb, wrist and hand. In: Musculoskeletal System, Part 1: Anatomy, Physiology and Metabolic Disorders. NJ: Ciba-Geigy; 1987:55-73.
5. McNally EG. Upper limb: Anatomy and technique. In: Practical Musculoskeletal Ultrasound. Philadelphia, PA: Elsevier Churchill Livingstone; 2005:1-21.
6. Martinoli C, Serafini G, Bianchi S, et al. Ultrasonography of peripheral nerves. J Peripher Nerv Syst. 1996;1(3):169-178.
7. Beggs I, Bianchi S, Bueno A, et al. Musculoskeletal Ultrasound Technical Guidelines: III. Wrist. Vienna, Austria: European Society of MusculoSkeletal Radiology. Available at http://www.essr. org/html/img/pool/wrist.pdf
8. Timins ME. Muscular anatomic variants of the wrist and hand: findings on MR imaging. AJR Am J Roentgenol. 1999;172(5):1397-1401.
9. Harvie P, Patel N, Ostlere SJ. Prevalence and epidemiological variation of anomalous muscles at Guyon's canal. J Hand Surg Br. 2004;29(1):26-29.
10. Zeiss J, Guilliam-Haidet L. MR demonstration of anomalous muscles about the volar aspect of the wrist and forearm. Clin Imaging. 1996;20(3):219-221.
11. Anderson MW, Benedetti P, Walter J, et al. MR appearance of the extensor digitorum manus brevis muscle: a pseudotumor of the hand. AJR Am J Roentgenol. 1995;164(6):1477-1479.
12. Gama C. Extensor digitorum brevis manus: a report on 38 cases and a review of the literature. J Hand Surg Am. 1983;8 (5, pt 1):578-582.
13. Ogura T, Inoue H, Tanabe G. Anatomic and clinical studies of the extensor digitorum brevis manus. J Hand Surg Am. 1987;12(1):100-107.
14. Sanger JR, Krasniak CL, Matloub HS, et al. Diagnosis of an anomalous superficialis muscle in the palm by magnetic resonance imaging. J Hand Surg Am. 1991;16(1):98-101.
15. Smith RJ. Anomalous muscle belly of the flexor digitorum superficialis causing carpal-tunnel syndrome. Report of a case. J Bone Joint Surg Am. 1971;53(6):1215-1216.
16. Touborg-Jensen A. Carpal-tunnel syndrome caused by an abnormal distribution of the lumbrical muscles. Case report. Scand J Plast Reconstr Surg. 1970;4(1):72-74.
17. Roberts PH. An anomalous accessory palmaris longus muscle. Hand. 1972;4(1):40-41.
P. 101

18. Polesuk BS, Helms CA. Hypertrophied palmaris longus muscle, a pseudomass of the forearm: MR appearance—case report and review of the literature. Radiology. 1998;207(2): 361-362.
19. Genc H, Cakit BD, Tuncbilek I, et al. Ultrasonographic evaluation of tendons and enthesal sites in rheumatoid arthritis: comparison with ankylosing spondylitis and healthy subjects. Clin Rheumatol. 2005;24(3):272-277.
20. Backhaus M. Ultrasound and structural changes in inflammatory arthritis: synovitis and tenosynovitis. Ann N Y Acad Sci. 2009;1154:139-151.
21. Boutry N, Morel M, Flipo RM, et al. Early rheumatoid arthritis: a review of MRI and sonographic findings. AJR Am J Roentgenol. 2007;189(6):1502-1509.
22. Sommer OJ, Kladosek A, Weiler V, et al. Rheumatoid arthritis: a practical guide to state-of-the-art imaging, image interpretation, and clinical implications. Radiographics. 2005;25(2):381-398.
23. Koch AE. Review: angiogenesis: implications for rheumatoid arthritis. Arthritis Rheum. 1998;41(6):951-962.
24. Bianchi S, Della Santa D, Glauser T, et al. Sonography of masses of the wrist and hand. AJR Am J Roentgenol. 2008; 191(6):1767-1775.
25. Filippucci E, Gabba A, Di Geso L, et al. Hand tendon involvement in rheumatoid arthritis: an ultrasound study. Semin Arthritis Rheum. 2012;41(6):752-760.
26. Kotob H, Kamel M. Identification and prevalence of rheumatoid nodules in the finger tendons using high frequency ultrasonography. J Rheumatol. 1999;26(6):1264-1268.
27. Wick MC, Weiss RJ, Arora R, et al. Enthesiopathy of the flexor carpi ulnaris at the pisiform: findings of high-frequency sonography. Eur J Radiol. 2011;77(2):240-244.
28. Nagaoka M, Matsuzaki H, Suzuki T. Ultrasonographic examination of de Quervain's disease. J Orthop Sci. 2000;5(2):96-99.
29. Jeyapalan K, Choudhary S. Ultrasound-guided injection of triamcinolone and bupivacaine in the management of De Quervain's disease. Skeletal Radiol. 2009;38(11):1099-1103.
30. Chhabra A, Soldatos T, Thawait GK, et al. Current perspectives on the advantages of 3-T MR imaging of the wrist. Radiographics. 2012;32(3):879-896.
31. Owers KL, Lee J, Khan N, et al. Ultrasound changes in the extensor pollicis longus tendon following fractures of the distal radius—a preliminary report. J Hand Surg Eur Vol. 2007;32(4):467-471.

32. Santiago FR, Plazas PG, Fernández JM. Sonography findings in tears of the extensor pollicis longus tendon and correlation with CT, MRI, and surgical findings. Eur J Radiol. 2008;66(1):112-116.
33. Kleinbaum Y, Heyman Z, Ganel A, et al. Sonographic imaging of mallet finger. Ultraschall Med. 2005;26(3):223-226.
34. Lopez-Ben R, Lee DH, Nicolodi DJ. Boxer knuckle (injury of the extensor hood with extensor tendon subluxation): diagnosis with dynamic US—report of three cases. Radiology. 2003;228(3):642-646.
35. Jeyapalan K, Bisson MA, Dias JJ, et al. The role of ultrasound in the management of flexor tendon injuries. J Hand Surg Eur Vol. 2008;33(4):430-434.
36. de Gautard G, de Gautard R, Celi J, et al. Sonography of Jersey finger. J Ultrasound Med. 2009;28(3):389-392.
37. Al-Qattan MM. Type 5 avulsion of the insertion of the flexor digitorum profundus tendon. J Hand Surg Br. 2001;26(5):427-431.
38. Klauser A, Frauscher F, Bodner G, et al. Finger pulley injuries in extreme rock climbers: depiction with dynamic US. Radiology. 2002;222(3):755-761.
39. Martinoli C, Bianchi S, Nebiolo M, et al. Sonographic evaluation of digital annular pulley tears. Skeletal Radiol. 2000;29(7):387-391.
40. Hauger O, Chung CB, Lektrakul N, et al. Pulley system in the fingers: normal anatomy and simulated lesions in cadavers at MR imaging, CT, and US with and without contrast material distention of the tendon sheath. Radiology. 2000;217(1):201-212.
41. Le Viet D, Rousselin B, Roulot E, et al. Diagnosis of digital pulley rupture by computed tomography. J Hand Surg Am. 1996;21(2):245-248.
42. Parellada JA, Balkissoon AR, Hayes CW, et al. Bowstring injury of the flexor tendon pulley system: MR imaging. AJR Am J Roentgenol. 1996;167(2):347-349.
43. Gabl M, Rangger C, Lutz M, et al. Disruption of the finger flexor pulley system in elite rock climbers. Am J Sports Med. 1998;26(5):651-655.
44. Bianchi S, Martinoli C, Abdelwahab IF. High-frequency ultrasound examination of the wrist and hand. Skeletal Radiol. 1999;28(3):121-129.
45. Tagliafico A, Resmini E, van Holsbeeck MT, et al. Sonographic depiction of trigger fingers in acromegaly. J Ultrasound Med. 2009;28(11):1441-1446.
46. Guerini H, Pessis E, Theumann N, et al. Sonographic appearance of trigger fingers. J Ultrasound Med. 2008;27(10):1407-1413.
47. Peters-Veluthamaningal C, van der Windt DA, Winters JC, et al. Corticosteroid injection for trigger finger in adults. Cochrane Database Syst Rev. 2009;21(1):CD005617.
48. Benson LS, Ptaszek AJ. Injection versus surgery in the treatment of trigger finger. J Hand Surg Am. 1997;22(1):138-144.
49. Rajeswaran G, Lee JC, Eckersley R, et al. Ultrasound-guided percutaneous release of the annular pulley in trigger digit. Eur Radiol. 2009;19(9):2232-2237.
50. Wright TW, Del Charco M, Wheeler D. Incidence of ligament lesions and associated degenerative changes in the elderly wrist. J Hand Surg Am. 1994;19(2):313-318.
51. Schweitzer ME, Brahme SK, Hodler J, et al. Chronic wrist pain: spin-echo and short tau inversion recovery MR imaging and conventional and MR arthrography. Radiology. 1992;182(1):205-211.
52. Timins ME, Jahnke JP, Krah SF, et al. MR imaging of the major carpal stabilizing ligaments: normal anatomy and clinical examples. Radiographics. 1995;15(3):575-587.
53. Schmid MR, Schertler T, Pfirrmann CW, et al. Interosseous ligament tears of the wrist: comparison of multi-detector row CT arthrography and MR imaging. Radiology. 2005;237(3):1008-1013.
54. Zanetti M, Saupe N, Nagy L. Role of MR imaging in chronic wrist pain. Eur Radiol. 2007;17(4):927-938.
55. Griffith JF, Chan DP, Ho PC, et al. Sonography of the normal scapholunate ligament and scapholunate joint space. J Clin Ultrasound. 2001;29(4):223-229.
56. Jacobson JA, Oh E, Propeck T, et al. Sonography of the scapholunate ligament in four cadaveric wrists: correlation with MR arthrography and anatomy. AJR Am J Roentgenol. 2002;179(2):523-527.
57. Dao KD, Solomon DJ, Shin AY, et al. The efficacy of ultrasound in the evaluation of dynamic scapholunate ligamentous instability. J Bone Joint Surg Am. 2004;86-A(7):1473-1478.
58. Finlay K, Lee R, Friedman L. Ultrasound of intrinsic wrist ligament and triangular fibrocartilage injuries. Skeletal Radiol. 2004;33(2):85-90.
59. Boutry N, Lapegue F, Masi L, et al. Ultrasonographic evaluation of normal extrinsic and intrinsic carpal ligaments: preliminary experience. Skeletal Radiol. 2005;34(9):513-521.
60. Lacelli F, Muda A, Sconfienza LM, et al. High-resolution ultrasound anatomy of extrinsic carpal ligaments [in English, Italian]. Radiol Med. 2008;113(4):504-516.
61. Chiou HJ, Chang CY, Chou YH, et al. Triangular fibrocartilage of wrist: presentation on high resolution ultrasonography. J Ultrasound Med. 1998;17(1):41-48.
P. 102

62. Keogh CF, Wong AD, Wells NJ, et al. High-resolution sonography of the triangular fibrocartilage: initial experience and correlation with MRI and arthroscopic findings. AJR Am J Roentgenol. 2004;182(2):333-336.
63. Heuck A, Bonél H, Stäbler A, et al. Imaging in sports medicine: hand and wrist. Eur J Radiol. 1997;26(1):2-15.
64. Klauser AS, Tagliafico A, Allen GM, et al. Clinical indications for musculoskeletal ultrasound: a Delphi-based consensus paper of the European Society of Musculoskeletal Radiology. Eur Radiol. 2012;22(5):1140-1148.

65. Moser T, Khoury V, Harris PG, et al. MDCT arthrography or MR arthrography for imaging the wrist joint? Semin Musculoskelet Radiol. 2009;13(1):39-54.
66. Watanabe A, Souza F, Vezeridis PS, et al. Ulnar-sided wrist pain. II. Clinical imaging and treatment. Skeletal Radiol. 2010;39(9):837-857.
67. Ebrahim FS, De Maeseneer M, Jager T, et al. US diagnosis of UCL tears of the thumb and Stener lesions: technique, pattern-based approach, and differential diagnosis. Radiographics. 2006;26(4):1007-1020.
68. Shinohara T, Horii E, Majima M, et al. Sonographic diagnosis of acute injuries of the ulnar collateral ligament of the metacarpophalangeal joint of the thumb. J Clin Ultrasound. 2007;35(2):73-77.
69. Noszian IM, Dinkhauser LM, Orthner E, et al. Ulnar collateral ligament: differentiation of displaced and nondisplaced tears with US. Radiology. 1995;194(1):61-63.
70. Descatha A, Huard L, Aubert F, et al. Meta-analysis on the performance of sonography for the diagnosis of carpal tunnel syndrome. Semin Arthritis Rheum. 2012;41(6):914-922.
71. Klauser AS, Halpern EJ, Faschingbauer R, et al. Bifid median nerve in carpal tunnel syndrome: assessment with US cross-sectional area measurement. Radiology. 2011;259(3):808-815.
72. Ghasemi-Esfe AR, Khalilzadeh O, Vaziri-Bozorg SM, et al. Color and power Doppler US for diagnosing carpal tunnel syndrome and determining its severity: a quantitative image processing method. Radiology. 2011;261(2):499-506.
73. Wilder-Smith EP, Therimadasamy A, Ghasemi-Esfe AR, et al. Color and power Doppler US for diagnosing Carpal tunnel syndrome and determining its severity. Radiology. 2012; 262(3):1043-1044; author reply 104.
74. Pfirrmann CW, Zanetti M. Variants, pitfalls, and asymptomatic findings in wrist and hand imaging. Eur.J.Radiol. 2005;56(3):286-295.
75. Klauser AS, Halpern EJ, De Zordo T, et al. Carpal tunnel syndrome assessment with US: value of additional cross-sectional area measurements of the median nerve in patients versus healthy volunteers. Radiology. 2009;250(1):171-177.
76. Marshall S, Tardif G, Ashworth N. Local corticosteroid injection for carpal tunnel syndrome. Cochrane Database Syst Rev. 2007;18(2):CD001554.
77. El-Karabaty H, Heyzel A, Galla TJ, Horch RE, Lücking CH, Glocker FX. The effect of carpal tunnel release on median nerve flattening and nerve conduction. Electromyogr Clin Neurophysiol 2005;45(4):223-227.
78. Vögelin E, Nüesch E, Jüni P, et al. Sonographic follow-up of patients with carpal tunnel syndrome undergoing surgical or nonsurgical treatment: prospective cohort study. J Hand Surg Am. 2010;35(9):1401-1409.
79. Elias DA, Lax MJ, Anastakis DJ. Musculoskeletal images. Ganglion cyst of Guyon's canal causing ulnar nerve compression. Can J Surg. 2001;44(5):331-332.
80. Cooke R, Lawson I. Use of Doppler in the diagnosis of hypothenar hammer syndrome. Occup Med (Lond). 2009;59(3):185-190.
81. Felman AH, Fisher MS. The radiographic detection of glass in soft tissue. Radiology. 1969;92(7):1529-1531.
82. Horton LK, Jacobson JA, Powell A, et al. Sonography and radiography of soft-tissue foreign bodies. AJR Am J Roentgenol. 2001;176(5):1155-1159.
83. Bradley M. Image-guided soft-tissue foreign body extraction —success and pitfalls. Clin Radiol. 2012;67(6):531-534.
84. Jacobson JA, Powell A, Craig JG, et al. Wooden foreign bodies in soft tissue: detection at US. Radiology. 1998;206(1): 45-48.
85. Rubin JM, Adler RS, Bude RO, et al. Clean and dirty shadowing at US: a reappraisal. Radiology. 1991;181(1):231-236.
86. Bianchi S, van Aaken J, Glauser T, et al. Screw impingement on the extensor tendons in distal radius fractures treated by volar plating: sonographic appearance. AJR Am J Roentgenol. 2008;191(5):W199-W203.
87. Teefey SA, Dahiya N, Middleton WD, et al. Ganglia of the hand and wrist: a sonographic analysis. AJR Am J Roentgenol. 2008;191(3):716-720.
88. Wang G, Jacobson JA, Feng FY, et al. Sonography of wrist ganglion cysts: variable and noncystic appearances. J Ultrasound Med. 2007;26(10):1323-1328.
89. Breidahl WH, Adler RS. Ultrasound-guided injection of ganglia with coricosteroids. Skeletal Radiol. 1996;25(7): 635-638.
90. Kransdorf MJ, Murphey MD, Smith SE. Imaging of soft tissue neoplasms in the adult: benign tumors. Semin Musculoskelet Radiol. 1999;3(1):21-38.
91. Middleton WD, Patel V, Teefey SA, et al. Giant cell tumors of the tendon sheath: analysis of sonographic findings. AJR Am J Roentgenol. 2004;183(2):337-339.
92. De Schepper AM, Hogendoorn PC, Bloem JL. Giant cell tumors of the tendon sheath may present radiologically as intrinsic osseous lesions. Eur Radiol. 2007;17(2):499-502.
93. Murphey MD, Rhee JH, Lewis RB, et al. Pigmented villonodular synovitis: radiologic-pathologic correlation. Radiographics. 2008;28(5):1493-1518.
94. Bianchi S. Ultrasound of the peripheral nerves. Joint Bone Spine. 2008;75(6):643-649.
95. Reynolds DL Jr, Jacobson JA, Inampudi P, et al. Sonographic characteristics of peripheral nerve sheath tumors. AJR Am J Roentgenol. 2004;182(3):741-744.
96. Parizel PM, Simoens WA, Matos C, et al. Tumors of peripheral nerves. In: Imaging of Soft Tissue Tumors. 2nd ed. Berlin, Heidelberg, NY: Springer; 2006:301-330.
97. Baek HJ, Lee SJ, Cho KH, et al. Subungual tumors: clinicopathologic correlation with US and MR imaging findings. Radiographics. 2010;30(6):1621-1636.
98. Drapé JL, Idy-Peretti I, Goettmann S, et al. Subungual glomus tumors: evaluation with MR imaging. Radiology. 1995;195(2):507-515.
99. Hwang S, Adler RS. Sonographic evaluation of the musculoskeletal soft tissue masses. Ultrasound Q. 2005;21(4): 259-270.

100. Fornage BD, Tassin GB. Sonographic appearances of superficial soft tissue lipomas. J Clin Ultrasound. 1991;19(4): 215-220.
101. Inampudi P, Jacobson JA, Fessell DP, et al. Soft-tissue lipomas: accuracy of sonography in diagnosis with pathologic correlation. Radiology. 2004;233(3):763-767.